NUMERICAL INVESTIGATIONS OF WEATHERED LEDA CLAY SLOPE STABILITY DUE TO RAINFALL INFILTRATION EXTENDING THE MECHANICS OF UNSATURATED SOILS

ALPESH RAMESH SENGHANI

Thesis submitted to the University of Ottawa in partial Fulfillment of the requirements for the Master of Applied Science in Civil Engineering

Under the supervision of Dr. Sai K. Vanapalli

Department of Civil Engineering

Faculty of Engineering

University of Ottawa

ABSTRACT

The slope stability analyses in Leda clays deposits of Ottawa and Quebec region which are sensitive in nature are based on conventional soil mechanics assuming saturated soil conditions. The gradual weathering associated with environmental factors contribute to cracks in the surface layer of Leda clay slopes that significantly escalate the susceptibility of slope failures. The Leda weathered clay surface slope and a certain depth of intact soil immediately below it is typically in a state of unsaturated condition. The hydro-mechanical behaviour of the unsaturated weathered crust of Leda clay is highly sensitive to snow melt and rainfall water infiltrates to greater depths. Due to this reason, the conventional slope stability analyses in geotechnical engineering practice based on the principles of saturated soil mechanics may not be reliable. During the last two decades, slope stability analyses based on numerical simulation techniques extending the principles of unsaturated soil mechanics proposed in the literature are being implemented in practice for conventional soils. In these numerical techniques, the hydro-mechanical soil property functions that are required are predicted using the saturated coefficient of permeability, effective shear strength parameters and the soil water characteristics curve (SWCC). The SWCC used in these numerical techniques of conventional soils behavior is unimodal in nature that has only a single air-entry value (AEV), which are representative of a typical intact soil behavior.

There are limited slope stability analyses reported in the literature of Leda clay deposits considering the principles of unsaturated soil mechanics. In addition, information about the SWCC of Leda clay is scarce. For rigorous analyses, it is important to consider the influence of soil properties of in-situ weathered crust and the soil below it. The SWCC features for considering such a scenario should consider the influence of bi-modal nature of the SWCC. For this reason, the focus of this thesis has been directed towards developing simple techniques for estimating both

the mono and bimodal SWCC of Leda clay and use them in the slope stability extending numerical techniques. As a part of this study, models have been developed for estimating the SWCC using the grain size distribution curve and soil properties collected from geotechnical reports of various projects in the Ottawa region. A range of AEVs were estimated to reasonably represent considering the typical in-situ weathered Leda clay crust behavior. Three unimodal SWCCs were estimated utilizing the lower, upper, and median AEV (i.e., 5 kPa, 80 kPa, 15 kPa). Using this information, a bimodal SWCC is approximated by superimposing two unimodal SWCCs to conduct slope stability analysis.

In this thesis, a numerical model has been established to examine the slope stability of weathered Leda clay considering the influence of different rainfall infiltration scenarios. This model utilizes a coupled hydro-mechanical stress analysis to perform numerical analysis using commercial GeoStudio software that includes SEEP/W, SIGMA/W and SLOPE/W. To ensure accuracy, the soil properties used in the numerical modelling are derived through an extensive literature review of Leda clay slopes.

Extensive numerical studies were undertaken to understand the impact of various soil properties on the factor of safety (FS). Pore water pressure (PWP) profiles variation demonstrate influence of rainfall infiltration in the surficial layer. Coupled analysis shows a faster downward movement of the wetting front than uncoupled analysis due to the influence of hydraulic and mechanical stresses, resulting in soil softening and volume change upon wetting. The faster rate of wetting also contributes to a rapid loss of shear strength, consequently, resulting in a lower FS than uncoupled analysis. The numerical technique proposed in this thesis is useful for the geotechnical engineers who routinely assess the stability of Leda clay slopes for rationally assessing the potential landslide hazards triggered by snow melt and rainfall events.

ACKNOWLEDGEMENTS

I would like to take a moment to express my sincere gratitude and appreciation to the individuals who have played a critical role in supporting and guiding me throughout my master's thesis journey.

First and foremost, I would like to recognize my supervisor, Dr. Sai K. Vanapalli, for his unwavering support and guidance. He has been a mentor and father figure to me, providing me with both professional and personal growth opportunities. I will forever cherish the academic and life experiences he has shared with me, and I am grateful for his steadfast support even during the most challenging times.

I would also like to extend my appreciation to my senior colleagues at the University of Ottawa. Mengxi (Meghan) Tan, thank you for your availability and assistance with my research inquiries. Your support during the numerical modelling phase was invaluable. Additionally, I would like to acknowledge Roberto Alves for his generous sharing of prediction model experiences and willingness to discuss my problems. N'eem Tavakkoli's guidance on data collection from geotechnical reports for Leda clay in the Ottawa region was also incredibly helpful. I would like to thank Xavier, Susan, Aaron, and Pan for their unique forms of support during my research days among the group.

Finally, I would like to thank my family for their patience and support throughout the completion of this thesis. A special appreciation goes to my wife, Darshna, for her understanding and sacrifices to help see this through. Thank you for your support.

TABLE OF CONTENTS

LIST OF FIGURES

LIST OF TABLES

CHAPTER 1: INTRODUCTION

1.1 Background

The climate in the Ottawa region, located towards Southeastern Ontario in Canada, is generally categorized as a "humid continental climate with warm, humid summers and cold, snowy winters" (Walsh and Patterson 2022). The Ottawa region's climate has been changing over the years, and trends show an increase in both temperature and precipitation. In the decades to come, the Ottawa region may have wetter springs, much warmer winters, and increased summer days above 30°C. These changes bring extreme weather events such as heat waves, floods, and ice storms (City of Ottawa 2020; Climate Atlas of Canada 2021). The variable climatic conditions directly impact the welfare of the people, infrastructure, the economy, and the environment. The cost of damages due to climate change is estimated to be between $21 billion and $43 billion annually by 2050 (Infrastructure Canada 2006).

Along with the change in climatic conditions, there has also been reasonable growth in the population over time. The population of the Ottawa-Gatineau Metro region increased from approximately 100,000 in the 19th century to about 282,000 in 1950. In 2020, the region's population was 1.4 million and will rise to 1.6 million by 2045 (Walsh and Patterson 2022). Consequently, there will be an increase in demand for housing and infrastructure in the region. According to the City of Ottawa (2019), there were 404,400 private homes in the area in 2018. These numbers will rise to about 599,200 private homes in 2046, an increase of 194,800 homes.

The City of Ottawa is extensively built on massive deposits of Leda clay, a sensitive clay with characteristics that may lead to flowslides when exposed to external loads, earthquakes, predominant rainfalls, excavation, or construction activities. These sensitive clays are also known

as Leda clay in the Ottawa region, Champlain Sea clay in Quebec, and Quick clay in the Scandinavian regions. In Eastern Canada, Leda clay deposits are sediments from the Champlain Sea that occupied the St. Lawrence lowlands during the late glacial period 10000 years ago, between Quebec City and Brockville, Ontario, extending up to the Ottawa River valley (Quigley 1980). One of the significant challenges around the region is the stability of Leda clay slopes. Figure 1.1 illustrates the extent of Leda clay in the area and the locations of landslides over the years.

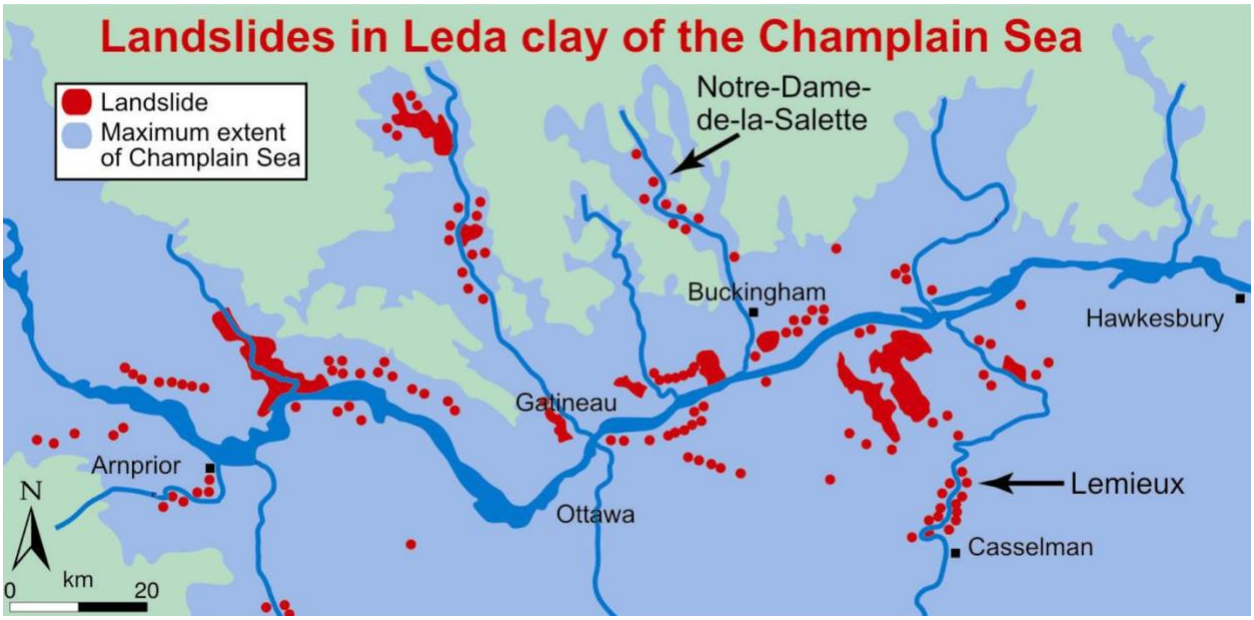

Figure 1.1 Landslide footprints over Leda Clay around the Ottawa region (Source: NRCAN)

The typical "house of cards" of Leda clay structure is held together by dissolved salts which provide electrolytic bond to the structure in its undisturbed state. However, these bonds are vulnerable to leaching, breaking down the flocculated structure into a dispersed one (Kerr 1963). The most challenging behaviour of Leda clay is associated with its sensitivity, which is defined as the ratio of undisturbed shear strength over the remoulded shear strength. The sensitive clay is

mostly spread over the industrial population of Canada and can lead to catastrophic failures of geotechnical structures, including slopes and foundations in the region (Law and Bozozuk 1988).

Climate Atlas of Canada (2021) presents numerous climate change data including annual and seasonal precipitation levels for Ottawa municipality. The data is predicted based on low or high carbon emissions future. Figure 1.2 presents historical and future precipitation data assuming high carbon emissions future. The average precipitation levels by 2050 are estimated to be 1031 mm/year, while by 2090, it may reach 1068 mm/year. However, the minimum (i.e., 10th percentile) and maximum (i.e., 90th percentile) for the range of prediction values should also be recognized. Therefore, it is essential to understand the impact of precipitation in the form of rainfall on the slope stability of weathered Leda clay slopes.

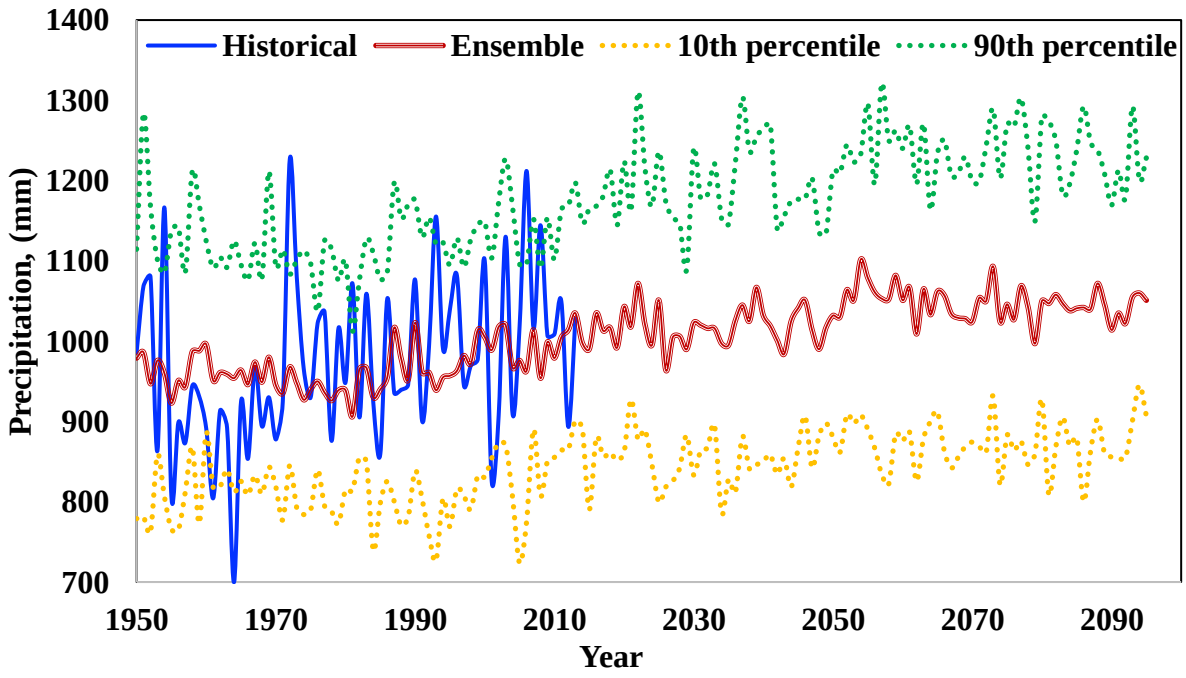

Figure 1.2 The historical and future climate change predictions for Ottawa Municipality (Climate Atlas of Canada 2021)

The climate of Eastern Canada has four different seasons around the year: spring, summer, autumn, and winter. Leda clay slopes exposed to these variations in weather around the year undergo physical and chemical weathering. This creates a layer of weathered crust on the surficial layer of Leda clay. The thickness of the weathered crust in Eastern Canada varies and may extend to depths of approximately 3 m to 6 m (Eden and Hamilton 1957; Eden 1966; Lefebvre et al. 1987; McRostie et al. 1996; Perret et al. 2019). Generally, the weathered crust is assumed to be at depths of roughly 3 m around the Ottawa region (Eden and Crawford 1957; Lefebvre and Poulin 1979; Garga et al. 2006). A typical slope of the Ottawa region with Leda clay consists of an unsaturated and saturated zone, as illustrated in Figure 1.3.

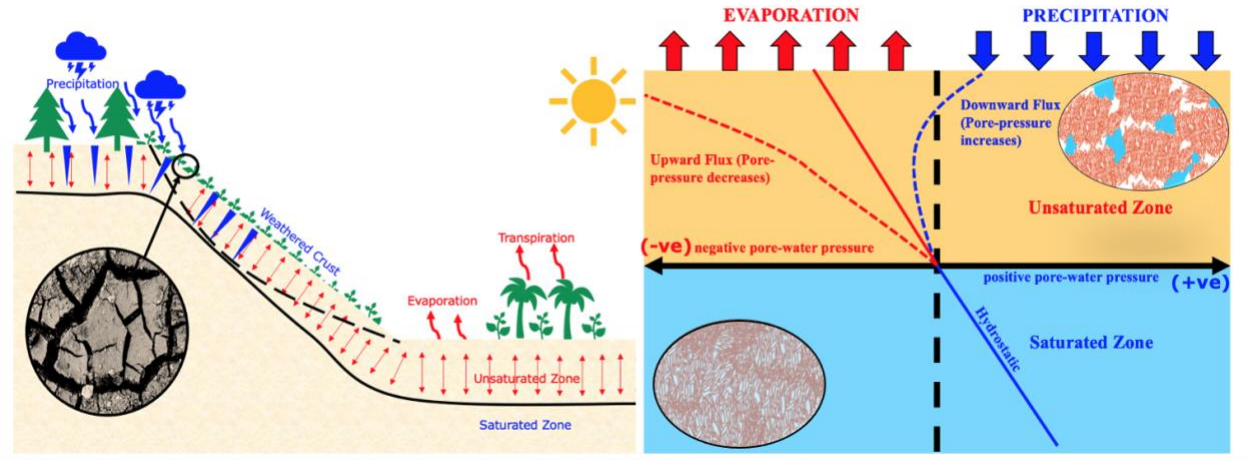

Figure 1.3 Influence of climate on unsaturated soil slopes

The weathered crust of Leda clay consists of unsaturated soil characteristics. The soil properties of the weathered crust differ from the soil properties of the intact layer (i.e., the saturated zone in Figure 1.3). The variation of soil properties results from the numerous drying and wetting and or freezing and thawing cycles (Pineda et al. 2014). Hence, the surficial layer can be assumed to be a separate layer when conducting coupled hydro-mechanical slope stability analysis (Qi and Vanapalli 2015a).

Historically, slope stability analyses have been conducted using the conventional methods that are based on the principles of saturated soil mechanics. However, research related to the unsaturated soil mechanics principles has emerged in recent decades that is useful in providing rational explanations. The general assumption is that the slope will eventually attain a fully saturated condition over a specific rainfall infiltration period (Fredlund 2015). However, this may not always be true, especially in arid and semi-arid regions with deeper groundwater tables (Azam and Ito 2011; Qi and Vanapalli 2015a; c; Tan and Vanapalli 2021).

Unsaturated soil properties are generally expressed as a function of soil suction. The direct measurement of the soil property functions is time-consuming and expensive and requires extensive equipment facilities that are not available in conventional laboratories. The principles of unsaturated soil mechanics can be used to analyze both saturated and unsaturated zones, while the principles of saturated soil mechanics can only interpret the saturated zone. For example, in Figure 1.4, saturated soil mechanics principles can analyze the moisture flow below the phreatic line but cannot analyze the moisture flow in the unsaturated soil. The fundamental differences between saturated and unsaturated soil mechanics principles (Table 1.1) explain the latter's versatility in solving complex soil mechanics problems.

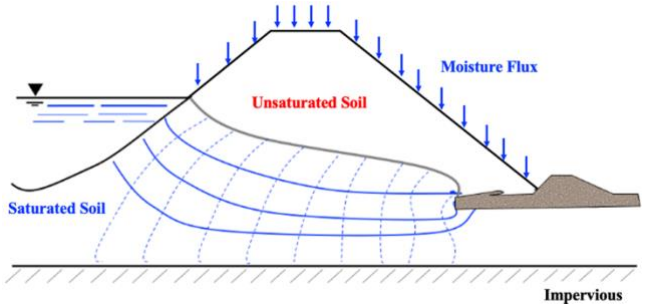

Figure 1.4 Limitations of using saturated soil mechanics principles (modified after Fredlund 2015)

Rainfall and snowmelt (i.e., precipitation) have mainly been responsible for several landslides in the Ottawa region (Crawford and Eden 1967; Mitchell 1969; Eden and Mitchell 1970; Mitchell and Markell 1974; Williams et al. 1979; Hugenholtz and Lacelle 2004; Al-Umar 2018). Numerous research works have been conducted to study the influence of rainfall on Leda clay slope stability (Oh et al. 2014; Al-Umar 2018; Panikom 2020; Al-Umar et al. 2022). However, the soil water characteristics curve (SWCC) used in these analyses does not consider the weathered crust on the surface of the Leda clay slopes. Oh et al. (2014) uses a SWCC derived from compacted Leda clay, while Al-Umar (2018), Panikom (2020), and Al-Umar et al. (2022) use SWCC derived from Leda clay collected below 8 m, which is much deeper than the weathered zone in Leda clay slopes.

Table 1.1 Saturated and unsaturated soil mechanics principles (After Fredlund 2015)

Saturated Soil Mechanics	Unsaturated Soil Mechanics
Soil properties are constants, c', ϕ', k, c_v	Soil properties are functions of suction
Soil properties are measured on undisturbed samples	Soil properties are estimated from Soil Water Characteristic Curve (SWCC)
Linear soil mechanics problems	Non-linear soil mechanics problems

In addition, there is limited data available in the literature for the SWCC that represents the weathered crust of Leda clay. The SWCC data available for Leda clay in the literature (Oh et al. 2014; Aldaeef and Rayhani 2015; Han et al. 2022) are developed on compacted samples. Moreover, the cost and duration of conducting laboratory tests to measure SWCC are limitations (Fredlund 2015). As a result, prediction models are generally used to compute the SWCC. Several models available in the literature (Arya and Paris 1981; Burger and Shackelford 2001; Fredlund et

al. 2002; Aubertin et al. 2003; Satyanaga et al. 2013; Wijaya and Leong 2016; Satyanaga and Rahardjo 2019) can predict or estimate SWCC using soil properties based on simple soil properties information that include grain size distribution, void ratio, and water content.

Several factors influence soil behaviour through various stresses, including thermal(T), hydrological(H), mechanical(M), and chemical(C) stresses (i.e., THMC). The complexity of understanding the soil behaviour increases as the number of different stresses is considered for analysis. In recent years, coupled hydro-mechanical slope stability analyses have been undertaken to simulate the influence of hydraulic and mechanical stresses in slope failures (Qi and Vanapalli 2015; Tan and Vanapalli 2021; Das et al. 2022).

The SWCC can be unimodal or bimodal, depending on the soil characteristics. The weathering of the surficial layer involves drying and wetting cycles that influence the soil packing and arrangement over several cycles. Consequently, the surficial layer develops both macro and micropores, which influences its hydro-mechanical soil properties. This can result in a bimodal SWCC demonstrating the dual porosity nature of the soil (Qi and Vanapalli 2015c). The weathering phenomenon does not influence the soil layer at a greater depth which is intact and maintain its original structure. Therefore, unimodal SWCC is sufficient for representation of the intact layer in slope stability analyses.

Saturated soil mechanics principles may not provide comprehensive understanding of the rainfall's influence on the slope stability. The principles of unsaturated soil mechanics can help predict and monitor landslides by estimating the pore-water pressure considering different scenarios that typically are encountered in practice (Zhang et al. 2004). For example, the slope failure period can be estimated with relative accuracy that help carry out evacuation measures to avoid catastrophic human and animal losses. In other words, principles of unsaturated soil

mechanics provide a critical role in understanding the slope stability of Leda clay to monitor, design current and future geotechnical structures considering the influence of climate changes associated with global warming.

1.2 Research Objective

The main objective of this thesis is directed towards estimating the bi-modal SWCC for weathered Leda clay using in situ data collected from the geotechnical reports for various government projects around the Ottawa region. The estimated bimodal SWCC that is reasonably representative of the weathered crust and the intact soil (i.e., unimodal SWCC) below is used as a tool to numerically model the slope stability analyses extending the state-of-the-art understanding of the mechanics of unsaturated soils. In addition, the influence of rainfall on pore-water pressure distribution and the safety factor of the weathered slope is examined extending coupled and uncoupled analysis on the safety factor.

1.3 Thesis Outline

The thesis is presented in five chapters. Chapter 1 provides a brief introduction and background relating to the thesis topic. The research objectives and the chronology of the thesis chapters are presented.

Chapter 2 presents a literature review, that includes: (i) information related to Leda clay in Eastern Canada, focusing more on its characteristics in the Ottawa region; (ii) stability of slopes in the Ottawa region, including formation of valleys and types of landslides; (iii) unsaturated soil mechanics, including SWCC, using SWCC for predicting design parameters, and SWCC curve fitting equations.

Chapter 3 presents a brief background on SWCC prediction models. Procedures for data collection and analysis to predict the SWCC are presented. Unimodal and bimodal SWCCs used in numerical modelling analyses are estimated and presented.

Chapter 4 presents a numerical model considering the influence of boundary conditions, input material (i.e., soil properties) and dimensions for rationally determining the slope stability safety factor extending the mechanics of unsaturated soils. Numerical modelling is conducted using the Geo Studio software (i.e., SLOPE/W, SEEP/W and SIGMA/W) considering both coupled and uncoupled analysis. Results and discussions are presented for various factors that influence the PWP profile variations and FS of the weathered Leda clay slopes.

Chapter 5 presents the conclusion and recommendations for future research work.

CHAPTER 2: LITERATURE REVIEW

2.1 Leda Clay – Background Information

Sensitive clays are widespread in Eastern Canada, Scandinavia, Northern parts of Russia, Alaska, and some Southern Hemisphere regions such as New Zealand (Torrance 1983). Sensitive clays are referenced with different names in different regions. Leda clay is used to identify and reference sensitive clays in Ontario province in Canada. The term Leda clay originated from the fossil *Leda glacialis*, which is abundantly present in sensitive clays and was originally introduced into the literature by the Canadian geologist Dr. J. W. Dawson (Bechai 1974). In Quebec, Canada, the term Champlain Sea clay is used for the sensitive clays due to its origins in the Champlain Sea. Lastly, the term Quick clays is widely used in Scandinavia, providing a reference to its sensitivity.

2.1.1 Introduction

The presence of sensitive clays in Canada can be attributed to the sedimentation process in proglacial and postglacial water bodies that existed as the Wisconsin ice sheet retreated between 18000 and 6000 years before present (BP). Figure 2.1 illustrates the vast areas covered by freshwater glacial lakes and inland marine seas during the retrieval of the Wisconsin ice sheet (Quigley 1980). During 18000 to 20000 BP, the extent of the Wisconsin ice sheet was at its maximum, with an ice thickness of almost 5000 m centred on the Hudson Bay area. As a result of the massive weight of the ice layer, the earth's crust around the Hudson Bay region depressed to about 1000 m, and the ocean water levels were at least 120 m below the current levels due to the mass of water captured in the enormous ice layer (Andrews 1972; Quigley 1980).

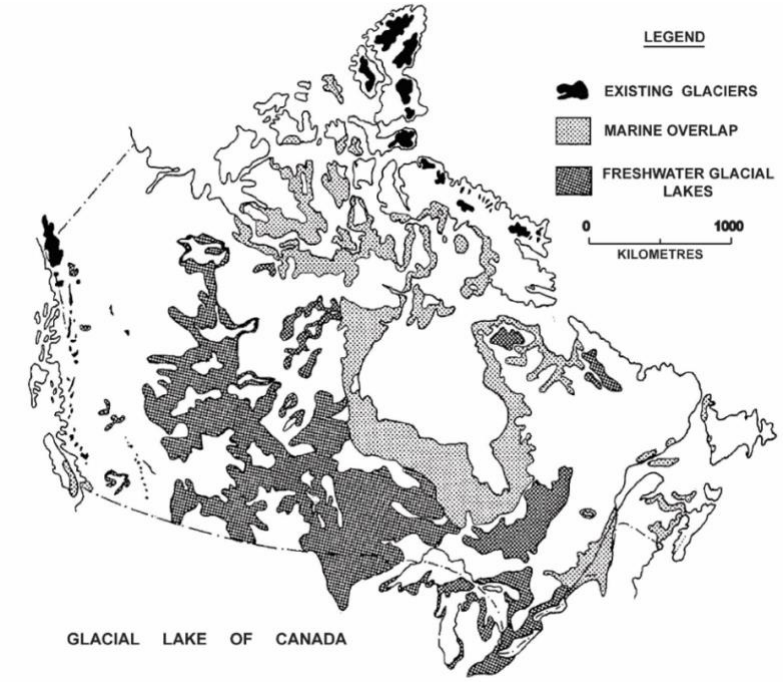

Figure 2.1 Distribution of Marine and freshwater glacial and postglacial lakes of Canada (Panikom 2020; Quigley 1980)

The climate began to warm around 18000 BP, and the Wisconsin ice sheet began to retreat. The Wisconsin glacier retreat occurred in stages where small and large proglacial lakes were created depending on the rate of the melting water at the ice fronts. Major re-advances of the ice overran soft soil deposits during 13500-, 11800- and 8200-years BP (Quigley 1980). As the ice layer thinned and moved North, isostatic rebounding of the land surface occurred. The rebounding process is relatively slow in that it continues in some regions today. Figure 2.2 illustrates the extent of rebounding around the Ottawa area, approximately 200 m (Quigley 1980; Lefebvre 1996).

The rate of ice-sheet melting, which led to the rise in sea level, was a much faster process than the rebounding of the land surface as the ice sheet retreated. However, the isostatic rebound was much more significant than the rise in sea level. The interaction between fluctuating land surface elevations and sea levels resulted in a period of inundation. Eventually, it resurfaced certain

portions of the continental land mass between the melting ice sheet and the present day (Lefebvre 1996).

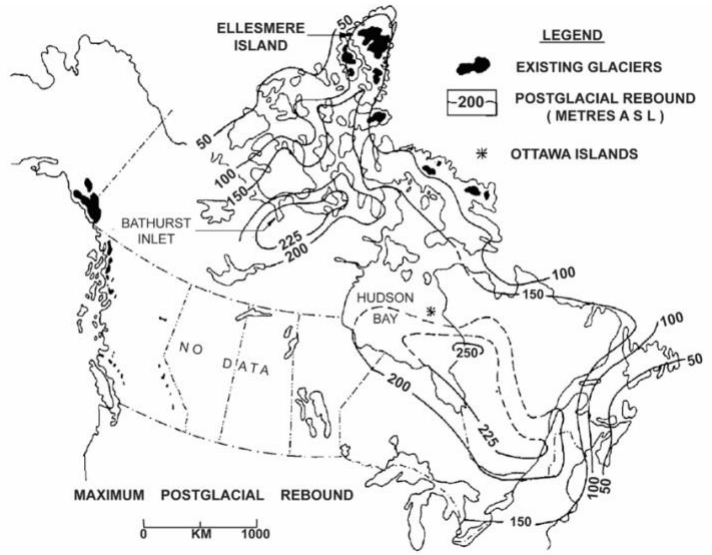

Figure 2.2 The maximum postglacial rebound of Eastern Canada (Andrews 1972; Quigley 1980; Panikom 2020)

Sensitive clays are considered to have been deposited in marine or brackish water bodies. The Champlain Sea is believed to have existed between 12500 and 10000 BP (Figure 2.3). The largest deposits of postglacial marine clays were formed in the Champlain Sea, which inhibited the St. Lawrence lowlands from the Gulf of St. Lawrence to the region around Ottawa City (Elson 1969; Gadd 1975; Lefebvre 1996). The salty water from the Champlain Sea flowed into the freshwater lakes in the valleys, and marine clays were deposited over freshwater varved clays in many regions, including the Ottawa area. Since the ice front experienced melting and freezing in some regions of the boundary, it resulted in layers of marine and freshwater clay deposits. The interlayered deposits of clay, sand, gravel, or glacial till can be found at the boundary of the Champlain Sea, while deep and thick clay deposits can be found around the centre of the Champlain Sea (Gadd 1975; Quigley 1980).

Figure 2.3 **Evolution of major glacial lakes of Canada 11800 BP (modified after Quigley 1980 & Panikom 2020)**

2.1.2 Sedimentology of Leda Clay

The study of sedimentology within the existing postglacial lakes and marine estuaries can be helpful in further understanding its impact on the geology and geotechnical characteristics of soft clay soils. Table 2.1 lists various significant soft clay deposits that may be encountered in geotechnical practice. Waterlaid tills, lacustrotills, and mudflow deposits may have coarse-grained materials inside a fine clayey matrix. Varved and marine clays consist mainly of uniform, fine-textured, silty clays (Quigley 1980).

Dreimanis (1976) suggests that waterlaid till is a stratified variety of till deposited in water. May (1977) describes waterlaid tills as lacustrine clays deposited at a floating ice sheet with a short water column that minimizes the grain-size segregation. Lacustrotills are "till-like sediments deposited in a lacustrine environment primarily by flow mechanisms" (May 1977). Lacustrotills are submarine mudflow in proglacial lakes that may result from waterlaid tills. Lacustrotills may disperse towards the shores to form turbidity current deposits interbedded with varved clays if the initial mudflow has underwater momentum (Morgenstern 1967).

Table 2.1 Different types of soft clay deposits (After **Quigley 1980**)

Type of Deposit	Origin
1. Waterlaid tills	Unsorted lacustrine sedimentation below floating ice
2. Lacustrotills	Subaqueous, proximal, flow deposits in proglacial lakes
3. Mudflow deposits	Subaerial and submarine flows
4. Turbidity current flows	Heavy-density current deposits generated by mudflow dilution, floods, ice calving, slumping etc.
5. Varved clays	Turbidity current summer deposits and winter clay deposition by settling
6. Marine clays	Saltwater flocculation and sedimentation

Varved clays are the layered sediments deposited in proglacial freshwater lakes where a single varve represents one year of deposition. The layered sediments comprise clay deposition in winter and silt in summer. During the summer, a cold inflow (0-6°C) due to heavy ice melt of high density (1 g/l or more) can enter the lake, resulting in a high-density flow shown in Figure 2.4 (b). This is due to the density of water at this temperature range (0-6°C) being at maximum. The turbidity currents may occur continuously for several days, or they might be short daily pulses that can flow for miles on the flat lake bottom as they deposit graded silty sand and silt (Kenney 1976). During the winter, the inlet stream lacked sufficient sediments and thus was of low density. As a result, overflow would occur in winter conditions (Figure 2.4 (a)), gradually settling undisturbed clay particles to form the winter layer (Quigley 1980).

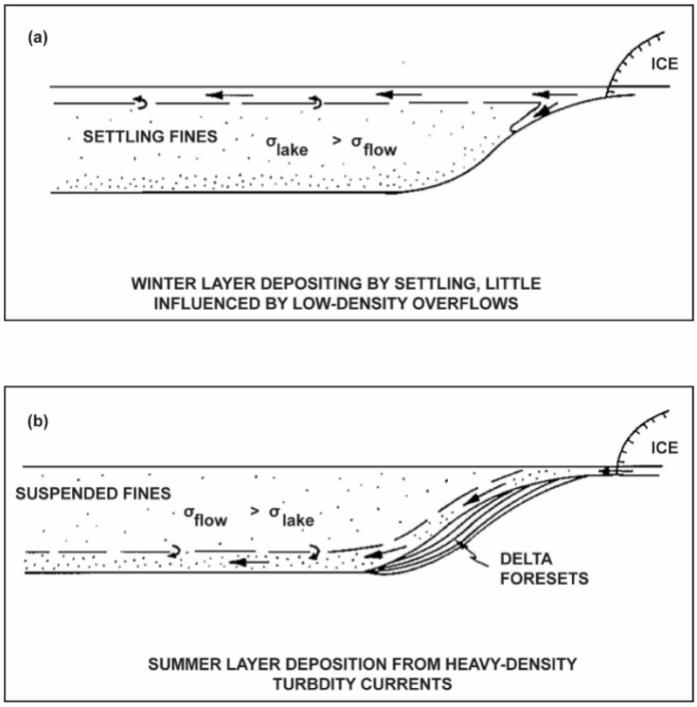

Figure 2.4 Deposition of varved clays (a) Winter layer deposition (b) Summer layer deposition (Panikom 2020; Quigley 1980)

The sediment density in the postglacial lake was approximately 0.1 g/l, lower than in proglacial lakes. Therefore, the inlet flow in this condition would enter the lakes as overflows and interflows. The deposition is consistent to proglacial lakes in that silty sand and silts are deposited during the summer, and clays that are deposited in the winter. However, the varved deposition would generally occur at the lake's inlet as the availability of sediments to produce varved deposits decreases as the distance from the inlet increases. The thickness of varved deposits quickly reduces with distance as massive clay deposits may be observed within 2km from the inlet (Smith 1978).

In the case of marine sea (for example, Champlain Sea) deposition, the meltwater or freshwaters would have generally entered the seas as overflows. Marine waters are of higher density due to dissolved salts (1020 g/l at 35% salinity) than meltwater (1000 g/l @ 4°C). The combination of freshwater and saltwater results in diffusion and turbulence down to a depth of 5m.

Low-salt flocculation of clay particles commences within the 5m depth. Below this depth, modification of clay floccules occurs by ingestion and excretion of plankton by a process called pelletization (Syvitski 1978, 1980; Syvitski and Murray 1981). This process produces fecal pellets and organic-rich floccules, which provide a fertile location for bacterial activity, which may be explained by observing black mottling in marine clays. Quigley (1980) summarizes that marine clays of proglacial origin have deep-water deposits composed of inorganic floccules, organic agglomerates, and fecal pellets, whose structure is retained in situ until damaged by consolidation.

2.1.3 Geochemical, Mineralogical and Structural Characteristics of Leda Clay

The study of mineral composition, pore-water chemistry, and the arrangement of these minerals in the structure can assist in understanding Leda clay's behaviour.

2.1.3.1 Mineralogical Characteristics

Leda clay consists of several minerals, which include quartz, feldspars, amphibole, illite, chlorite, calcite, amorphous matter, mica, phyllosilicates, iron oxides, dolomite, smectite, plagioclase, traces of kaolinite and vermiculite (Brydon and Patry 1961; Moum et al. 1968; Løken 1970; Quigley 1980; Locat et al. 1984; Torrance 1988). Bentley and Smalley (1978) summarize studies on the mineralogy of Leda clay for period of 1950s to the 1970s. The composition of minerals in Leda clay does not have significant differences when analyzing samples from different sites. The most prominent minerals found in Leda clay include quartz, feldspars, amphiboles, micas, and chlorites (Brydon and Patry 1961).

The mineral composition in Norwegian quick clay and Canadian Leda clay (both sensitive marine clays) are relatively similar, with the presence of quartz, feldspars, amphibole, illite, chlorite, calcite, and iron oxides (Moum et al., 1968; Løken 1970; Torrance 1988, 2013). The

presence of silicates and phyllosilicates in the clay fraction varies in the two regions, where phyllosilicates are abundant in Scandinavia, and silicates in Eastern Canada. The Scandinavian source rocks provide an abundance of phyllosilicate greater than the igneous and metamorphic rocks of the Canadian Shield (Torrance 2013).

Iron oxides are regularly found in Leda clays. In Eastern Canada, hematite is predominantly found in the South Nation River landslide site, whereas magnetite is found mainly in St. Leons, Quebec (Torrance et al. 1986). The glacial debris was briefly exposed to sub-aerial weathering. However, iron oxide formation is limited to surface or sedimentary environments. Therefore, Hematite and magnetite are products of the glacial grinding of iron oxides in the Canadian Shield's rock and iron ore deposits (Torrance 2013).

2.1.3.2 The Structure of Leda Clay

The structure of clay soil can be defined as the space occupied by solid particles held by plastic and rigid bonds. The fabric is the "size, shape and geometric arrangement of particles," which can be in a random or card-house orientation. The structure of quick clays is sensitive to deformation, and its structural properties change dramatically when strained (Crawford 1968).

Penner (1965) explains the electrokinetic theory in Leda clays using the clay-water system. The electrokinetic phenomena arise when charges are separated randomly as clay particles and water are brought into contact. The negatively charged surface of clay particles generally attracts the positive hydrogen ions. The bonding of clay particles and water results in repulsion among the clay particles and propagates soil swelling.

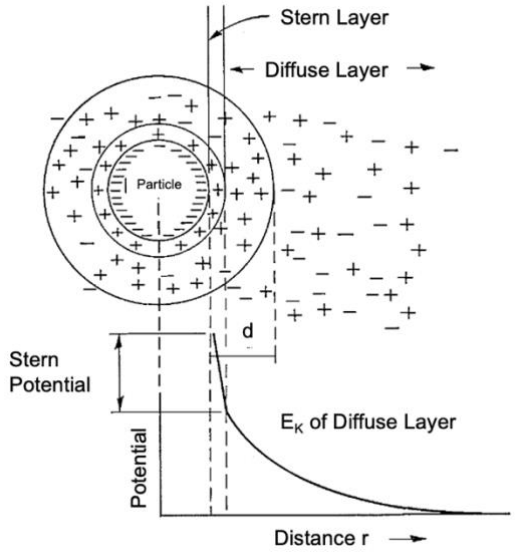

Figure 2.5 The electrokinetic potential E_K and the electrical double layer (adapted from **Alexander and Johnson 1949 and Penner 1965)**

The bonding produces a diffuse double layer whose prominent features are illustrated in Figure 2.5, as portrayed by Alexander and Johnson (1949). A fixed negative charge is found around the surface of the clay particle. The Stern layer consists of a fixed positive layer next to the surface where the potential drops linearly with distance. Therefore, the Stern potential can be defined as the difference between the surface potential and the potential of the fixed layer on the outer limit. After the Stern fixed layer is the diffuse layer, like the Gouy model, where there is an exponential drop of potential with distance. The positively charged diffuse layer is attracted toward the cathode when an external electrical potential is applied to the surface. On the other hand, the negatively charged particle with the adsorbed layer of water (immobile layer) will be attracted toward the anode (Penner 1965).

The potential difference between the clay particles and the surrounding liquid is the electrokinetic potential. The electrokinetic potential may be measured using numerous methods,

including electroosmosis, electrophoresis, streaming potential, and sedimentation effect (Penner 1965).

Leda clays are presumed to have a "house of cards" structure like other sensitive clays due to their deposition environment, age and geologic history (Law and Bozozuk 1988). The coarser particles are generally spherical and are of inert materials. In contrast, finer particles are comprised of elongated and plate-shaped clay materials. Moreover, Leda clays are generally "inactive" (Eden and Crawford 1957; Penner 1965; Crawford 1968).

The flocculated particles in marine water form a loose, porous structure which consists of a mixture of clay, silt, and sand. Flocculation does not occur in freshwater; the clay particles remain dispersed and settle slower than the silt and sand particles. The clay particles assume a parallel orientation (Figure 2.6 (b)) due to the repulsive forces and the slow settling. The card-house structure (Figure 2.6 (a)) generally results from electrostatic attraction between the particles' negatively charged faces and positively charged edges (Bennet 1976; Gillot 1987).

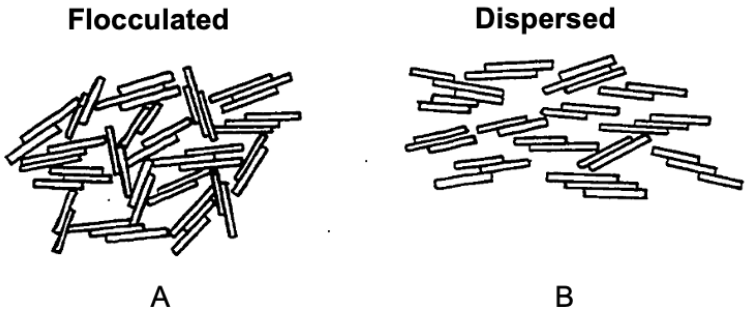

Figure 2.6 Particle arrangement in clay sediment (A) Open, random, house of cards arrangement; (B) Parallel or sub-parallel arrangement (Bennet 1976)

The arrangement of clay particles in the clay structure also influences the mechanical properties of sensitive soil and the engineering response of the soil. The microstructure (<1mm in size) and macrostructure (>1mm in size) influence can be recognized in a clay structure. These

micro and macrostructure characteristics provide evidence of a clay deposit's entire geologic and stress history. Figure 2.7 illustrates scanning electron images of the clay deposits chronology to form the microstructure and macrostructure. At the early stage, clay particles flocculate to create domains which are submicroscopic fabrics. The domains would then aggregate to form clusters visible through an optical microscope. Biogeochemical processes in soil lead to the clusters holding on to each other in clumps visible to the naked eye, known as peds.

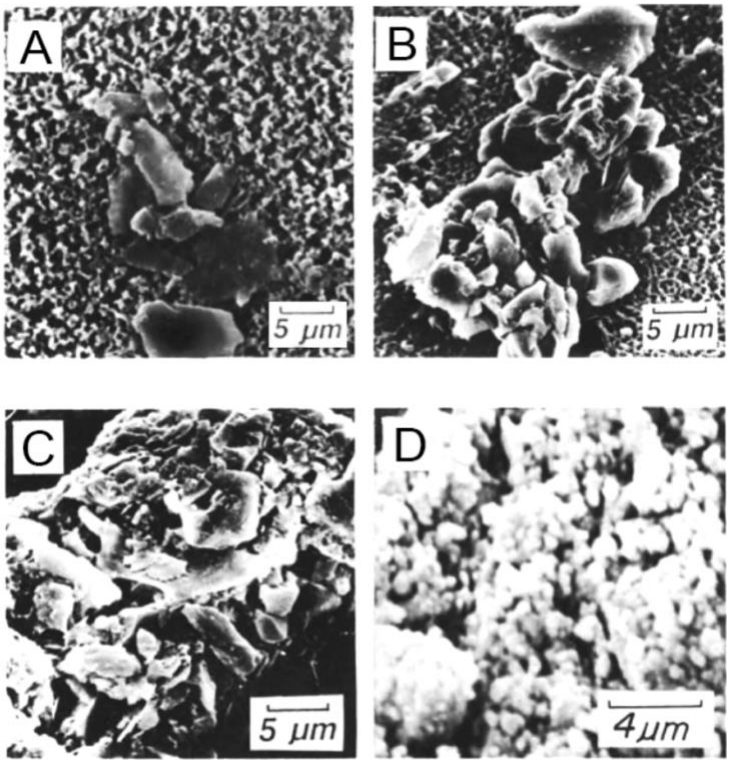

Figure 2.7 Scanning electron micrograph images of clay microstructures and macrostructures (A) A small edge-to-edge floccule (a domain); (B) A large face-to-face floccule (a cluster); (C) A ped formed by a mineral-bearing fecal pellet; (D) Microstructures and macrostructures in Leda clay (adapted from Quigley 1983)

The pores (voids) generally change shape as the surrounding pressure changes. This has not been the case around the Ottawa region, as the pore structure is intact despite the pressure of several metres of overburden strata that lie above Leda clay. The slow rate of deposition of

sediments and the development of ionic bonds between clay particles to form a “card-house” structure resulted in the retention of the original porosity of Leda clay (Quigley 1980).

Two types of pores are found in Leda clay: macropores and micropores. Macropores are large, open spaces between the larger aggregates (clusters and peds), called inter-aggregate pores. On the other hand, micropores are small spaces between the constituent particles of the aggregates, also called intra-aggregate pores.

2.1.3.3 Porewater Chemistry

Torrance (1979) reported pore-water chemistry for four sites in the Ottawa area: Treadwell, Touraine, Chelsea, and Angers. The current cation concentration in the pore water (i.e., during the study in 1979) is compared to the initial cation concentration in the sediment.

The chemical conditions of the depositional and post-depositional environment change in the pore-fluid chemistry influence the behaviour of Leda clay. These deposits have pores filled with freshwater despite evidence of marine remains. The contents of these deposits can be used to examine the original properties, depositional environment, and weathering (Torrance 1979).

Typically, low salinity levels in Touraine, Chelsea and Angers regions are due to the probable influence of leaching and weathering. However, Treadwell region showed high salinity levels. Torrance (1979) provides a detailed discussion of the results from the four sites reported regarding the porewater cation variance with depth. There is a minimum concentration of the porewater salinity required for rapid flocculation of suspended materials, which was exceeded. The minimum value depends on the concentration of suspended solids, approximately 2–3%. The maximum salinity for Ottawa area sediments is about 21% (Torrance 1979). The post-depositional chemical changes that influence the porewater chemistry of the sedimentary clay deposits of the Ottawa area include salt leaching, salinity increase, and weathering.

2.1.3.3.1 Salt Leaching

There are signs of leaching in all the different sites reported by Torrance (1979) in the Ottawa area. The humid-weather marine deposits uplifted above the sea level are prone to salt leaching through other mechanisms. One of the mechanisms involves the downward movement of rainwater entering the surface and percolation through the deposit. The upward movement of water may also be possible due to the influence of artesian pressures at the base of the deposits. The soil's hydraulic gradient and conductivity influence the leaching rate (Moum et al. 1971; Torrance 1979).

The salt leaching does not necessarily take place in the vertical direction but may also occur through the diffusion of salts towards zones of low salt concentrations. These low-concentration zones may be found on the surface or in sand layers at different depths, influencing the rapid horizontal flow of groundwater that increases the leaching rate. Even though the leaching process through diffusion is slow in thick deposits, the ultimate low-concentration zone reached in different parts of the deposit may impact its behaviour. The salt diffusion effect reduces the salt removal rate during the downward flow leaching phenomenon. The leaching process may be controlled if the rate of the downward water flow under the imposed hydraulic gradient is equal to or less than the rate at which salt diffuses under the salt concentration gradient that develops in the deposit (Torrance 1979).

The consequence of the leaching phenomenon on the illitic–chloritic marine clays is the decrease in pore-water salinity, which reduces the remoulded shear strength to a point where the soil behaves as a liquid at particularly low concentration zones (Rosenqvist 1953; Mitchell and Houston 1969; Torrance 1975, 1979).

The sensitivity of Leda clay increases as the influence of leaching increases. The sensitivity relationship with pore-water cations for the four sites near the Ottawa area (Treadwell, Touraine,

Chelsea, and Angers) indeed confirms the influence of salt leaching. For example, the Treadwell site shows a maximum sensitivity value of 26 at a depth of 15 m, with low salt concentration. The sensitivity value did not rise above 12 between depths of 15m to 90m, as the salt concentration was considerably high in this depth range (Figure 2.8 (a)). Torrance (1975) illustrated the impact of salt addition to highly leached debris of the Chelsea landslide, where the remoulded strength increased from 0.1 kN/m^2 to 1.5 kN/m^2.

Quigley (1980) also provides a geochemical and mineralogical profile for Leda clay studies conducted on four boreholes around Hawkesbury, Ontario (Figure 2.8 (b)). Similar trends concerning sensitivity can be observed: high sensitivity values when salinity levels are low in the first 0-10 m and relatively low sensitivity numbers when the salinity increases with an increase in depth. Therefore, the salinity of the pore-water influences the remoulded shear strength and, ultimately, the sensitivity of the soil (Torrance 1979).

The pore-water salinity has a recognizable impact on the sensitivity of Leda clay. However, low pore-water salinity on its own only sometimes results in higher sensitivity of the soil. Several researchers suggest various factors contribute to the high sensitivity nature of Leda clay including Penner (1965), Moum et al. (1971), and Torrance (1975, 1979). Table 2.2 succinctly summarizes the factors producing high sensitivity in clayey sediments.

2.1.3.3.2 Weathering

The isostatic rebounding uplifted the land out of the sea, allowed the rivers to flow through the landscape, and exposed the Leda clay deposit to oxidative subaerial weathering, forming a surficial crust. The surface crust was created by "additions, removals, transformations, and translocation of soil materials" (Brady and Weil 2008; Torrance 2013).

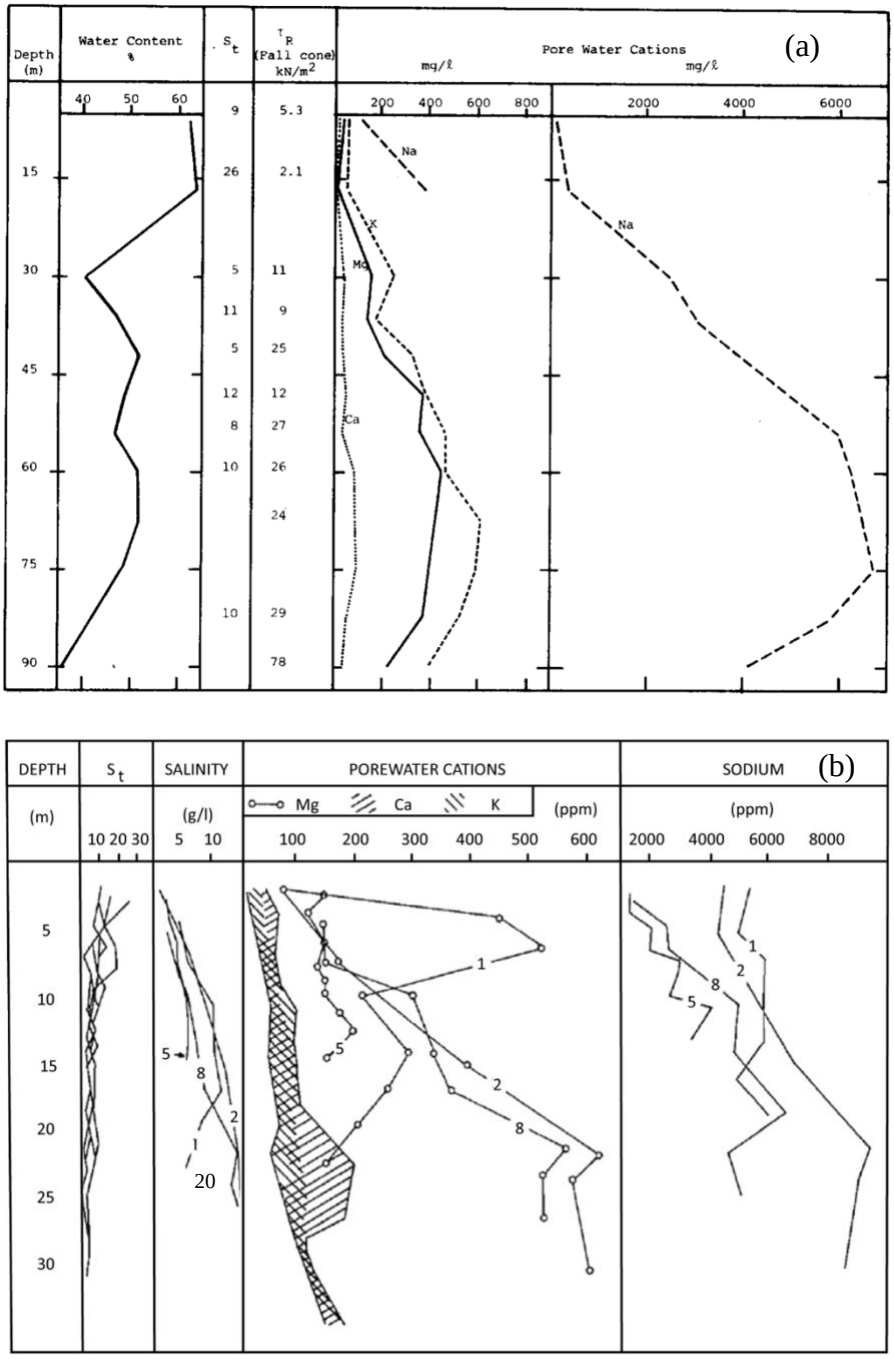

Figure 2.8 Sensitivity and pore-water cation chemistry vs depth for Leda clay: (a) Treadwell Site (b) Hawkesbury, Ontario (Torrance 1975; Quigley 1980)

Table 2.2 Factors producing high sensitivity in clayey sediments (Compiled after Quigley 1980; Torrance 1983)

Depositional	Post-depositional
Factors producing high undisturbed strength	
Flocculation[a,b] • Salinity[a] • Divalent cation adsorption[b] • High suspension concentration	Cementation bonds • Rapidly developed • Slowly developed Slow load increase • Time for cementation Other time-dependent processes • Diagenetic change
Factors producing low remoulded strength	
Material properties • Low-activity minerals dominate[a,b]	Decrease in liquid limit > decrease in water content • Leaching of salt[a] • Dispersants[b] Minimal consolidation

[a] Essential in marine clays
[b] Essential in freshwater clays

The minerals, such as carbonates and iron-bearing silicates, were weathered by soil acids and oxidation. The release of soluble Ca, K, and Mg ions influences the pore-water chemistry and cation balance changes, which may initiate downward leaching. Over time, Ca, K, and Mg produced by weathering in the overlying soil, and along rock joints are carried within the deposit by downward, upward, and lateral water flows. Eventually, the ions are transported to the cation exchange sites where they replace adsorbed Na, thus gradually increasing the remoulded strength and reducing the sensitivity (Moum et al. 1971; Torrance 2013).

Environmental factors caused a network of cracks to be formed near the weathered surface and slopes, forming nodular structures as referred to by Eden and Mitchell (1970). The crust thickness varies according to the local conditions; it has a greater thickness at the slope crest, and the thickness reduces towards the slope base. The direction of water flow in the soil controls the

variation in crust thickness. A thick crust is associated with a downward flow of water, whereas high artesian pressures will limit the depth of surface oxidative by upward and lateral water flow (Rankka et al. 2004; Torrance 2013).

2.1.4 Sensitivity of Leda Clay

The sensitivity of the soil is generally defined as the ratio of undisturbed shear strength over the remoulded shear strength with a dimensionless unit. Eq. 2.1 can be used to determine a numerical value that can be used to categorize the vulnerability of a particular sensitive clay sample (Skempton and Northey 1952). Quigley (1980) summarized some factors influencing these marine clay sediments' undisturbed and remoulded strengths. Torrance (1983) amends the summary by including a horizontal division distinguishing the requirements during sediment deposition and post-deposition (Table 2.2).

$$s_t = \frac{s_{u_{undisturbed}}}{s_{u_{remoulded}}} \qquad \textbf{Eq. (2-1)}$$

where; s_t= sensitivity, s_u = shear strength

Skempton and Northey (1952) were the earliest researchers who classifies clayey soils based on their sensitivity values (see Table 2.3).

Table 2.3 Sensitivity Scale after Skempton and Northey (1952)

Sensitivity	Classification
1	Insensitive clays
1-2	Clays of low sensitivity
2-4	Clays of medium sensitivity
4-8	Sensitive clays
>8	Extra sensitive clays
>16	Quick clays

Rosenqvist (1953) suggests the sensitivity classification in Table 2.4 for the Norwegian quick clays. The Scandinavian quick clays have very high sensitivities, and Skempton and Northey (1952) attempts to modify the classification to accommodate higher sensitivity values.

Table 2.4 Sensitivity Scale after Rosenqvist (1953)

Sensitivity	Classification
1	Insensitive clays
1-2	Slightly sensitive clays
2-4	Medium sensitive clays
4-8	Very sensitive clays
8-16	Slightly quick clays
16-32	Medium quick clays
32-64	Very quick clays
>64	Extra quick clays

Amendments were made to the Scandinavian sensitivity scale such that the classification ranges were reduced to three, as summarized in Table 2.5. A different concept of "rapidity number" was introduced by Soderblom (1974), which provided additional information regarding the work required to remould the soil. Torrance (1983) suggested that the rapidity number concept would be helpful, but the sensitivity measurement procedure would be complicated. Norwegian and Swedish geotechnical institutes prefer to use the scale shown in Table 2.5 (Rankka et al. 2004; Torrance 1983).

Table 2.5 Sensitivity scale after Rankka et al. (2004) and Norsk Geoteknisk Forening (1974)

Sensitivity	Classification
< 8	Low sensitivity
8-30	Medium high sensitivity
>30	High sensitivity*

* The term "quick clay" can be used when the remoulded shear strength is <0.5kPa and the remoulded soil behaves like a liquid

Holtz et al. (1981) reports the sensitivity (Table 2.6) scale used in the United States of America (USA) for sensitive clays. The scale resembles the original classification proposed by Skempton and Northey (1952). On the other hand, the Canadian Geotechnical Society (CGS) initially adopted a sensitivity scale (Table 2.7) similar to the Scandinavian scale (Table 2.5). The CFEM (2006) Errata recommended an updated sensitivity scale (Table 2.8) resembling the original classification Skempton and Northey provided (1952).

Table 2.6 Sensitivity scale after Holtz et al. (1981)

Sensitivity	Classification
2-4	Low sensitivity
4-8	Medium sensitivity
8-16	High sensitivity
>16	Quick clays

Table 2.7 Sensitivity scale after CFEM (2006)

Sensitivity	Classification
<10	Low sensitivity
10-40	Medium sensitivity
>40	High sensitivity

Table 2.8 Sensitivity scale after CFEM (2006) Errata

Sensitivity	Classification
< 2	Low sensitivity
2-4	Medium sensitivity
4-8	Sensitive
8-16	Extra (High) sensitivity
> 16	Quick

2.2 Stability of Slopes in the Ottawa Region

The landscape of the Ottawa region has been influenced by massive ancient landslides (Aylsworth et al. 2000), large modern landslides along large river valleys such as the South Nation River (SNR), and small modern landslides along small river valleys such as Green's Creek and Mud Creek.

The magnitude of the massive ancient landslides ranges from 10^6 to 10^8 m^3, while the modern landslides range from 10^3 to 10^6 m^3. Another apparent difference between the old and contemporary landslides is the mode of triggering slope failures. Earthquakes triggered the ancient landslides, while seismic activities have minimal influence on modern landslides. It can be argued that several modern landslides are triggered due to increasing precipitation levels associated with the climate change (Gadd 1976; Hugenholtz and Lacelle 2004).

The two groups of modern landslides differ in size, geotechnical setting, and characteristics of Leda clay. The small modern landslides typically occur in slopes with a thick layer of weathered Leda clay exposed to the surface. Although some landslides are categorized as flowslides and retrogressive slides, the landslides mainly occur in the weathered Leda clay layer and rarely extend down to the sensitive clay. On the other hand, the larger modern landslides along the South Nation River (SNR) occur where the slopes are topped by a thick sandy layer and underlain by interbedded silt and clay layers (Fransham and Gadd 1977; Hugenholtz and Lacelle 2004).

The top layer of slopes in Leda clay may consist of silts, sands, and weathered Leda clay crust. Figure 2.9 illustrates a simple soil stratigraphy that may be encountered in Leda clay slopes in the Ottawa region. The till layer suggested by Lefebvre (1986) may only sometimes be present in Leda clay slopes, and intact Leda clay may be found directly on the bedrock. The surficial and till layers are more permeable than the intact ones. The difference in permeability between intact

Leda clay and its boundary layers (i.e., surficial and till layers) can range from 100 to 1000 times. The increase in permeability may not necessarily be instantaneous, but a gradual increase from intact clay to boundary layers is expected.

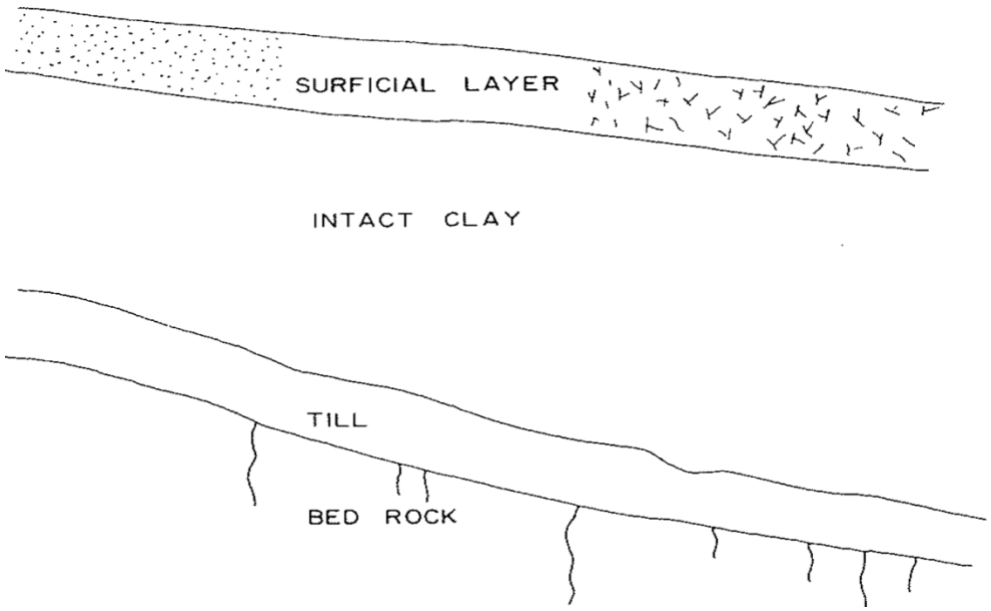

Figure 2.9 Typical stratigraphy in Leda clay slopes (Lefebvre 1986)

The general stratigraphy illustrated in Figure 2.9 can be observed in young valleys of the Ottawa region, such as Mud Creek. However, there are certain regions where the intact clay layer lies directly on the bedrock, which may bring disparities between the ground flow regimes in the slope model presented by Lefebvre (1986). Therefore, one must ensure proper site investigation studies before using the model to design geotechnical structures (Hugenholtz and Lacelle 2004).

2.2.1 Formation of valleys

Slope stability in the Ottawa region is greatly influenced by valley formation; landslides are essential to valley formation. The toe of the slope erodes due to a stream or river and, consequently, leads to a landslide. The landslide intensity contributes to the valley formation's

deepening and widening. Figure 2.10 displays the different phases of valley formation in Leda clay.

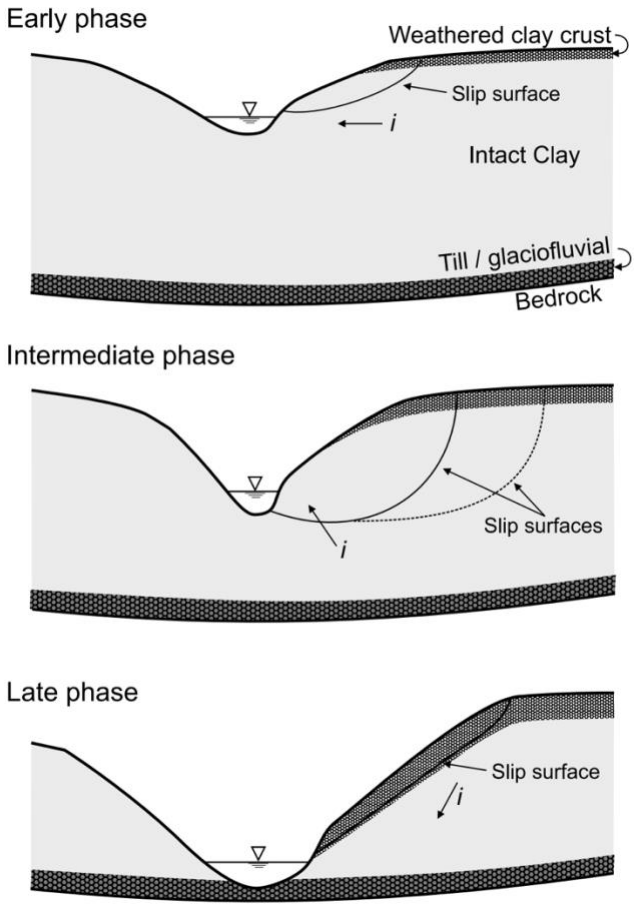

Figure 2.10 Simplified model of valley formation in Leda clay (Lefebvre 1986)

The early phase of the valley formation generally has its valley bed at the top of the intact clay layer. The groundwater flow in this phase is generally downwards in the weathered crust layer and upwards towards the valley bed in the intact layer. The intact Leda clay layer is highly resistant to erosion; therefore, small rotational slides are expected in the weathered crust.

In the intermediate phase, the valley deepens into the intact layer, where the groundwater gradient from the till layer influences the slope stability. The groundwater flow around the toe of the slope creates a favourable environment for deep landslides, which may also damage the

riverbed. Since the pore-water pressure changes are experienced within the intact layer, the vulnerability to large flowslides is increased due to sensitive Leda clay. The increase in porewater pressure would lead to the leaching of salt ions in Leda clay, thus diminishing the shear strength of the soil. Therefore, the penetration of porewater into the sensitive clay layer beneath the weathered crust can result in deep landslides in the form of large flowslides. Lefebvre (1986) believes that the intermediate phase generally experiences an increase in landslide activities and leads to fast-paced valley erosion.

In the final phase, the formation of the valley reaches the depth of the pervious till layer. This allows the groundwater to merge with the river and create a downward gradient in the slope. The intact clay should experience a strong downward gradient, which is helpful in terms of effective stress, shear strength and, ultimately, slope stability. As illustrated in Figure 2.10, the weathered crust will gradually form on the slope's surface in the final stage. The slope failures in this phase would generally be shallow failures within the weathered crust. Therefore, valley formation will continue along the banks until sufficient low-lying areas are developed along the river. Large flowslides may not be possible in this phase due to the inability of the shallow failures to penetrate the intact layer and increase the magnitude of slope failure.

2.2.2 Types of Landslides

Cruden (1991) defines a landslide as the “movement of a mass of rock, earth or debris down a slope.” In addition, (Varnes 1958) described a landslide as the “downward and outward movement of slope forming materials composed of natural rocks, soil, artificial fill or a combination of these materials.” These two definitions for landslides are simple yet elaborate at the same time. There are different ways of classifying different types of landslides.

The sensitive clays of Canada mainly give rise to single rotational slides, multiple retrogressive slides, translational progressive landslides, and spreads (Eden and Mitchell 1970; Tavenas F. 1984; Hugenholtz and Lacelle 2004; Locat 2012).

2.2.2.1 Rotational Slides

The single rotational slide failures are recognized by the rupture surface that tends to concave upwards. The mass of the ruptured surface tends to move along the concaved failure surface in the early phase, as shown in Figure 2.10. Single rotational slides are standard in slopes with weathered crust in Leda clay slopes. The water infiltration rate in the surface layer is much higher than the intact clay layer, and the permeability difference between the layers can be up to a magnitude of 2 to 3. Therefore, the slip surface is generally within the weathered crust, which shields the intact soil beneath (Ter-Stepanian 2000). The rotational slides are predominantly observed in the initial stages of various types of landslides. The magnitude of the failure is influenced by the weathered crust and intact clay layer arrangement in the slope profile (Ter-Stepanian 2000).

2.2.2.2 Retrogressive Slides – Flowslides

Flow slides occur on stable slopes after an initial slope slide. This categorizes it as a retrogressive type of landslide (Thakur and Dedago 2014). Issler et al. (2014) define flows as several retrogressive slides from an initial slide with remoulded debris flowing out of the crater. This forms an unstable scarp that may result in another slide with debris flowing out of the crater, creating another unstable scarp. The cycle continues until a stable scarp is formed (Figure 2.11).

There are in situ soil properties that encourage the occurrence of flowslides in Leda clay. Leda clays with a remoulded shear strength (Cr) of < 1 kPa may be vulnerable to flow slides with retrogression distance (L_R) >100m (Mitchell and Markell 1974). Demers et al. (2014) and Thakur

and Dedago (2014), through further studies, confirmed that Cr <1 kPa may be used to define the threshold for the occurrence of large landslides in the Canadian and Norwegian regions. Another critical requirement is the sensitive clay's liquidity index (IL). Sensitive clays with IL >1.2 are susceptible to multiple retrogressive slides (Leroueil et al. 1996). Thakur and Dedago (2014) point out that IL >1.2 may only be possible when the Cr <1; therefore, Cr can be used to determine the potential of a flowslide.

The failure surface does not necessarily occur along the riverbank; due to the retrogressive characteristics of flowslides, it creates multiple failures at a higher elevation, as seen in Figure 2.12(a) (Demers et al. 2014; Locat et al. 2017). Therefore, river erosion can provide initial conditions for the landslide to occur and propagate up the slope retrogressively.

2.2.2.3 Lateral Spreads

Spreads feature expansion and dislocation of the soil mass on the failure surface, which forms characteristic horsts and grabens (Figure 2.12 (c)) that drop in the remoulded layer in the shear zone (Cruden and Varnes 1996). Grabens can be identified with a flat horizontal or inclined top that may retain some vegetation. Horsts are blocks with pointed tips generally pointing upwards (Locat et al. 2017).

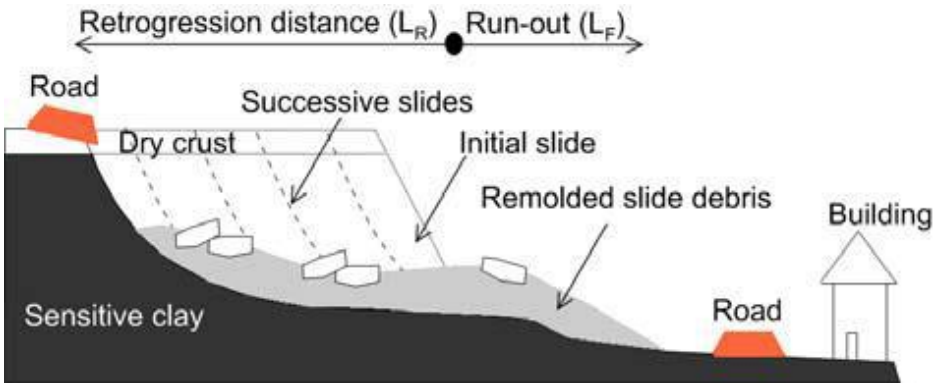

Figure 2.11 Flowslides in sensitive clay (Thakur and Dedago 2014)

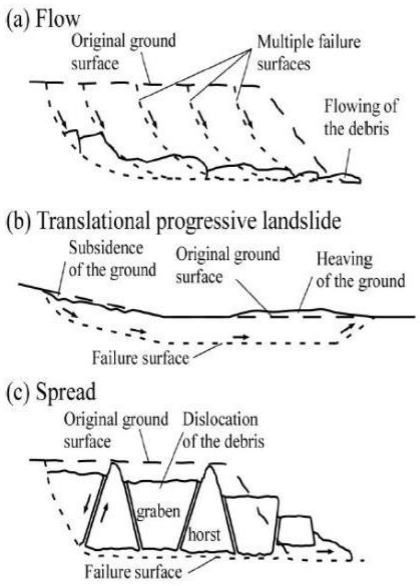

Figure 2.12 Common types of landslides in sensitive clay in Eastern Canada (Locat et al. 2017)

2.2.2.4 Translational Slides

Translational landslides occur due to increased shear force in the surface parallel to the ground surface. As a result, the soil mass is transported downhill (Cruden and Varnes 1996; Issler et al. 2014). Du et al. (2020) explain that with the combined effect of pressure from "trailing edge water" and the "uplift pressure of the potential sliding surface," the land mass moves on the surface layer as the layer deforms and fails. Figure 2.12 (b) shows subsidence of the ground at the head of the slope and a heaved surface at the toe. Overall, Petley et al. (2002) agree with the definitions above and state that translational landslides may occur due to a rise in multiple shear forces on the surface layer or sliding on an existing surface.

2.2.3 Mechanism of Landslides in Surficial Weathered Leda Clays

A weathered crust develops in the surficial layer of Leda clay slopes that can likely extend to depths of 10 m in the Ottawa region. The extent of the weathered crust can be identified by decreasing undrained shear strength values with depth to a minimum strength value as measured

by field vane shear tests, and then an increase with depth subsequently. The point of minimum strength value marks the extent of weathered crust (Eden and Crawford 1957; Eden 1975).

The weathered crust structure consists of closely spaced fissures or planes of weakness in the clay. When the weathered Leda clay undergoes shearing, it breaks down into small blocks and nodules. The mode of fracturing (i.e., either small blocks or nodules) depends on the type of shearing induced. Simple bending action yielded well defined surfaces of small blocks, while torsional shear yielded the nodular structure. The breaking down of the clay into nodules indicates the association of dilatant behaviour after failure. If the nodules of the fissured clay can be thoroughly remolded, it can be broken down to a quasi-liquified state that suggests that the weathered clay is sensitive and may have a natural water content greater than the liquid limit (Eden 1975).

Mitchell (1970) studies on the shear strength behaviour of weathered Leda clays revealed three distinct behaviours of Leda clay depending on the level of mean normal stress. The shear strength envelope depicted in Figure 2.13 illustrates the relationship between the maximum deviatoric stress (q) and the mean normal stresses (p), which range from 0 to 2.8 kg/cm^2 (or 0 to 274.6 kN/m^2) in a clay with a preconsolidation pressure of about 2 kg/cm^2 (or 196 kN/m^2). When the stress levels exceed the preconsolidation pressure, any increase in shear or deviatoric stress results in significant volume changes in the clay. The strength of the clay is directly proportional to the level of mean normal stress. The clay's structure is entirely disrupted, and this behavior is referred to as "work hardening plastic flow".

When the mean normal stress levels are below the preconsolidation pressure (ranging from 1.0 to 2.0 kg/cm^2 (or 98.07 to 196.14 kN/m^2) as shown in Figure 2.13, the shear strength remains almost unchanged. It is believed that the strength in this stress range largely relies on the bonds

between the clay particles. Mitchell (1970) demonstrated that the strength exhibits more anisotropic effects within this range compared to higher or lower stress ranges. Shear takes place with minimal volume change along clearly defined failure planes. The shear behavior in this range is typical of a brittle material (Eden 1975).

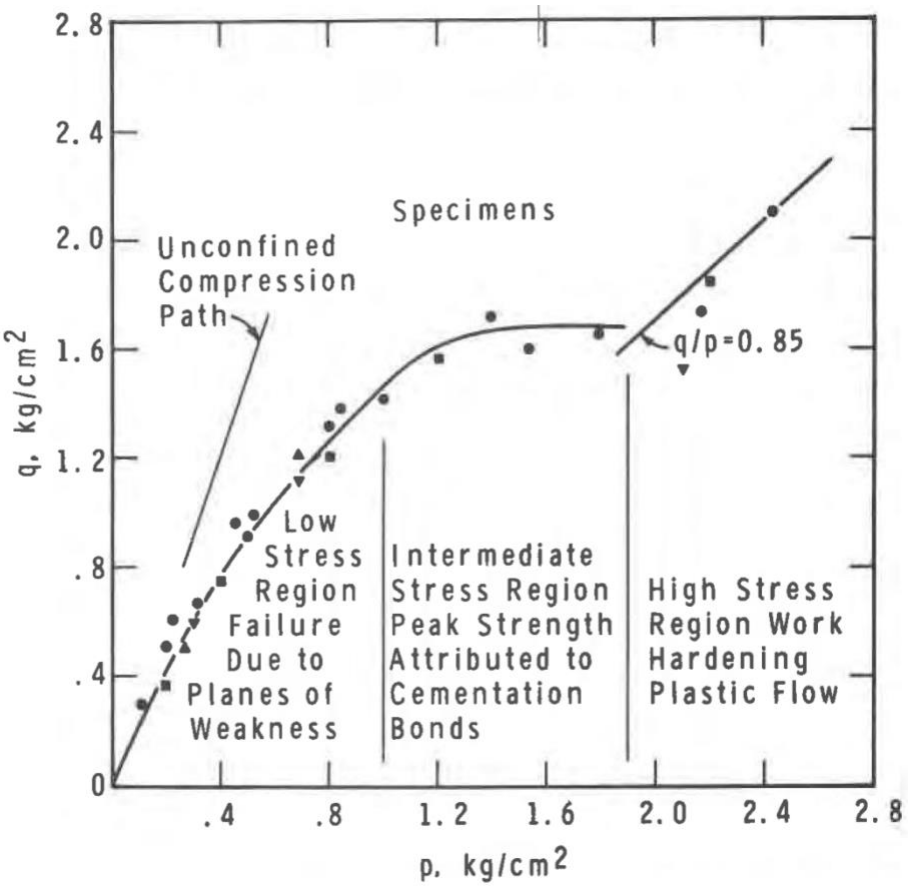

Figure 2.13 Mechanical strength of Leda clay (Mitchell 1970)

When the mean normal stress levels are low (ranging from 0 to 1.0 kg/cm^2 (or 0 to 98.07 kN/m^2) as shown in Figure 2.13, a distinct type of shear behavior is observed due to the existence of closely packed fissures. The clay behaves like a densely packed granular material, with one particle moving relative to another under shear strain. This movement results in a volume increase and draws water into the shear zone. This characteristic is crucial for maintaining slope stability,

as numerous landslides have occurred when there was an available source of free water on the ground surface, either from rain or melting snow (Eden 1975).

Therefore, the shear strength behavior of weathered Leda clay can be described in three different ways depending on the mean normal stress levels. Eden (1975) suggests that the behavior in the low stress range is most relevant for considerations of slope stability. This is because this behavior explains many of the features observed in landslides such as tension cracks, evidence of creep, and the correlation of landslide activity with water supply.

2.3 Mechanics of Unsaturated Soils

The weathered crust of Leda clay slopes displays characteristics of unsaturated soils. The soil properties of the weathered crust are most likely to differ from the soil properties of the intact layer, as discussed in section 2.2 above. Some varying properties include matric suction, permeability, and shear strength. The properties of unsaturated soils are mainly expressed as a function of the matric suction.

The matric suction, (u_a - u_w) can be defined as the difference between the atmospheric pore-air pressure, (u_a) and the pore-water pressure, (u_w). Since the matric suction is calculated with reference to the atmospheric pressure, matric suction can also be referred to as negative pore-water pressure. The environmental changes directly influence the negative pore-water pressures in Leda clay slopes. For example, during the spring, heavy rainfall and snow melt would increase water infiltration into the soil, increasing the pore-water pressure and reducing the soil's suction and shear strength. On the other hand, during the summer, evaporation reduces the soil's water content and increases the soil's negative pore-water pressure and shear strength.

There are numerous methods to measure the suction using direct or indirect methods. The direct methods measure the pore water energy to provide a suction value. In contrast, the indirect

methods determine different parameters (e.g., relative humidity, moisture content, conductivity, and resistivity) that may relate to soil suction and calibrate using known suction values (Catana 2006). The direct measurement techniques include tensiometers, pressure and suction plates, and pressure membranes, while the indirect measurement techniques include thermocouple psychrometers, filter paper, and thermal conductivity sensors.

2.3.1 Soil Water Characteristics Curve (SWCC)

. The SWCC is the relationship between the degree of saturation or water content (gravimetric or volumetric) and matric suction. It is used as a tool to understand, interpret, and predict the behavior of several unsaturated soil properties. Three distinctive zones can be identified from the drying SWCC as shown in Figure 2.13, that include the boundary effect, transition, and residual zones. In addition, two more characteristic features of the SWCC can be identified as air entry value (AEV) and residual suction value (RSV). The AEV and RSV can be estimated with reasonable accuracy using graphical construction or computational techniques from the SWCC (Vanapalli et al. 1996; Vanapalli et al. 1998).

Figure 2.14 shows SWCC for sandy, silty, Indian Head Till and clayey soil; the desaturation rate varies in soils with varying pore sizes. Sandy soil with large, interconnected pores tends to desaturate much faster than clayey soil; the desaturation rate decreases with finer particles. Therefore, soils with high plasticity can hold water at higher matric suction values, and the RSV tends to be much higher (Vanapalli 1994). Strong relationships have been established between the SWCC and the non-linear properties of unsaturated soils can also be extended to analyze Leda clay slopes. Such approaches are useful in alleviating the limitations of the time-consuming and expensive test procedures for determining soil properties (Vanapalli 1994; Catana 2006).

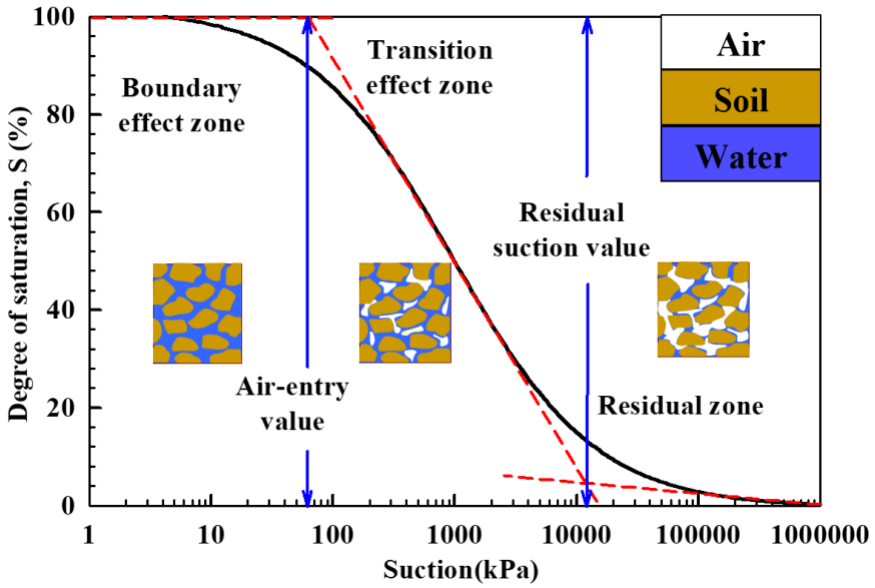

Figure 2.14 Three distinct zones of the SWCC (Vanapalli et al. 1996)

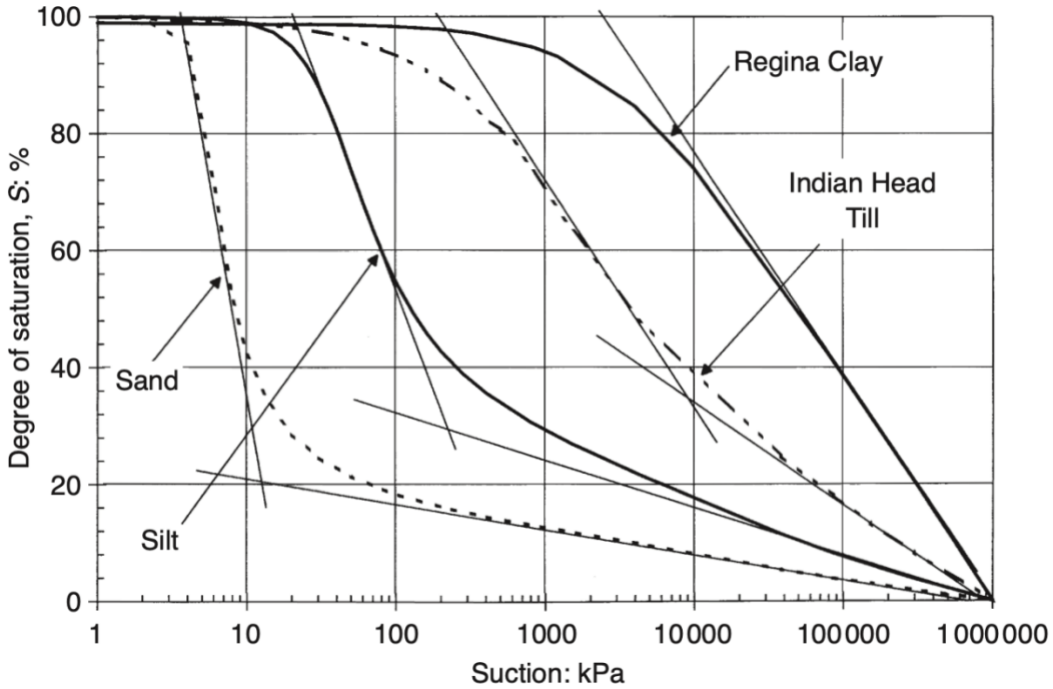

Figure 2.15 SWCC for soils with varying particle sizes (Vanapalli et al. 1999)

2.3.2 Estimation of Design Parameters using SWCC

Various researchers have proposed approaches in the literature for using the SWCC as a tool for analyzing volume change, seepage, and shear strength problems (e.g., van Genuchten 1980, Mualem 1986; Barbour 1998; Fredlund 2000; Catana 2006). Fredlund (2004) suggested a technique to estimate the unsaturated soil property functions using saturated soil properties, the SWCC, and an additional soil parameter (Eq. 2.2).

$$\text{Unsaturated Soil Property} = [\text{Saturated Soil Property}]\,f(\text{SWCC})^{\text{Soil parameter}} \qquad \text{Eq. (2-2)}$$

2.3.2.1 Estimating hydraulic conductivity using SWCC

Several mathematical techniques are proposed to estimate the hydraulic conductivity of unsaturated soils. These models can be divided into empirical and theoretical equations derived as statistical models (Mualem 1986). Empirical equations typically describe the relationship between the water coefficient of permeability and soil suction or volumetric water content. On the other hand, the theoretical models are further categorized into two (i.e., microscopic and macroscopic approaches): the statistical assumptions regarding pore distributions and the interpretation applied to the SWCC.

The macroscopic models generally provide an analytical, closed-form equation for unsaturated soil permeability function with the general form presented in Eq. 2.3 (Fredlund 2006). This equation is relatively similar to the technique and template proposed in Eq. 2.2 for estimating unsaturated soil properties such as coefficient of permeability. van Genuchten (1980) presented the closed-form permeability function (Eq. 2.4) by using the statistical permeability model by (Mualem 1976) and the SWCC curve fitting equation.

$$k_r = S_e^{\eta} \quad \textbf{Eq. (2-3)}$$

$$k_r(\psi) = \frac{\{1 - (\alpha\psi)^{n-1}[1 + (\alpha\psi)^n]^{-m}\}^2}{[1 + (\alpha\psi)^n]^{0.5}} \quad \textbf{Eq. (2-4)}$$

where; k_r = relative permeability (i.e., $k_r = \frac{k_{unsat}}{k_{saturated}}$); S_e= effective water degree of saturation (i.e., $S_e = \frac{\theta - \theta_r}{\theta_s - \theta_r}$, where θ_s and θ_r are volumetric saturated and residual water content, respectively); η = fitting constant; ψ = soil suction range; α, n, m = curve fitting parameters.

2.3.2.2 Shear strength of unsaturated soils

The shear strength of soil is an essential property in the design and analysis of geotechnical structures that include slopes, embankments, and foundations. In saturated soils, the shear strength can be expressed by Eq. 2.5. One of the methods of determining the shear strength of saturated soils involves plotting Mohr circles (i.e., failure conditions). A tangent line is plotted to denote the failure envelope, which may provide both the total and effective shear strength parameters (i.e. depending on the type of analyses, short-term or long-term stability); $c - \phi$ and $c' - \phi'$ respectively.

$$\tau = c' + (\sigma - u_w)\tan\phi' \quad \textbf{Eq. (2-5)}$$

where: τ = shear stress at failure, c' = effective soil cohesion, ϕ' = effective angle of friction.

Fredlund et al. (1978) extended the Mohr-Coulomb failure criterion of saturated soils to unsaturated soils. The linear shear strength equation (Eq. 2.6) was introduced for unsaturated soil mechanics, incorporating the theory of two independent stress state variables presented by Fredlund and Morgenstern (1977).

$$\tau_{unsat} = c' + (\sigma_n - u_a)\tan\phi' + (u_a - u_w)\tan\phi^b \quad \textbf{Eq. (2-6)}$$

where; τ_{unsat} = shear strength of unsaturated soil, c' = cohesion intercept when the two stress variables $(\sigma - u_a)$, and $(u_a - u_w)$ are zero (i.e., effective cohesion of a saturated soil), ϕ' = friction angle with respect to changes in $(\sigma_n - u_a)$ when $(u_a - u_w)$ is held constant (i.e., effective angle of shearing resistance for a saturated soil), ϕ^b = friction angle due to the contribution of $(u_a - u_w)$ when $(\sigma - u_a)$ is held constant (i.e., angle of shearing resistance with respect to matric suction), $(\sigma - u_a)$ = net normal stress on the plane of failure at failure, and $(u_a - u_w)$ = matric suction of the soil on the plane of failure.

Fredlund et al. (1978) suggested the linear planar failure envelope based on the shear strength data of unsaturated soils published in the literature mostly on fine-grained soils whose matric suction range is 0 kPa to 200 kPa. However, numerous studies after that have shown that for higher suction values (i.e., 0 to 500 kPa), the failure envelope for unsaturated soil concerning matric suction is generally non-linear (Figure 2.15 (b)). The shear strength of unsaturated soil typically increases linearly until the AEV, $\phi^b = \phi'$. As the soil transitions from saturated to unsaturated conditions, the shear strength increases non-linearly where ϕ^b becomes less than ϕ' (Fredlund 2006; Vanapalli 2010; Al-Khazaali 2019).

Since the experimental procedures of obtaining shear strength values of unsaturated soils are both time-consuming and expensive, several empirical models have been proposed in the literature for reasonably predicting the shear strength of the unsaturated soils. Vanapalli et al. (1996) proposed the semi-empirical model (Eq. 2.7 and 2.8) that allows the relationship between shear strength and SWCC; it enables the non-linear relationship between shear strength and suction to be predicted and modelled as shown in Figure 2.15 (b).

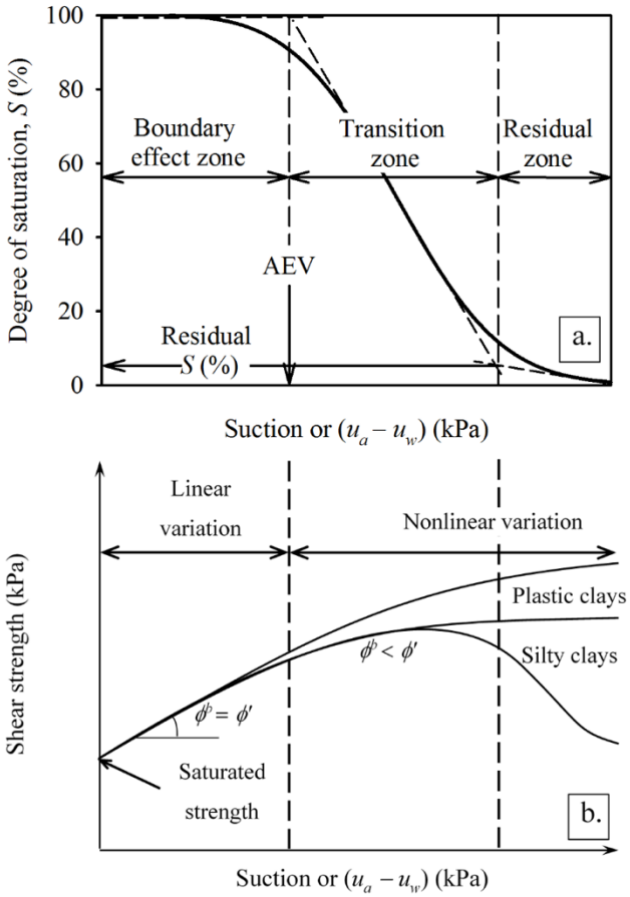

Figure 2.16 (a) SWCC displays different suction zones and, (b) the variation of shear strength of unsaturated soils in various zones of unsaturation of different soils (Vanapalli 2010; Al-Khazaali 2019)

$$\tau_{unsat} = c' + (\sigma_n - u_a)\tan\phi' + (u_a - u_w)\left[(\tan\phi')\left(\frac{\theta_w - \theta_r}{\theta_s - \theta_r}\right)\right] \qquad \textbf{Eq. (2-7)}$$

$$\tau_{unsat} = c' + (\sigma_n - u_a)\tan\phi' + (u_a - u_w)\left[(\tan\phi')\left(\frac{S - S_r}{100 - S_r}\right)\right] \qquad \textbf{Eq. (2-8)}$$

where; θ_w = volumetric water content, θ_r = residual volumetric water content, θ_s = saturated volumetric water content, S = degree of saturation, and S_r = residual degree of saturation.

Several curve fitting and estimating models have been developed over the years to determine respective SWCC, which can be further applied to solve complex engineering problems.

2.3.3 SWCC curve fitting equations

A mathematical equation is typically used to fit the SWCC data points measured from laboratory tests that is representative of the soil behavior over a large suction range. Several curve-fitting equations for SWCC are available in the literature, including Gardner (1958), Brooks and Corey (1964), Farrell and Larson (1972), van Genuchten (1980), Williams et al. (1983), and Fredlund and Xing (1994). From these equations and many others available in the literature, van Genutchen (1980) (Eq. 2.9) and Fredlund and Xing (1994) (Eq. 2.10 & Eq. 2.11) are commonly used. The equation presented by van Genutchen (1980) (Eq. 2.9) furnishes a comprehensive analytical expression for relative hydraulic conductivity. On the other hand, Fredlund and Xing (1994) model can be used for the variation of non-linear properties of unsaturated soils over the entire suction range from 0 to 10^6 kPa that represents fully saturated to dry conditions.

These curve-fitting equations can be helpful when there is a deficiency in data available to carry out preliminary design calculations in practice. There are also several SWCC estimation models that are derived from the information of soil properties (e.g. grain size distribution, Atterberg limits and dry density) that are easy to collect (Fredlund 1999; Vanapalli and Catana 2005).

In this thesis, Fredlund and Xing's (1994) equation is used for SWCC estimations (more details in Chapter 3). This research uses simple techniques available in the literature to estimate the SWCC and perform slope stability analysis using numerical modelling.

$$w(\psi) = \frac{w_s}{[1 + (a\psi)^n]^m} \qquad \textbf{Eq. (2-9)}$$

$$w(\psi) = C(\psi)\frac{w_s}{\left\{ln\left[e + \left(\frac{\psi}{a}\right)^n\right]\right\}^m} \quad \textbf{Eq. (2-10)}$$

$$C(\psi) = \left[1 - \frac{ln\left(1 + \frac{\psi}{\psi_r}\right)}{ln\left(1 + \frac{1,000,000}{\psi_r}\right)}\right] \quad \textbf{Eq. (2-11)}$$

$$w(\psi) = w_s\left[\frac{1}{\left\{ln\left[e + \left(\frac{\psi}{a}\right)^n\right]\right\}^m}\right]\left[1 - \frac{ln\left(1 + \frac{\psi}{\psi_r}\right)}{ln\left(1 + \frac{1,000,000}{\psi_r}\right)}\right] \quad \textbf{Eq. (2-12)}$$

where $w(\psi)$ is the water content at any soil suction, w_s is the saturated water content, ψ = soil matric suction, ψ_r is the soil suction at residual conditions, $a, n,$ and m are fitting soil parameters associated with the SWCC, e is the base of the natural logarithm, $C(\psi)$ is the correction factor.

2.4 Summary

The background information presented in this chapter will be used to serve as the foundation for numerical investigations in this study. As discussed, weathering phenomenon influences the hydro-mechanical soil properties of unsaturated Leda clay slopes of the surficial layer compared to the intact layer. Due to this reason, numerical investigations which cannot be modeled using a unimodal SWCC. Due to the influence of cracking, the weathered Leda clay exhibits a dual porosity structure, that has macropores (i.e., the cracks) and micropores (i.e., intra-aggregate pores), which can result in a bimodal SWCC (Qi and Vanapalli 2015). The weathering phenomenon does not affect the intact layer and maintains its structure with micropores. Therefore, a unimodal SWCC is typically sufficient to characterize the in-situ soil conditions. A simple

technique that can be used to estimate the bimodal SWCC for the weathered Leda clay crust is summarized in Chapter 3.

As discussed in Chapter 1, the weathered surficial layer is typically in an unsaturated condition; hence, saturated soil mechanics principles may not be sufficient to fully address the non-linearity of the soil mechanics problems (Fredlund 2015). Therefore, the background information for unsaturated soil mechanics principles will be used to facilitate the SWCC estimations in chapter 3 as well as the slope stability analyses in Chapter 4.

CHAPTER 3: A TECHNIQUE FOR THE ESTIMATION OF BIMODAL SWCC OF WEATHERED LEDA CLAYS

3.1 Introduction

The unsaturated soil property functions need to be obtained in a timely and cost-effective approach such that they can be used in the numerical investigations for modeling the behavior of unsaturated soils. There is a significant difference in the laboratory costs of determining unsaturated soil property functions compared to saturated soil properties. The cost of measuring an unsaturated permeability or shear strength function, may be approximately 10 times higher than that of saturated soil properties (Fredlund et al. 2002). The SWCC can be measured in the laboratory at a much lower cost than the unsaturated property functions, but the tests are complex and time-consuming. The SWCC is an essential tool for predicting hydro-mechanical unsaturated soil properties (for example, permeability and shear strength) using semi-empirical models (Li and Vanapalli 2022).

Rapid and reliable measurement, estimation, or prediction techniques are essential to minimize the costs of laboratory measurements of the SWCC and the unsaturated property functions. Such estimation or prediction techniques facilitate for implementing the state-of-the-art understanding of unsaturated soil mechanics principles in the design of numerous geotechnical structures (Fredlund et al. 2002; Li and Vanapalli 2022b).

The SWCC and saturated soil properties are typically used to estimate and predict the unsaturated soil property functions. Therefore, estimating SWCC using easy-to-obtain soil properties such as grain size distribution (GSD), porosity, and Atterberg limits reduces the time and cost of the measurements. Several estimation methods have been introduced by researchers

over the years using various soil properties to improve the accuracy of the estimations (Fredlund et al. 2002; Aubertin et al. 2003; Catana et al. 2006; Li and Vanapalli 2022b).

3.2 Background Information

As discussed in Chapter 2, Leda clay slopes tend to develop a weathered crust in the surficial layer due to environmental fluctuations from seasonal changes around the year. The weathered crust of the slope typically shows characteristics of unsaturated soil with the presence of soil, air, and water phases. To conduct numerical modelling for Leda clay slopes, it is essential to have a SWCC that represents both the weathered crust and the intact layer for a credible analysis.

3.2.1 Leda Clay SWCCs Available in the Literature

Limited data is available in the literature concerning the measurement, estimation, or prediction of SWCC for Leda clay. Table 3.1 summarizes available SWCC-measured data from the published literature for Leda Clay that was used in different research studies. The soil particle packing state is highlighted to recognize the need for more information concerning SWCC data related to the weathered crust of Leda clay.

Taha (2010) tested undisturbed Leda clay samples collected at a depth ranging from 8 to 12 m in the Ottawa area. Several soil properties of Leda clay were also measured, including the Atterberg limits, GSD, specific gravity, shear strength, void ratio, and salt concentration. The weathered crust in the Ottawa region typically ranges between 3 to 6 m; however, an average depth of 3 m is widely used as an approximation (Eden and Crawford 1957; Garga et al. 2006). The SWCC measured by Taha (2010) using WP4 Dewpoint Potentiometer represents the behavior of intact layer of Leda clay slopes. The intact layer is the soil layer where the weathering phenomenon is absent, and the soil properties are significantly different from that of the weathered crust. The

depth of the weathered crust as discussed earlier typically ranges from 0 to 3 m. In contrast, the intact layer depth depends on the soil stratigraphy, but generally, it is below 4 m and extends up to bedrock or glacial till, typically in the Ottawa region.

Table 3.1 Leda Clay SWCCs available in the Literature

#	Soil Particle Packing	Research Work	Reference
1	Intact Layer (8-12 m depth)	Interface shear behavior of sensitive marine clays	(Taha 2010)
2	Compacted Leda clay	Slope stability analysis	(Oh et al. 2014)
3	Compacted Leda clay + 5% Bentonite	Hydraulic performance of compacted clay liners	(Aldaeef and Rayhani 2015)
4	Compacted Leda clay (0-3m depth)	Resilient modulus and suction for compacted subgrade soils	(Han and Vanapalli 2016)

Oh et al. (2014) investigated the slope stability of Champlain Sea clay slopes extending unsaturated soil mechanics principles. The research aimed to propose an approach that could estimate the pore-pressure distribution profiles and subsequently determine the safety factors of the Champlain Sea clay slopes. The commercial finite element software Geo Studio, which includes SEEP/W and SLOPE/W software that conducts seepage and slope stability analysis, respectively, was used in the research. The finite element analysis, FEA, requires specific unsaturated soil properties to be defined, which includes the SWCC, hydraulic conductivity function, and the shear strength function. The SWCC in Oh et al. (2014) was measured using the pressure plate method on a statically compacted sample.

Aldaeef and Rayhani (2015) researched the hydraulic performance of compacted clay liners (CCL) under simulated daily thermal cycles. One of the test soils included Leda clay extracted from the Navan Landfill in the Ottawa region. The Leda clay was mixed with 5% bentonite to

understand its influence on the CCL in their research investigations. Therefore, the SWCC measured (using the axis-translation technique for a suction range of 0-1500 kPa and WP4 Dewpoint Potentiometer technique for higher suction values) in their study corresponds to the Leda clay and bentonite mixture.

Han and Vanapalli (2016) examined the relationship between the resilient modulus and suction for compacted subgrade soils, which included Leda clay found in the Ottawa region. The SWCC measured on Leda clay samples were obtained at a depth ranging from 0 to 3 m, which represents weathered crust. Furthermore, the samples were compacted to simulate the soil condition in the field; therefore, the SWCC curve measured (using the axis-translation technique and filter paper method) reflects a compacted sample using the weathered crust Leda clay sample.

In summary, the SWCCs available in the literature do not resemble the in-situ conditions of a weathered Leda clay crust. For this reason, there is a need to explore alternative methods to derive the SWCC that are representative for weathered Leda clay.

3.2.2 Estimation Models for SWCCs

The historical development of the SWCC in terms their understanding together with the estimation and prediction techniques have been presented by Barbour (1998). Zapata (1999) and Fredlund et al. (2002) list three categories of techniques primarily used in the literature to estimate the SWCC, which can be summarized below:

1. Statistical estimation of water content at specific matric suction values,
2. Estimation of conventional soil properties and fitting parameters of the SWCC using correlation based on regression analysis and
3. Physico-empirical models (pedotransfer functions) use the GSD curve to predict SWCC.

Li and Vanapalli (2022) provide a similar list of techniques but focus on models that specifically use GSD curves to estimate the SWCC. Zapata (1999) suggests that models that estimate SWCCs using the third technique provides a better estimation than the other two techniques. This research concerns Leda clay; therefore, physico-empirical models are used in the SWCC estimation.

A pedotransfer function (PTF) uses simple soil properties such as the GSD and generates a soil property function (Bouma 1989). There are numerous PTF models proposed in the literature that provide an estimate of SWCC using the GSD and simple soil properties (e.g., Arya and Paris 1981; Tyler and Wheatcraft 1989; Fredlund et al. 1997, 2002; Arya et al. 1999; Alves et al. 2020).

Arya and Paris (1981) developed the first widely recognized PTF model highlighting the similarities between the SWCC and the GSD. The model requires the GSD and the bulk density as input data to estimate the SWCC. The GSD is generally divided into fractions with mean pore radius to determine the volumetric water content (VWC), while the capillary theory was used to estimate the matric suction. The pore radius estimation resulted from assumptions of spherical and cylindrical soil particles and pores, respectively. There are several modifications made to improve the Arya and Paris (1981) model to demonstrate shape similarity between the SWCC and cumulative GSD for sandy soils (Haverkamp and Parlange 1986), modelling intra-aggregate pores (Gupta and Ewing 1989), and estimation of VWC and matric suction using statistical regression analysis (Fredlund et al. 2002).

Fredlund et al. (2002) enhanced the Arya and Paris (1981) model by implementing the results of parametric studies on numerous SWCC data sets in the original model. The Arya and Paris (1981) model did not consider the in-situ density in its estimation of the SWCC, while Fredlund et al. (2002) enhanced the model by using a packing arrangement factor to consider the in-situ porosity of a particular grain size.

Initially, the GSD best that best fits using the Fredlund et al. (1997) unimodal equation (i.e., Eq. 3.1) to generate a continuous GSD curve representing the entire range from coarse to fine-grained soils. The distribution data from the mathematical fit is then used in a new algorithm that predicts the SWCC. A combination of the capillary model and the particle size variation in the GSD is used to estimate the SWCC. Fredlund et al. (2002) describe the new technique using a series of theorems:

(i) A soil with entirely uniform and homogeneous particle size has a unique drying SWCC,

(ii) The air-entry value (AEV) for each uniform and homogeneous particle size collection can be estimated using the capillary model to an acceptable accuracy and

(iii) The SWCC for soils with numerous particle sizes can be derived by summating individual particle sizes SWCCs.

$$P_p(d) = \frac{1}{ln\left[\exp(1) + \left(\frac{a_{gr}}{d}\right)^{n_{gr}}\right]^{m_{gr}}} \left\{1 - \left[\frac{\ln\left(1 + \frac{d_r}{d}\right)}{\ln\left(1 + \frac{d_r}{d_m}\right)}\right]^7\right\} \qquad \textbf{Eq. (3-1)}$$

where a_{gr} is a parameter related to the initial breaking point of the curve; n_{gr} is a parameter related to the steepest slope of the curve; m_{gr} is a parameter associated with the shape of the fines portion of the curve; d_r is a parameter related to the number of fines in the soil; d is the diameter of any particle size under consideration; and d_m is the diameter of the minimum allowable size particle.

The Fredlund and Xing (1994) equation (Eq. 2.12) is extended to model the estimated SWCC due to its capacity to fit the entire range of matric suction. The PTF was trained to determine the range of acceptable values for the packing arrangement (porosity) to estimate the SWCC. Overall, the SWCC estimation for sands and silts was better in comparison to finer particles like clays, which provide reasonable results. The packing arrangement of the particles has a more significant

influence on much finer particles, and Fredlund et al. (2002) suggested that more data sets need to be used to train the model.

3.3 Data Collection

As per the discussions in the earlier sections, information about the SWCC is required for rational numerical analysis on the stability of Leda clay slopes in the Ottawa region. For achieving this objective, simple techniques are used for the estimation of SWCC based on the soil properties that correspond to the weathered crust of Leda clay.

Several geotechnical reports are available from government resources documenting numerous geotechnical projects in the Ottawa region. These geotechnical reports contain borehole logs which provide useful soil properties, including Atterberg limits, groundwater level, soil profile, N-value, and undrained shear strength (Field and Laboratory Vane Shear tests). In addition, some of these geotechnical reports include GSD curves, e-log p curves (i.e., consolidation curve data), and relevant project drawings that are beneficial in understanding the soil properties at different locations in Ottawa region.

3.3.1 Data Resources

The geotechnical reports of City of Ottawa (2023) and MTO (2022) are valuable resources that can provide reliable soil properties information within the Ottawa region. The procedure to collect relevant data from these two sources is briefly detailed in the subsequent sections.

3.3.1.1 Ministry of Transportation Ontario (MTO)

MTO (2022) provides an interactive mapping tool that contains a library of foundation engineering reports (i.e., publicly accessible reports) submitted to the MTO over the years. Figure

3.1 illustrates the MTO Foundation Library's webpage, which can extract geotechnical reports from different parts of Ontario.

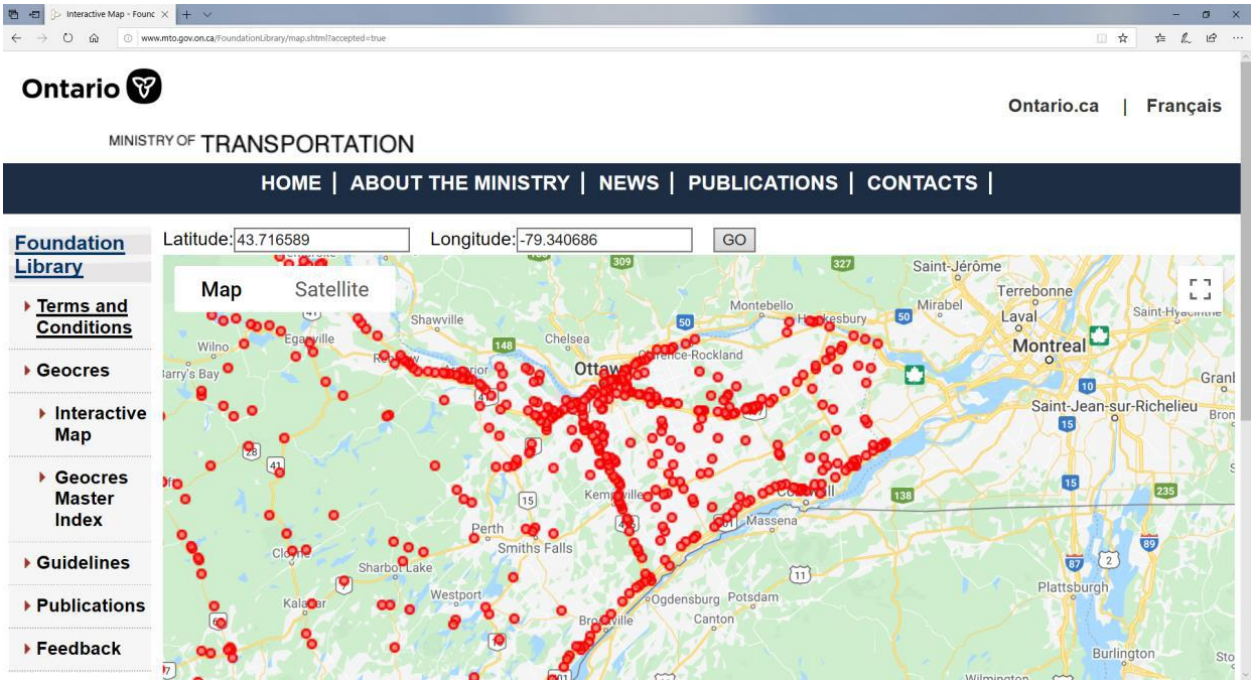

Figure 3.1 MTO Foundation Library (MTO 2022)

The research mainly focuses on Leda clay, typically predominant in southeastern Ontario or the Ottawa region. Therefore, using the interactive mapping tool together with surficial geology maps published by the Ontario government simplifies the task of browsing Leda clay geotechnical reports. Surficial geology maps (Ministry of Mines 2023) can be obtained from an application by the Ontario Ministry of Mines, which are superimposed in the Google Earth Application.

Figure 3.2 displays a screenshot of surficial geology data superimposed on Google Earth for South-Eastern Ontario. The light-blue-coloured polygons represent Leda clay in the region. Therefore, Figure 3.1 and Figure 3.2 can be simultaneously referenced to extract geotechnical reports corresponding to Leda clay soil in the Ottawa region efficiently.

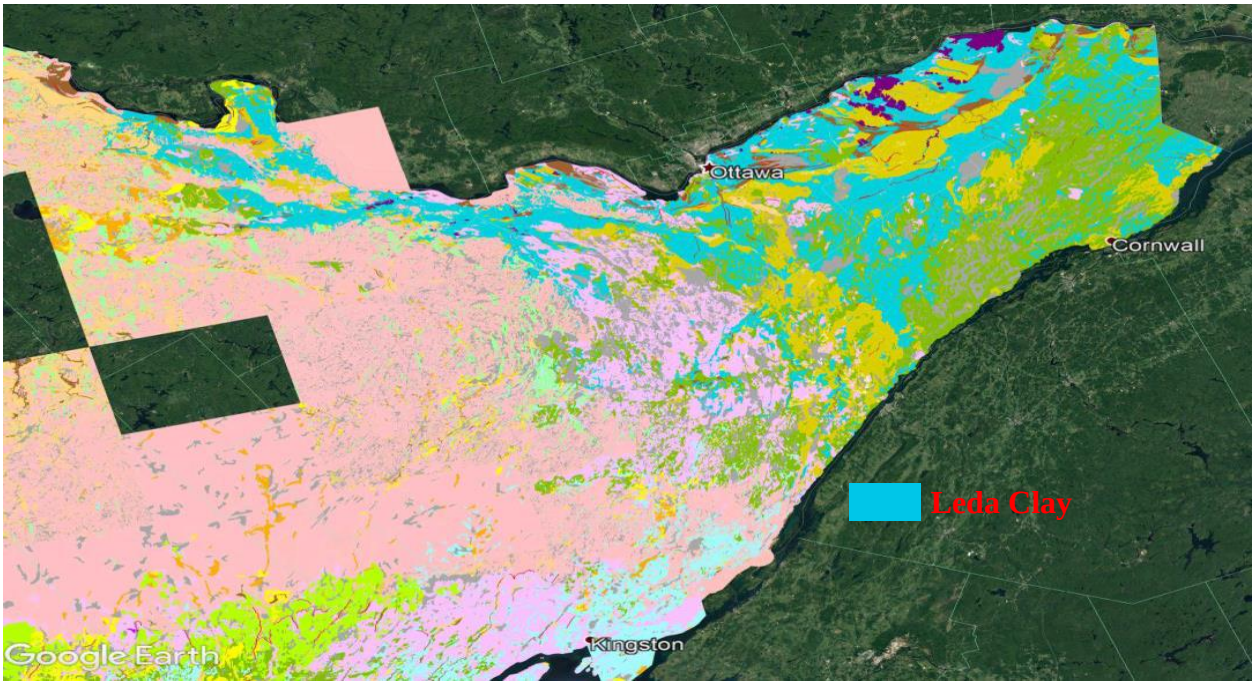

Figure 3.2 Surficial geology data superimposed on Google Earth

3.3.1.2 City of Ottawa

The City of Ottawa has an interactive webpage with numerous development projects that require public consultation (City of Ottawa 2023). The categories of projects compelling public consultation include:

1. Site Plan Control,
2. Official Plan Amendment,
3. Zoning By-law Amendment,
4. Demolition Control,
5. Plan of Subdivision and,
6. Plan of Condominium.

The development application search (DAS) tool (Figure 3.3) allows the City of Ottawa's residents to review the progress of development projects and provide feedback. The surficial soil

data and the DAS tool can be used simultaneously used to gather geotechnical properties of Leda clay soils.

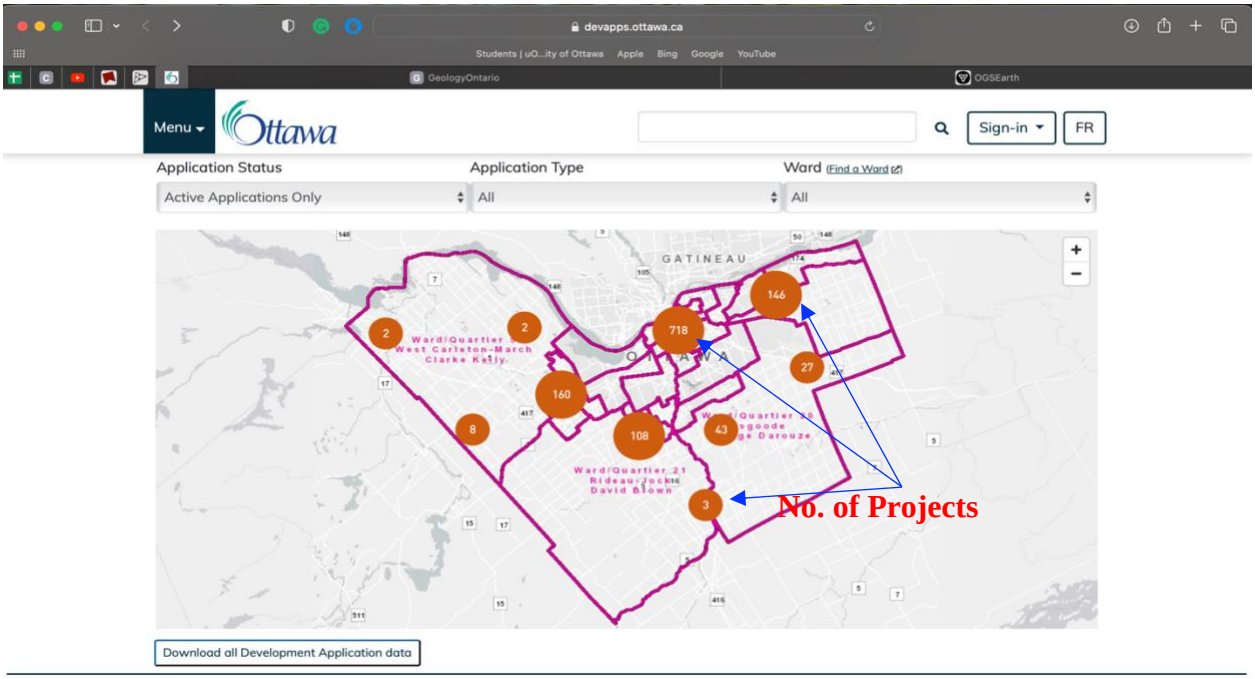

Figure 3.3 Development Application Search Tool (City of Ottawa 2023)

Other resources may not be open source, such as academic research projects and industrial projects by the private sector. For example, Table 3.1 consists of data collected from the literature. Industrial projects by private companies do not publish their geotechnical site investigation reports publicly. However, in such cases, the firm's geotechnical section or department can use its database internally for SWCC estimation and used them in the design of geotechnical structures extending unsaturated soil mechanics principles.

3.3.2 Weathered Leda Clay Soil Properties Collection

In the next step, continuing the chronology from the previous section, each site investigation report is then browsed to check if the borehole logs:

1. Contain weathered Leda clay at depths ranging from 0 to 3 m,

2. Contain data related to Atterberg limits,
3. Contain data related to GSD and,
4. Contains data related to the oedometer test (Consolidation – e-log curves).

Table 3.2 shows the data collected for 18 samples from borehole logs and site investigation reports from various locations across the Ottawa region. The GSD curves for all but three samples (i.e., No. 15, 16, 17) were retrieved from the site investigation reports. Similarly, the initial void ratio and Atterberg limits data were obtained from browsing e-log curves determined for Leda clay within the weathered crust. Figure 3.4 illustrates the locations of the site investigation reports and borehole logs referenced to collect the weathered Leda clay soil properties from the MTO Foundation Library.

The weathered Leda clay crust layer can be identified from a borehole log by reviewing several soil properties that distinguishes weathered clay from intact clay. Some of the criteria that can be used to identify weathered crust layer include variation of undrained shear strength, soil layer description, soil layer depth (i.e., 3 m for weathered Leda clay) and Atterberg limits. For example, the extent of the weathered crust in Leda clay can be quantified by analyzing the variations in undrained shear strength measurements from field vane shear tests. Typically, the undrained shear strength exhibits an initial decrease with increasing depth, reaching a minimum strength value, beyond which it begins to increase. This point of minimum strength serves as an indicator of the depth extent of the weathered crust (Eden 1975).

The accuracy and precision of inferencing data from borehole logs can be difficult when the reports are old and scanned copies are of poor quality. Therefore, understanding of the structure and process of generating the borehole log can be useful to extract information for various soil parameters with reasonable accuracy and precision.

Figure 3.4 Location of collected data from site investigation reports from MTO Foundation Library

3.4 Weathered Leda Clay SWCC Estimation Analysis

Section 3.2.2 summarized background information on some of the SWCC estimation models available in the literature. The literature summary highlights that there is limited data for undisturbed weathered Leda clay SWCC. Therefore, this research aims to propose a technique for the estimation of the bi-modal SWCC that can closely represent the in-situ weathered crust and intact soil layer in Leda clay slopes.

3.4.1 Estimation using Fredlund et al. (2002) Model

The procedure for Fredlund et al. (2002) model for SWCC estimation has been summarized in section 3.2.2. The input soil properties include GSD curves, unit weight of water, degree of saturation, dry unit weight, specific gravity of Leda clay, void ratio, and water content. It is essential to recognize that only specific soil parameters must be known, as others can be calculated using mass-volume phase relationships (Eq. 3.2 to 3.4).

$$G_s * w = S * e \qquad \textbf{Eq. (3-2)}$$

$$\gamma_{bulk} = \frac{G_s + Se}{1 + e} * \gamma_w \qquad \textbf{Eq. (3-3)}$$

$$\gamma_{dry} = \frac{G_s}{1 + e} * \gamma_w = \frac{\gamma_{bulk}}{1 + w} \qquad \textbf{Eq. (3-4)}$$

where G_s is the specific gravity of the soil, w is the water content, S is the degree of saturation, e is the void ratio, γ_{bulk} is the bulk unit weight of the soil, γ_w is the unit weight of water and, γ_{dry} is the dry unit weight of the soil.

As a first step, the unimodal GSD fitting equation (Eq. 3.1) is used to fit the GSD to determine the fitting parameters (i.e., a_{gr}, n_{gr}, and m_{gr}) to be used further in the estimation model. The soil properties representing a particular dataset (for example, No. 1 in Table 3.2) are then input into the model. The specific gravity, G_s for Leda clay can range between 2.70 and 2.80 (Leroueil 1997; Taha 2011; Taha and Fall 2014). In this research, G_s value of 2.7 has been assumed during the SWCC estimation. The G_s tends to increase with depth due to the increasing amount of rock flour in Leda clay from bedrock erosion (Rasmussen 2012; Nader 2014). Therefore, a value of 2.7 is reasonable for weathered Leda clay, typically found at shallow depths. In addition, a general assumption of 9.81 kN/m^3 is used for γ_w. The distribution data from the fitted GSD curve (see Appendix 1) is then used with a new algorithm to predict the SWCC. The algorithm utilizes the combination of the capillary model and particle size data from the GSD curve to estimate the SWCC. As discussed in section 3.2.2, the SWCC is estimated by summating (i.e., superimposing multiple SWCCs) the individual SWCCs derived from multiple particle sizes (i.e., each particle size is used to predict a SWCC) observed in the fitted GSD curve.

Table 3.2 Soil properties of weathered Leda clay collected from the Ottawa region

NO.	GEOCRES	Latitude	Longitude	Depth (m)	*w* (%)	e_0	LL (%)	PL (%)
1	31G00-059	45.340665	-74.906303	1.58	50.00	1.521	41.30	19.40
2	31G05-090	45.384658	-75.585005	1.78	58.00	1.702	63.00	23.00
3	31G00-240	45.338512	-75.473156	2.04	74.00	1.890	80.00	21.00
4	31G05-089	45.392850	-75.592395	2.10	56.00	1.472	64.00	25.00
5	31G05-088	45.384813	-75.584774	2.20	58.00	1.750	66.00	26.00
6	31G00-240	45.338512	-75.473156	2.34	74.00	1.955	70.00	23.00
7	31G00-240	45.338512	-75.473156	2.37	86.00	2.340	70.00	21.00
8	31G00-227	45.303810	-75.075760	2.60	49.90	1.465	54.00	20.00
9	31G00-227	45.303810	-75.075760	2.60	80.00	2.265	66.00	23.00
10	31G05-090	45.384658	-75.585005	2.70	60.00	1.058	52.00	24.00
11	31G00-227	45.303810	-75.075760	2.70	60.30	1.620	49.00	27.00
12	31G05-092	45.398661	-75.583259	2.85	52.00	1.604	67.00	25.00
13	31G05-079	45.389771	-75.590155	2.90	52.00	1.680	62.00	25.00
14	31G05-089	45.392850	-75.592395	2.90	50.50	1.398	53.00	24.00
15	31G05-087	45.396746	-75.596664	2.90	52.00	1.388	41.00	24.00
16	31G00-034	45.362308	-75.485387	3.08	87.50	2.340	77.00	26.00
17	31G05-143	45.494315	-75.484069	3.10	66.00	1.804	64.00	24.00
18	31G00-240	45.338512	-75.473156	3.12	80.00	2.140	73.00	31.00

where, ***w* (%)**, e_0, **LL (%)** and **PL (%)** represent **water content**, **initial void ratio**, **liquid limit,** and **plastic limit**, respectively. **GEOCRES** column references the MTO Foundation library database for individual site investigation reports.

There are three ways of representing SWCCs: gravimetric water content SWCC (*w*-SWCC), volumetric water content SWCC (θ-SWCC) and degree of saturation SWCC (*S*-SWCC). The information (i.e., AEV or RSV) provided by each of the SWCC may be different (Fredlund et al. 2018). If the soil does not undergo volume change with an increase in suction, then *w*-SWCC can be relied upon to extract information such as air entry value (AEV). However, Leda clay undergoes volume change behaviour, and *w*-SWCC cannot provide the true AEV. θ-SWCC or *S*-SWCC should be used to estimate the representative AEV of Leda clay; most preferably, *S*-SWCC should be referenced for AEV. The AEV measured from *S*-SWCC can be significantly higher than that from *w*-SWCC.

Figure 3.5 and Figure 3.6 display the predicted volumetric water content SWCC (θ-SWCC) and degree of saturation SWCC (*S*-SWCC), respectively. There are 15 SWCCs predicted using the fitted GSD curves shown in Appendix A and soil properties in Table 3.2. There are 3 datasets (i.e., #15, #16 and #17) whose GSD curves were not available in the reports. For this reason, they were not used for SWCC prediction using the Fredlund et al. (2002) model.

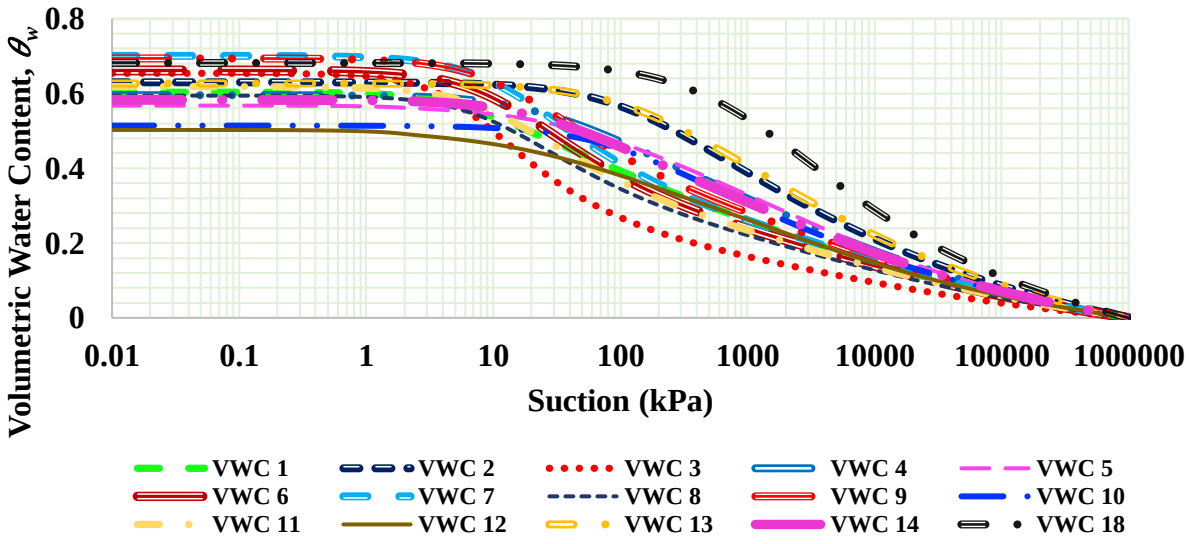

Figure 3.5 θ-SWCCs estimated using the Fredlund et al. (2002) model

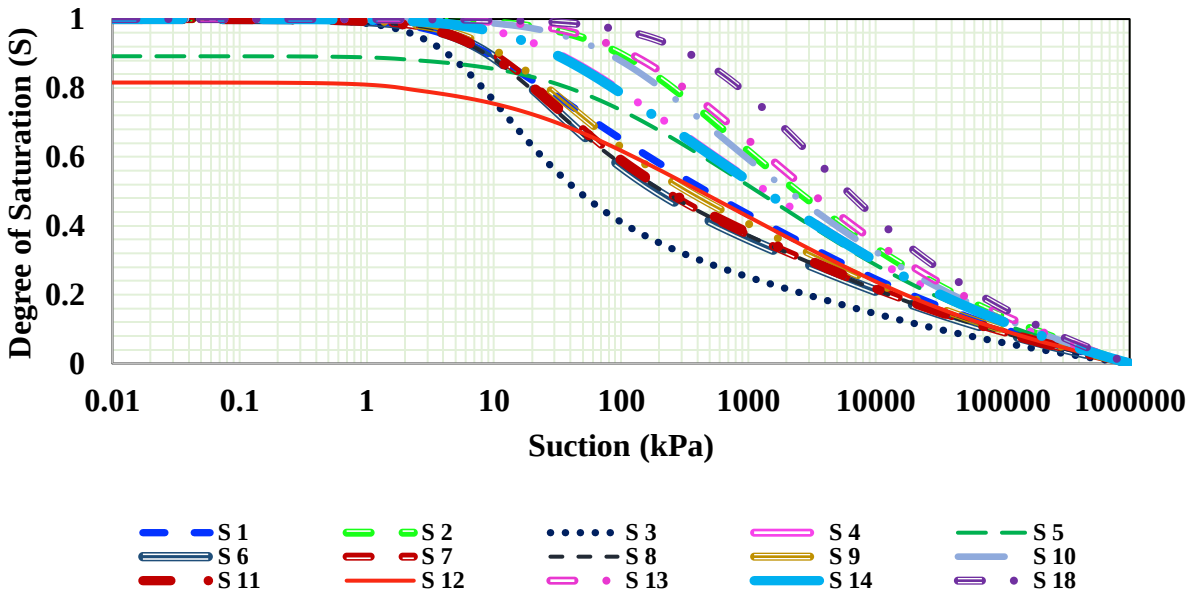

Figure 3.6 S-SWCCs estimated using Fredlund et al. (2002) model

Some anomalous curves can be neglected to achieve a reasonable range of AEVs. Figure 3.7 and Figure 3.8 illustrate the modified estimated θ-SWCC and *S*-SWCC, respectively. The anomalous curves were removed from the plot to improve the accuracy of the AEV estimation. The Fredlund et al. (2002) model typically predicts θ-SWCCs as output, which are useful as input parameters for numerical modelling software. However, at this estimation stage, *S*-SWCC provides essential information on the true AEV for Leda clay, as discussed above. Therefore, *S*-SWCC is used to approximate the range of AEV for the weathered crust of Leda clay. According to Figure 3.8, the estimated AEV (determined using the Vanapalli et al. (1998) construction method) ranges from 5 kPa to 80 kPa. An approximation for the median AEV can be presumed as 15 kPa.

The verification for using Fredlund et al.'s (2002) model cannot be conducted diligently due to the lack of measured data available for in situ weathered Leda clay SWCC. However, an attempt is made to verify using the intact layer SWCC measured by Taha (2010) using WP4

potentiometer. The GSD curve and soil properties presented by Taha (2010) are used in the model to estimate the SWCC. Figure 3.9 compares measured and predicted θ-SWCCs for Taha (2010) using Fredlund et al. (2002) model. The reported AEV value by Taha (2010) is approximately 350 to 400 kPa, while the model approximates the AEV between 250 to 300 kPa.

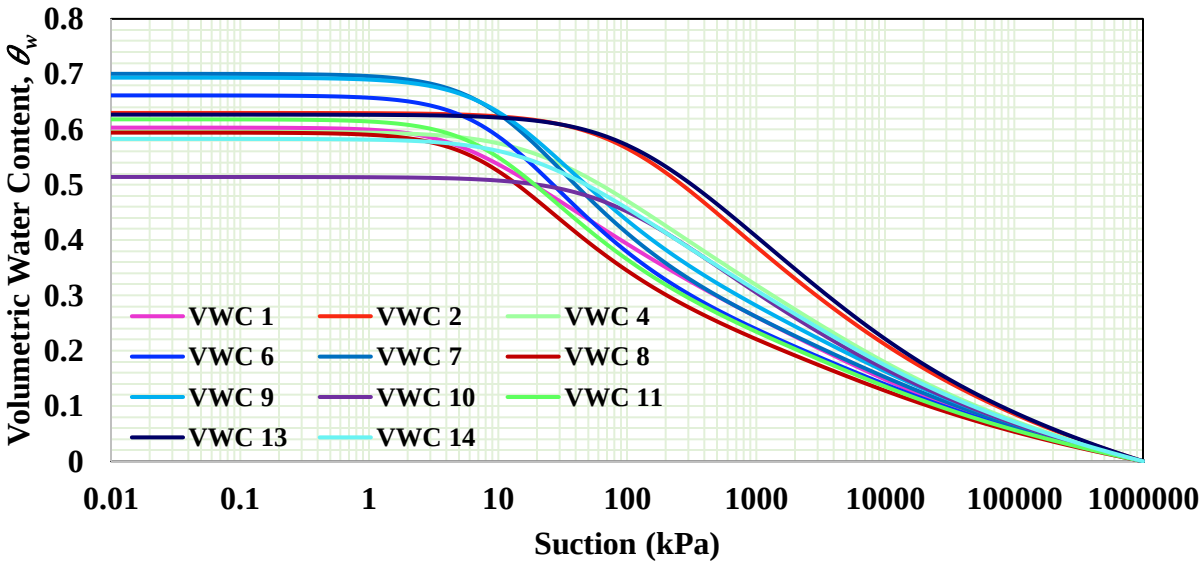

Figure 3.7 Modified θ-SWCCs estimated using the Fredlund et al. (2002) model

The comparison of the two SWCCs shows that the measured and predicted SWCCs do not match closely. However, it should be noted that Taha (2010) did not measure the SWCC in the low suction range (i.e., 0 kPa to 800 kPa) using the conventional axis-translation technique but is mainly based on the WP4 suction measurements, which is reliable for high suction range (i.e., 1000 kPa to 300000 kPa) compared to low suction range (Ebrahimi-Birang and Fredlund 2016). However, due to the lack of in-situ measured SWCC data for Leda clays, the Taha (2010) SWCC is used for providing comparisons in this study.

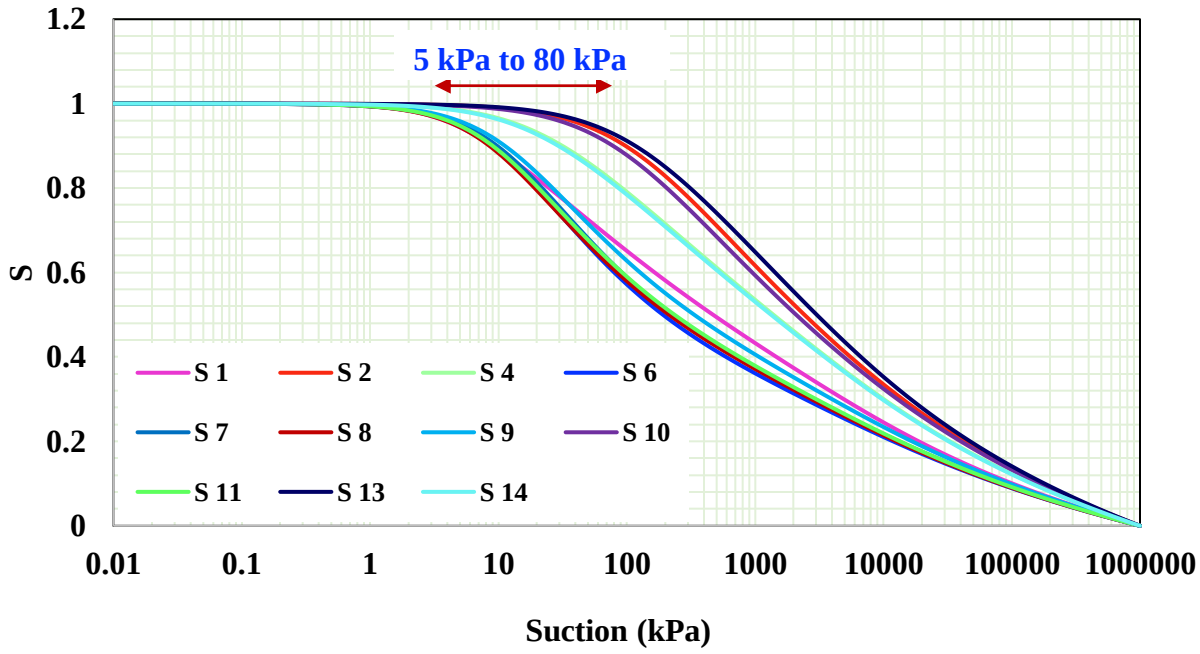

Figure 3.8 Modified S-SWCCs estimated using Fredlund et al. (2002) model

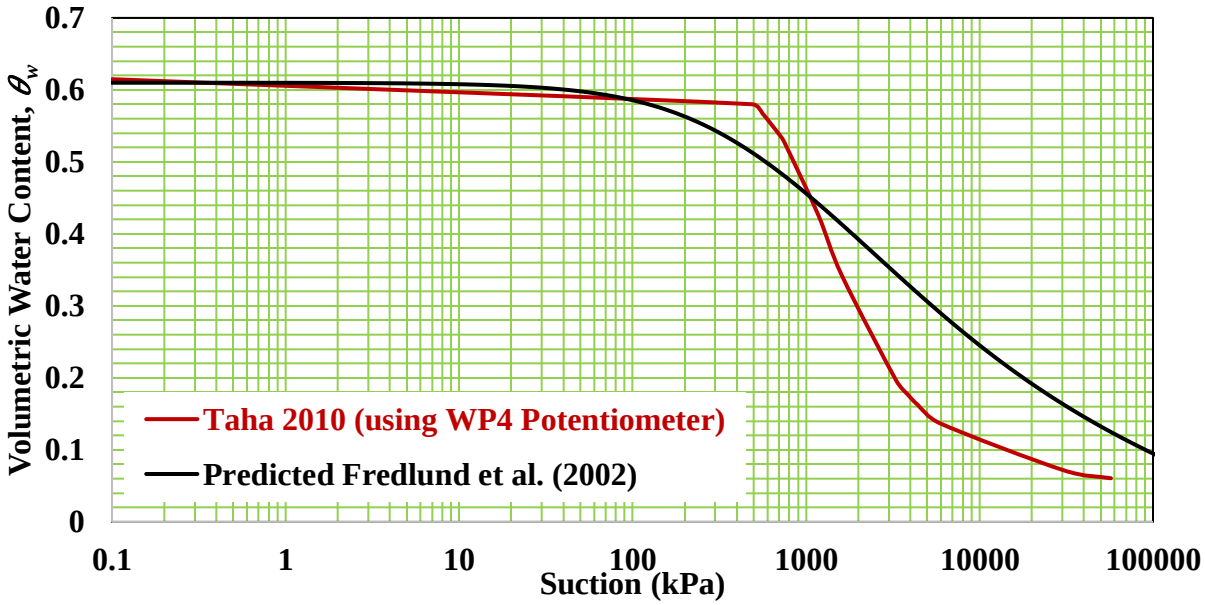

Figure 3.9 Predicted θ-SWCC using Fredlund et al. (2002) model for intact layer SWCC by Taha (2010)

3.4.2 Estimation using Aubertin et al. (2003) model

The model proposed by Aubertin et al. (2003) is a PTF based on adaptations of the model presented by Kovacs (1981). In contrast with Fredlund et al. (2002), this model does not use the entire GSD to estimate the SWCC. The diameter corresponding to 10% passing (D_{10}) and the coefficient of uniformity (C_U) are used to predict capillary retention in coarse-grained soils.

On the other hand, the model uses the information of liquid limit, LL to account for the retention properties of fine-grained soils. The model provided a reasonable variance between the measured and predicted SWCC for various materials (coarse and fine-grained materials). Therefore, the Aubertin et al. (2003) model provides a different means of relating the GSD and SWCC for prediction analysis (Alves et al. 2020). In the present research, this model is extended to estimate the SWCC for weathered Leda clay. A detailed breakdown of the model's procedures is available from Aubertin et al. (2003).

Figure 3.10 and Figure 3.11 displays plots of estimated θ-SWCC and S-SWCC using the Aubertin et al. (2003) model. The model provides an output with θ-SWCC, and S-SWCC is generally derived to improve the accuracy of the AEV measurement. The data used as input in this model can be referenced from Table 3.2. The approximate range for the AEV (determined using the Vanapalli et al. (1996) construction method) is 18 kPa to 40 kPa (Figure 3.11). In addition, similar to results summarized in Figure 3.9 using the Fredlund et al. (2002) model, Figure 3.12 also shows that there are differences between measured and predicted SWCC using the Aubertin et al. (2003) model.

One of the limitations of the Aubertin et al. (2003) model is that the data used to train and verify the model involved fine-grained soils that do not resemble the soil properties of Leda clay. For example, a significant disparity is seen in the void ratio values for Leda clay that has an initial

void ratio above 1.5. Such a trend in results may be associated with the Aubertin et al. (2003) model which focussed on soils with void ratios that are typically below 1.

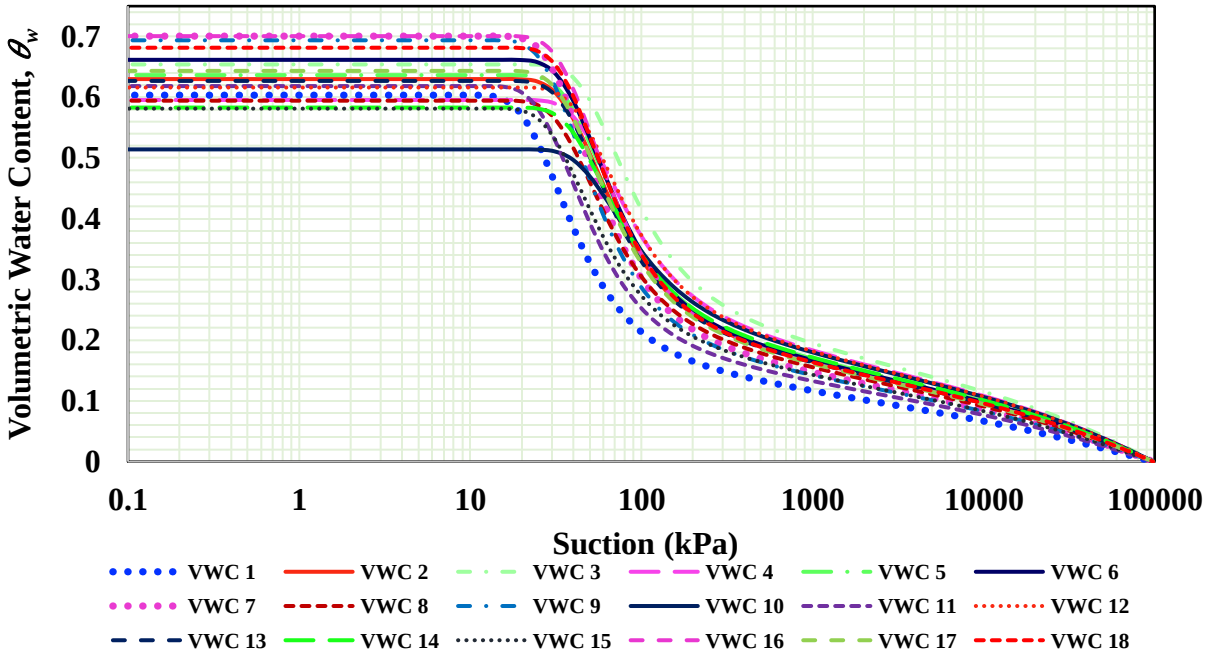

Figure 3.10 θ-SWCCs estimated using Aubertin et al. (2003) model

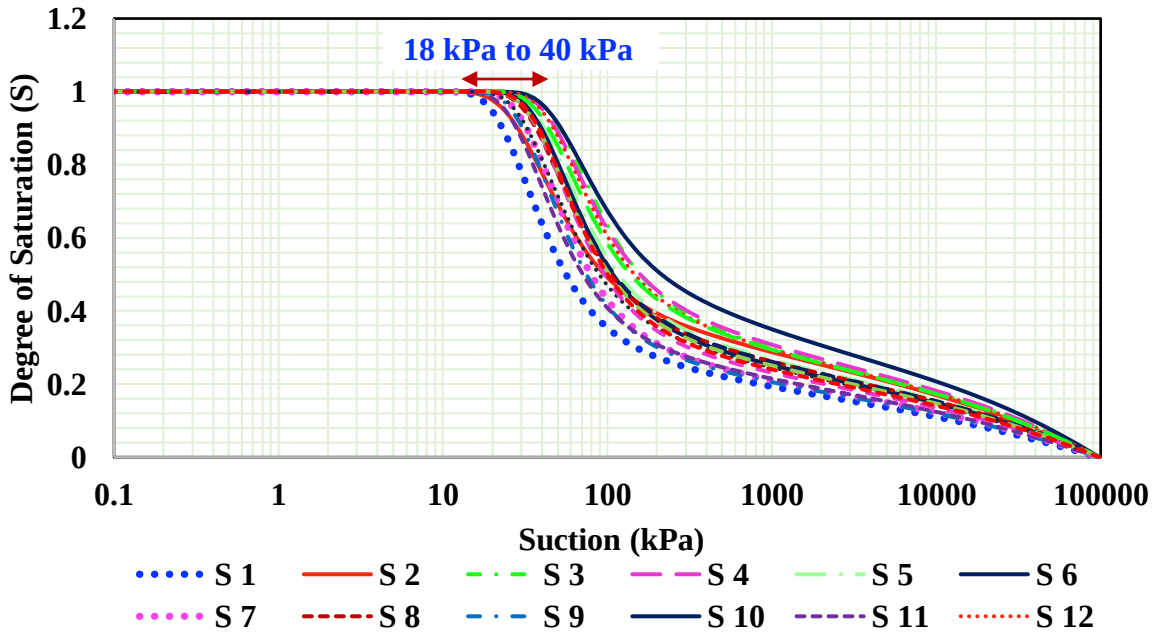

Figure 3.11 S-SWCCs estimated using Aubertin et al. (2003) model

In addition, the discussions in the previous section regarding the reliability of the measured SWCC (i.e., using WP4 potentiometer for low suction range measurements) data can also contribute to the variations to the two SWCCs comparisons. A detailed deliberation on the estimation models compared in this study is presented in the next section.

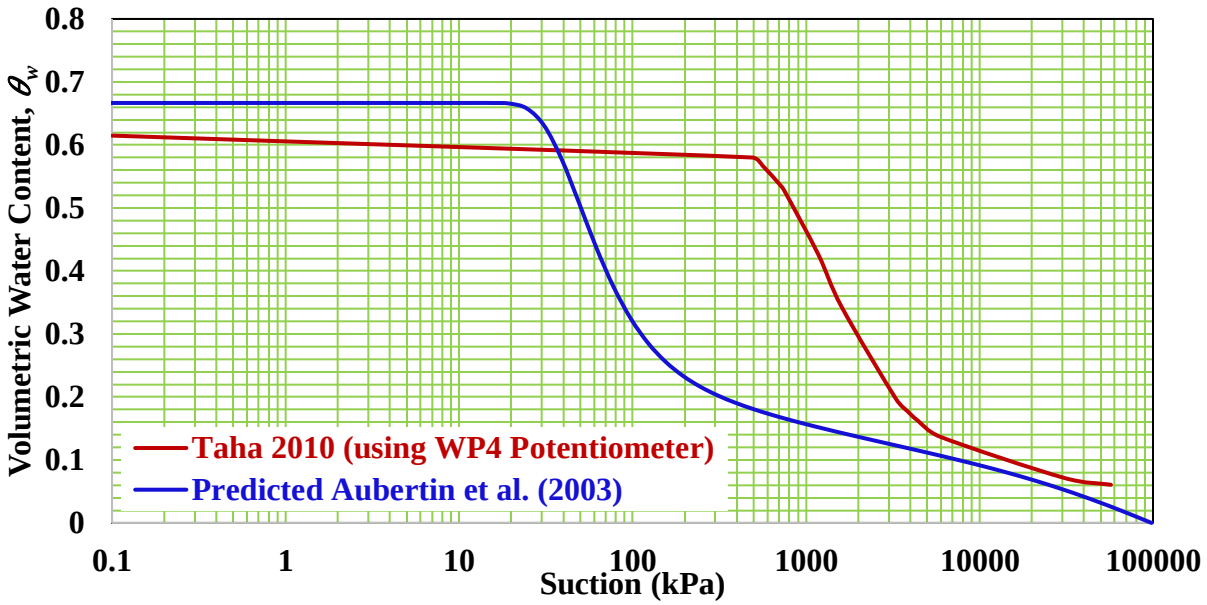

Figure 3.12 Predicted θ-SWCC using Aubertin et al. (2003) model for intact layer SWCC by Taha (2010)

3.4.3 Estimation models deliberation

The AEV values cannot be verified due to limitations discussed in section 3.2.1. However, an attempt has been made to investigate the influence of using in situ conditions in weathered Leda clay slopes. The estimation models use soil properties (Section 3.3) collected from borehole logs across the Ottawa region to facilitate representation of in situ soil conditions. Fredlund et al. (2002) and Aubertin et al. (2003) models are used to estimate the SWCC for weathered Leda clay using the data collected from numerous geotechnical reports around Ottawa (Figure 3.4 and Table 3.2).

The intact layer SWCC measured by Taha (2010) is utilized to provide a comparison of the prediction models. However, it should be noted that the accuracy of the two prediction models and

the measured Taha (2010) SWCC used in this study are difficult to verify due to reasons discussed in the earlier sections. As a result, this study attempts to use the average AEV range predicted by both Fredlund et al. (2002) (i.e., 5 kPa to 80 kPa) and Aubertin et al. (2003) (i.e., 18 kPa to 40 kPa) models. It can be noted that the AEV range from the Fredlund model is inclusive of the Aubertin model range. Therefore, the predicted range of AEV is utilized to assume the lower bound, upper bound, and average AEV value. As a reliable in-situ measured SWCC data is not available, it is difficult to select the most appropriate prediction model for rigorous verification. However, a simplistic approach is used in this study to provide a technique that can be used to reasonably predict the SWCC using in-situ soil properties.

The Fredlund et al. (2002) model that is used in this study provides a range of AEV (i.e., 5 kPa to 80 kPa) from the predicted SWCCs (see section 3.4.1). Since, there are various assumptions and simplifications used in this study, using a single SWCC to represent the weathered Leda clay may not be representative. The lower bound, upper bound, and the average AEV SWCC will be used to conduct certain numerical studies in the next chapter. However, the average AEV SWCC will be used extensively for numerical studies in this research.

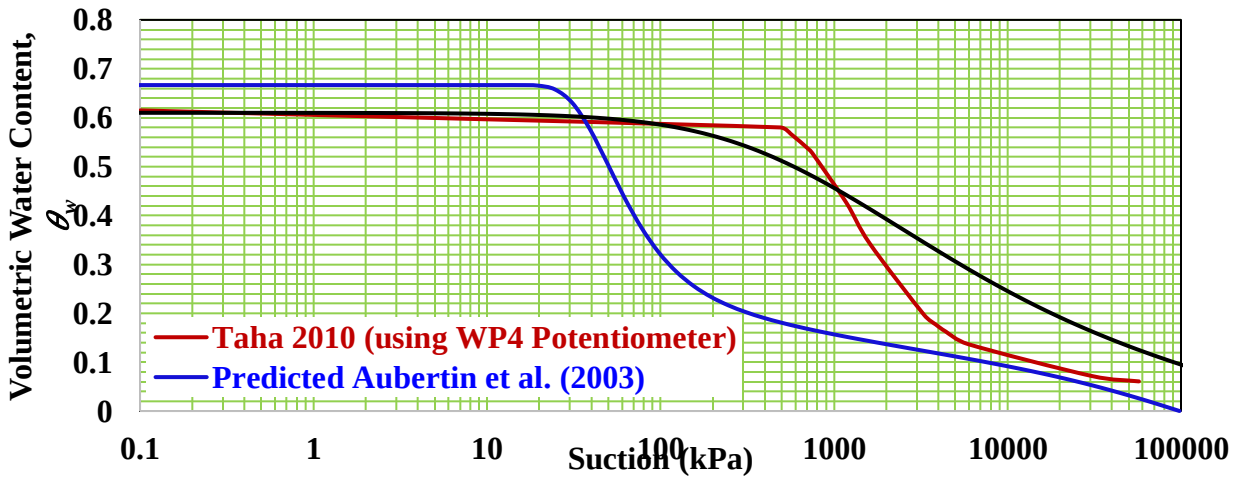

Figure 3.13 Comparison between the measured and predicted SWCCs using different models

3.4.4 Estimated SWCCs for numerical modelling

This section aims to present θ-SWCCs considering the AEV estimations of the previous section together with the database shown in Table 3.2. Three θ-SWCCs are to be estimated using the lower bound, upper bound, and average AEV.

The weathered crust of Leda clay forms due to numerous environmental cycles that erode the surface layer over time. These environmental fluctuations affect soils' hydro-mechanical behaviour (Wang et al. 2016). The soil properties of the weathered layer tend to be significantly different than the intact layer, especially the hydraulic conductivity and the SWCC.

The cracking of weathered Leda clay allows a dual porosity structure (Figure 3.14), including macropores (i.e., the cracks) and micropores (i.e., intra-aggregate pores), which can result in a bimodal SWCC (Qi and Vanapalli 2015c). The weathering phenomenon does not affect the intact layer and maintains its structure with micropores. Therefore, a unimodal SWCC is typically sufficient to characterize the in-situ soil conditions.

Figure 3.15 can be further used to understand the need for unimodal and bimodal SWCC to characterize Leda clay in the Ottawa region. The data projected is an extract of an ongoing research that aims to collect relevant soil properties for Leda clay around the Ottawa region. There is a considerable variation in void ratio at depths of 0 to 3 m. In contrast, the variation of void ratio reduces with an increase in depth. This shows that the weathered crust contains soil with variable pore sizes, while the intact layer tends to have a similar pore size at greater depths. Therefore, a rational analysis can only be conducted when a bimodal and unimodal SWCC is used to represent the weathered and intact layer of Leda clay slopes, respectively.

Figure 3.14 Illustration of macropores and micropores (Li and Vanapalli 2021)

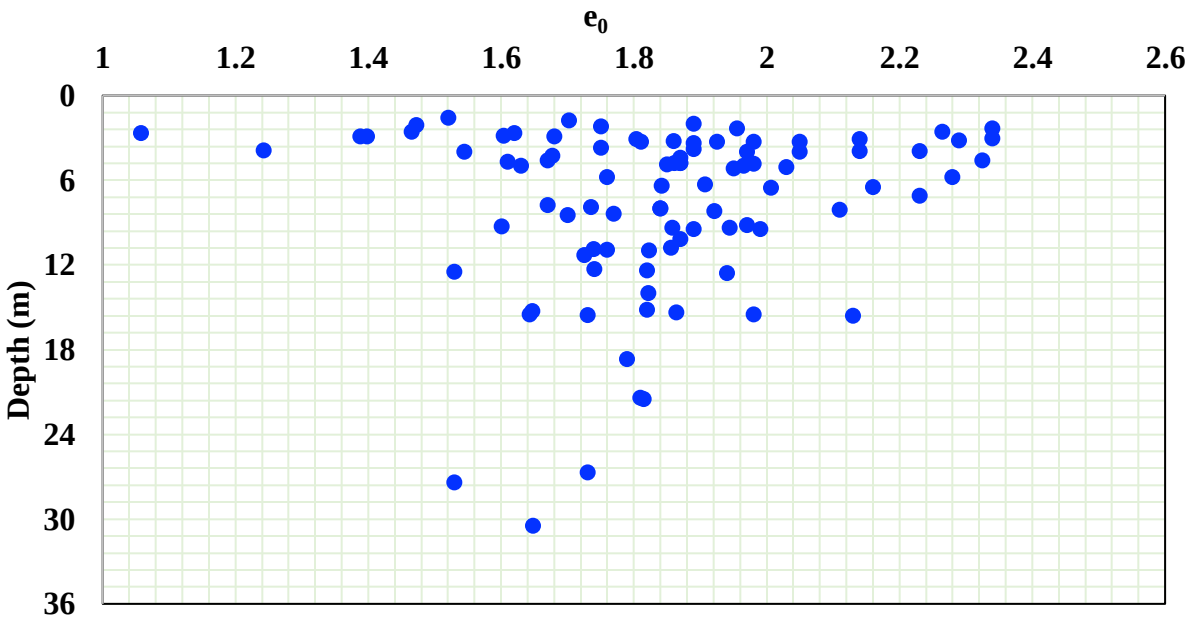

Figure 3.15 Variation of void ratio with depth for Leda clay around the Ottawa region

The unimodal SWCC can be plotted using several fitting equations available from the literature (see section 2.3.3). This study uses Fredlund and Xing's (1994) equation as the Fredlund et al. (2002) model also uses it for SWCC estimation. Fredlund et al. (2011) provide guidelines on

rearranging the SWCC fitting equations and using them to obtain suction values at various gravimetric water contents. The following steps can be used to generate a unimodal SWCC:

1. Choose a SWCC fitting equation and rearrange it to obtain the suction values (Eq. 2.12 is rearranged to Eq. 3.6; the correction factor is assumed to be 1.0 in this study)

$$\psi = a\left[e^{\left(\frac{w_s}{w}\right)^{\frac{1}{m}}} - e\right]^{\frac{1}{n}} \qquad \textbf{Eq. (3-5)}$$

2. Input data required, Initial saturated water content (w_s), fitting parameters *a, m,* and *n*
3. Determine w_s using the data collected from the borehole logs (Table 3.2)

$$w_s = \frac{S * e_0}{G_s}; S = 1 \qquad \textbf{Eq. (3-6)}$$

where S is the degree of Saturation, e_0 is the initial void ratio, and G_s is specific gravity.

4. Plot SWCC by varying the "*a*" parameter and keeping the "*m*" and "*n*" parameters constant.

The "*a*" parameter does not equal the AEV but is close to the AEV value. For example, the lower bound estimation for AEV is 5 kPa from the Fredlund et al. (2002) model; this does not mean that the "*a*" parameter will be 5 when plotting the SWCC.

Figure 3.16 and Figure 3.17 illustrates the estimated unimodal and bimodal SWCCs, respectively. The unimodal SWCC has been plotted using the procedures discussed above. In contrast, the bimodal SWCC has been devised by superimposing two unimodal SWCCs (i.e., SWCC from Figure 3.16 and Taha's (2010) intact layer SWCC). There are numerous models available in the literature that can be used to fit the bimodal SWCC using two unimodal SWCCs (Burger and Shackelford 2001; Satyanaga et al. 2013; Wijaya and Leong 2016; Satyanaga and Rahardjo 2019). However, the Geo Studio software contains a built-in function that allows the

fitting of bimodal SWCCs using the spline functions. The software provides tools to adjust the curve to best fit the SWCC. In addition, for this research, the accuracy of the spline function in the software is sufficient and has been incorporated by various researchers (Qi and Vanapalli 2015c; Tan and Vanapalli 2021).

There are recent advances in the prediction of unimodal and bimodal SWCCs using Artificial Intelligence (AI) as a tool (Schaap 1998; Koekkoek and Booltink 1999; Minasny and McBratney 2002; Li and Vanapalli 2021, 2022a; 2022b). The use of AI prediction methods is beyond the scope of the present research.

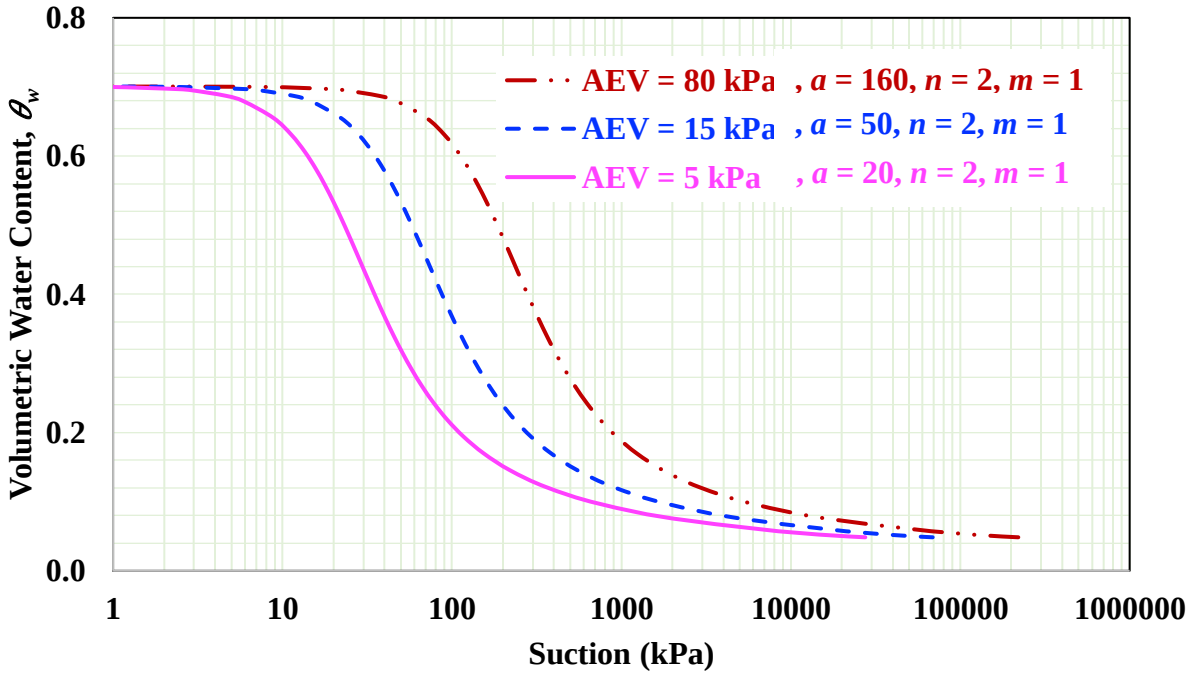

Figure 3.16 Unimodal SWCC for lower, upper, and median AEV

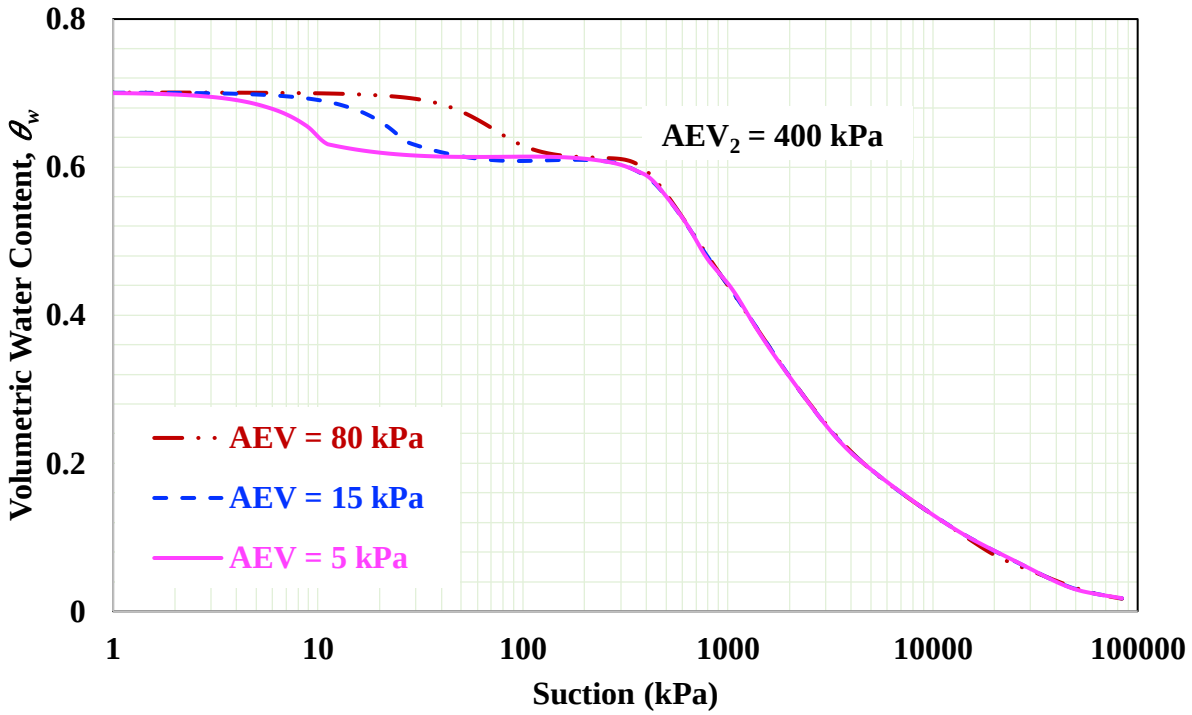

Figure 3.17 Bimodal SWCC for lower, upper, and median AEV

3.5 Conclusion

This chapter presents a technique for estimating the bimodal SWCC for weathered Leda clay that is required in the rigorous slope stability analyses of weathered surficial layer. Unfortunately, there is no information is available in the literature related to measured SWCC for Leda clay using in-situ soil sample. To address this gap in data, a simplistic representative SWCC is predicted using soil properties collected from borehole logs in the Ottawa region, utilizing the Fredlund et al. (2002) and Aubertin et al. (2003) estimation models.

The chapter provides information on the data collection procedure for gathering data on Leda clay in the Ottawa region. A comparison between two estimation models is conducted to use a model that can predict a reasonable SWCC that represents the in situ weathered conditions. The

AEV (i.e., 5 kPa, 15 kPa and 80 kPa) from the estimated model is used to plot the final unimodal and bimodal SWCC for numerical modelling analyses.

Reliable estimation of the most representative SWCC for the weathered Leda clay crust is a challenge due to the variability of soil properties and lack of measured in situ weathered Leda clay SWCC data. Therefore, this research is based on simplified assumptions to develop a theoretical background for performing numerical modeling studies for weathered crust in Leda clay slopes. While there are numerous approaches to estimating the SWCC, they have not been extended in this research due to various reasons; that include time, cost, scope, and complexity.

CHAPTER 4: NUMERICAL MODELLING ANALYSES OF WEATHERED LEDA CLAY SLOPE

4.1 Introduction

In this Chapter, the influence of rainfall infiltration on a weathered Leda clay slope is investigated. Leda clay slopes are typically in a state of unsaturated condition in the surficial weathered layer, which extends approximately to a depth of 3 m in the Ottawa region. As discussed in Chapter 2 (section 2.2.1), slope stability in the Ottawa region is vastly influenced by valley formation. The occurrence of landslides over a period tends to develop deeper V-shaped valleys in stages. These stages are shown in Figure 2.10 to visualize the development of the V-shaped valley. The figure also depicts the progression of the weathered layer as the valley deepens towards the "last stage" of the valley formation. The study aims to investigate the role of rainfall infiltration towards the slope stability of the weathered Leda clay slope. Therefore, the numerical model is largely based on the "last stage" slope illustrated in Figure 2.10. This is to represent the entire surficial layer as weathered Leda clay in the numerical studies.

The weathered crust of the Leda clay slope is generally in a state of unsaturated condition. Therefore, conventional slope stability analysis using saturated soil mechanics may not reasonably represent the in-situ conditions in the slope. Due to this reason, in this study the hydromechanical behavior of unsaturated soils is predicted using the SWCC and the saturated soil properties information. The key objective of this chapter is to perform studies on a weathered Leda clay slope considering the changes in the hydraulic and mechanical properties associated with the influence of rainfall on slope stability.

There are several numerical studies conducted in this chapter to fully comprehend the influence of rainfall influx on the stability of weathered slope. In this study, the hydro-mechanical behaviour is predicted using saturated soil properties and the SWCC. Moreover, the influence of unimodal (for intact soils) and bimodal (for considering the influence of weathered crust) SWCC on the factor of safety (FS) studies is examined. Furthermore, the effect of extending linear and non-linear shear strength equations to conduct SLOPE/W studies is assessed (extending background discussed in Chapter 2). Finally, the impact of varying rainfall intensity on slope stability is also considered.

4.2 Stability of Slopes in Unsaturated Soils

The weathered Leda clay undergoes hydro-mechanical changes during rainfall infiltration. The water infiltration through the unsaturated weathered soil influences both the seepage fields as well as the stress fields due to the volume change behaviour upon wetting. Therefore, a rigorous slope stability analysis should include the contribution of mechanical and hydraulic stresses for slope stability.

4.2.1 Governing Equations

The equations that govern the mechanical and water flow behaviour (i.e., hydro-mechanical behaviour) of unsaturated soil elements are the partial differential force equilibrium (Eq. 4.1) and water continuity equation (Eq. 4.2). The continuity equation for two-dimensional water flow should be used knowing that the water is assumed to be incompressible and have insignificant deformations (Richards 1931; Qi and Vanapalli 2015c)

$$\frac{\partial \sigma_{ij}}{\partial x_i} + b_j = 0 \qquad \textbf{Eq. (4.1)}$$

$$\frac{\partial q_i}{\partial x_i} + \frac{\partial \theta_w}{\partial t} = 0 \qquad \text{Eq. (4.2)}$$

where, σ_{ij} are components of total stress tensor, b_j are components of the body force vector. θ_w is the volumetric water content, and t is time; q_i are the flow velocities in the *i*- directions. Darcy's Law (Eq. 4.3) describes the relationship between flow velocities and hydraulic heads for water flow in unsaturated soils.

$$q_i = -k_{ij} \frac{\partial}{\partial x_j}\left(\frac{u_w}{\rho_w} + y\right) \qquad \text{Eq. (4.3)}$$

where k_i is the hydraulic conductivity in the *i* direction; u_w is the value of porewater pressure, ρ_w is the density of water, and y is the vertical coordinate (elevation).

4.2.2 Constitutive Relationships

The mechanical behaviour of unsaturated soils cannot be described by effective stress-strain relationship as in the case for saturated soils. The relationship between the water content and the stress state variables is required to sufficiently describe the mechanical behaviour of unsaturated soils (Qi and Vanapalli 2015c). The unsaturated soil constitutive relationships use the two stress state variables, namely net normal stress, $(\sigma_n - u_a)$ and matric suction, $(u_a - u_w)$. Eq. 4.4 and Eq. 4.5 shows the unsaturated soil constitutive relationship that is consistent with continuum mechanics principles after simplification:

$$d\varepsilon_{ij} = \frac{1+\mu}{E} d\sigma_{ij} - \frac{\mu}{E} d\sigma_{mean}\delta_{ij} - \frac{1}{H} du_w \delta_{ij} \qquad \text{Eq. (4.4)}$$

$$d\theta_w = \frac{3}{H} d\sigma_{mean} - \frac{1}{H_w} du_w \qquad \text{Eq. (4.5)}$$

where ε_{ij} are the components of the strain tensor, E is the elastic modulus of the soil, $\sigma_{mean} = (\sigma_x + \sigma_y + \sigma_z)/3$ which represents the average stress value in each direction, δ_{ij} is the Kronecker delta, H is the unsaturated soil modulus for soil structure with respect to $(u_a - u_w)$, $H = \frac{E}{1-2\mu}$. H_w

represents a modulus relating the variation in volumetric water content and variation in matric suction, and μ is the Poisson's ratio. Eq. 4.6 defines the relationship between the change in volumetric water content to the change in volume of soil structure which can be obtained by substituting Eq. 4.4 into Eq. 4.5.

$$d\theta_w = \frac{E}{H(1-2\mu)} d\varepsilon_v - \left(\frac{1}{H_w} - \frac{3\beta}{H}\right) du_w \qquad \textbf{Eq. (4.6)}$$

4.2.3 Numerical Uncoupled and Coupled Solutions

For uncoupled solutions, Eq. 4.2 with the application of Darcy's law (Eq. 4.3) can be used to estimate the unknowns such as pore-water pressure (PWP) with relative degree of accuracy. Eq. 4.7 is derived by substituting Eq. 4.3 into Eq. 4.2 and can be used to solve two-dimensional problems. The uncoupled numerical analysis can be implemented using the GeoStudio Software, SEEP/W (GeoSlope International Ltd. 2007c), which requires only hydraulic soil properties (e.g., SWCC and hydraulic conductivity functions) as input parameters.

$$\frac{\partial}{\partial x}\left[k_x \frac{\partial}{\partial x}\left(\frac{u_w}{\rho_w g} + y\right)\right] + \frac{\partial}{\partial y}\left[k_y \frac{\partial}{\partial y}\left(\frac{u_w}{\rho_w g} + y\right)\right] = \frac{\partial \theta_w}{\partial t} \qquad \textbf{Eq. (4.7)}$$

On the other hand, substituting Eq. 4.4 and Eq. 4.6 into Eq. 4.1 and Eq. 4.2 yields a coupled hydro-mechanical description of rainfall infiltration through an unsaturated porous media with two sets of unknowns including PWP and displacement. The commercial software SIGMA/W (GeoSlope International Ltd. 2007b) can solve for the two unknowns simultaneously which also incorporates the hydraulic analysis code (SEEP/W) and the static force equilibrium analysis to implement the coupled analysis (Qi and Vanapalli 2015c).

4.2.4 Shear Strength of Unsaturated Soils

The Mohr-Coulomb failure criterion (Eq. 4.8) is widely used to determine the shear strength for slope stability analysis in saturated soils.

$$\tau_{f_{sat}} = c' + (\sigma - u_w) \tan \phi' \qquad \textbf{Eq. (4.8)}$$

where, $\tau_{f_{sat}}$ is the shear strength of saturated soil, c' is the effective soil cohesion, ϕ' is the effective friction angle, and $(\sigma - u_w)$ is the effective stress. Vanapalli et al. (1996) proposed a semi-empirical model (Eq. 4.9) that can be used in prediction of the variation of shear strength with respect to suction using the SWCC as a tool. This model approximates a non-linear relationship between unsaturated shear strength and suction.

$$\tau_{f_{unsat}} = c' + (\sigma_n - u_a) \tan \phi' + (u_a - u_w) \left[\frac{\theta_w - \theta_r}{\theta_s - \theta_r}\right] (\tan \phi') \qquad \textbf{Eq. (4.9)}$$

where, $\tau_{f_{unsat}}$ is the shear strength of unsaturated soil, θ_w is the volumetric water content, θ_r is the residual volumetric water content, θ_s is the saturated volumetric water content, $(\sigma - u_a)$ is the net normal stress on the plane of failure at failure, and $(u_a - u_w)$ is the matric suction of the soil on the plane of failure.

Eq. 4.9 can be used for evaluating both the shear strength in saturated and unsaturated soil conditions. For a scenario the soil attains saturated conditions, ($u_a - u_w$) would be zero and the ratio of $\frac{\theta_w - \theta_r}{\theta_s - \theta_r}$ would equal to 1. This reverts Eq. 4.9 to Eq. 4.8, which represents the Mohr-Coulomb failure criterion's effective stress principle. Therefore, this semi-empirical model helps analyze slip surfaces that are partly saturated (e.g., below GWT) and unsaturated conditions (e.g., above GWT).

Figure 4.1 below shows the variation of shear strength with suction using Eq. 4.9 for the weathered (i.e., bimodal SWCC with AEV = 15 kPa) and intact (i.e., unimodal SWCC with AEV

= 400 kPa) layer. Due to the lower first AEV for the bimodal SWCC, the shear strength starts to decrease and then increase again towards the second AEV of approximately 400 kPa. The intact layer shear strength curve would continue to increase until the first AEV of 400 kPa. Eq. 4.9 can illustrate the non-linear behaviour of the shear strength as the matric suction increases beyond the AEV. In addition, the shear strength of the weathered layer represented by a bimodal SWCC can be lower than that of the intact layer with unimodal SWCC despite the same internal friction angle.

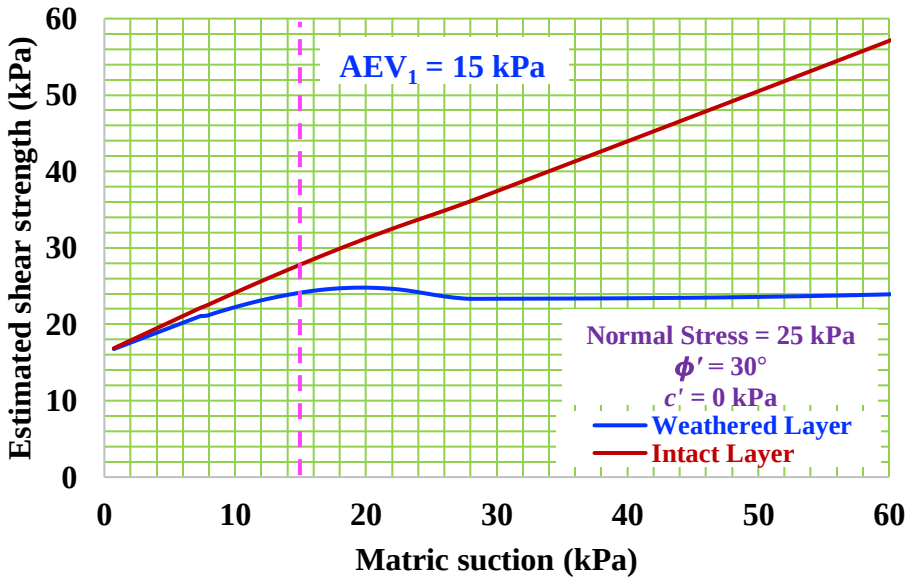

Figure 4.1 Variation of Shear strength with matric suction

4.2.5 Slope Stability

The factor of safety (FS) value is used for evaluating the stability of several geotechnical structures that include slopes, foundations, and retaining walls. Numerous approaches are available in the literature to solve for FS for slopes of 1, 2 and 3 dimensions in saturated or unsaturated conditions. This study analyzes 2-dimensional unsaturated slopes (e.g., Morgenstern and Price 1965). The limit equilibrium method (LEM) and finite element method (FEM) are two of the various approaches available to determine the FS for slopes.

The SLOPE/W software incorporates the calculation of FS using both the LEM and FEM according to the type of analyses (i.e., coupled or uncoupled). For uncoupled analyses, the SEEP/W software determines the hydraulic stresses and provides input parameters for SLOPE/W to conduct FS using LEM. On the other hand, for FEM, SIGMA/W software needs to determine the mechanical and hydraulic stress information to be used as input parameters for SLOPE/W analysis (GeoSlope International Ltd. 2007a).

One of the LEM techniques incorporated within the SLOPE/W software is the Morgenstern-Price method with the half sine side function which considers the interslice shear and normal forces that provides a conservative FS value. The Morgenstern-Price method is a general method of slices developed based on limit equilibrium. The equilibrium of forces and moments acting on the individual blocks (i.e., blocks created above the slip surface by dividing planes) needs to be satisfied. The FS is determined iteratively by adjusting inclination angles to achieve equilibrium. The factor of safety can be described by the ratio of soil shear strength (τ_f) to the shear stress (τ_s) on the specified slip surface (Eq. 4.10) (Morgenstern and Price 1965).

$$\boldsymbol{FS = \frac{\tau_f}{\tau_s}} \qquad \textbf{Eq. (4.10)}$$

It should be noted that there is an updated Morgenstern-Price method proposed by Ouyang et al. (2024) that improves several aspects of the traditional method. It replaces the traditional trial and error process to determine the scaling factor with an efficient search algorithm. Moreover, the updated method eliminates the need for dense slice mesh by using strategically placed gauss points on the slip surface. Since this study uses the GeoStudio software for slope stability analysis, the Morgenstern-Price method incorporated within SLOPE/W will be used for LEM.

4.3 Methodology for Slope Stability Analyses of Weathered Leda Clay

Figure 4.2 summarizes the procedure used in the evaluation of the slope stability of weathered Leda clay. The coupled analysis can be conducted using two different techniques: a strong-coupled analysis and a weak-coupled analysis. The strong-coupled analysis is undertaken by determining both the hydraulic and mechanical stresses within SIGMA/W software. On the other hand, a weak-coupled analysis uses a combination of SIGMA/W and SEEP/W for mechanical and hydraulic stresses, respectively. In this study, a strong-coupled analysis is used for evaluating the hydro-mechanical behaviour of weathered Leda clay.

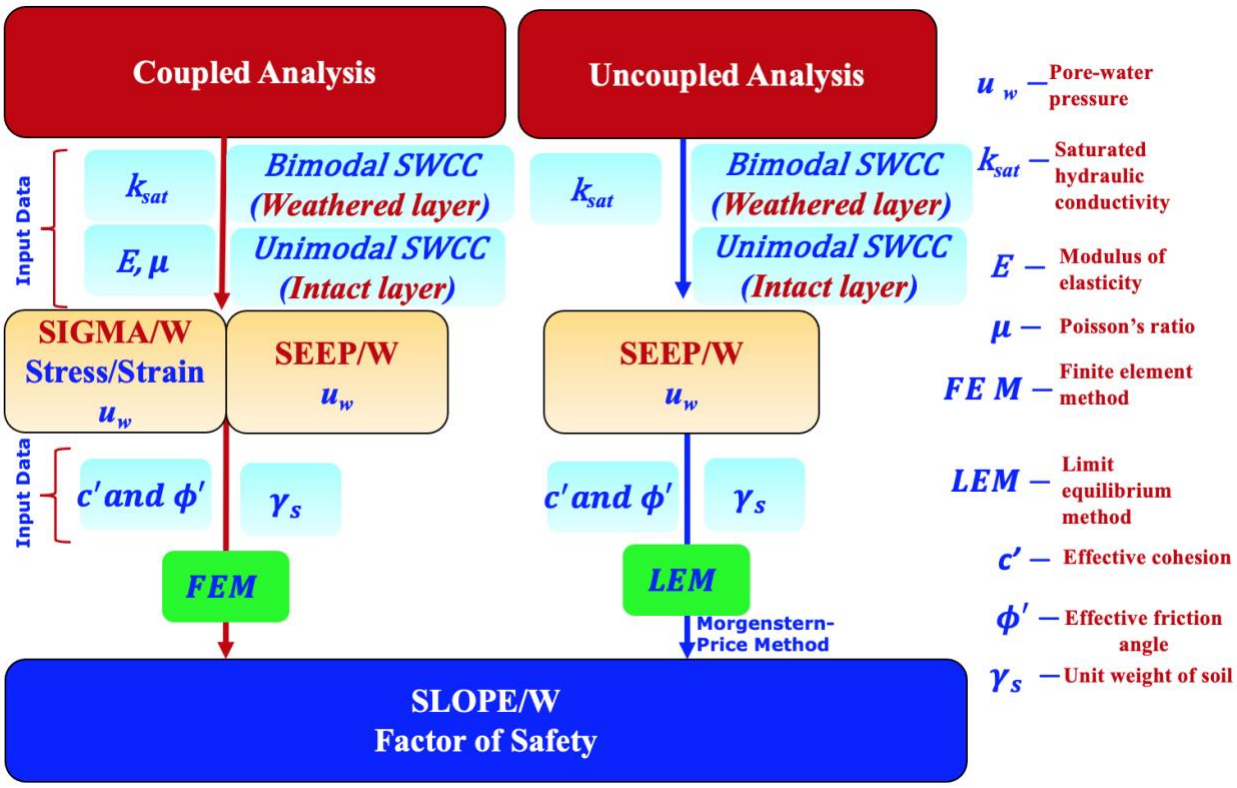

Figure 4.2 Slope stability analysis procedure based on coupled and uncoupled analyses

SEEP/W conducts the hydraulic stress analysis without incorporating mechanical stresses for uncoupled analysis. Therefore, for uncoupled analysis, only SEEP/W software can be utilized for hydraulic parameters required for slope stability analysis.

The input parameters for coupled analysis requires both the mechanical and hydraulic soil properties while only the hydraulic properties are sufficient for uncoupled analysis. The output from SIGMA/W and SEEP/W analyses are then input into the SLOPE/W software to complete the slope stability analyses of the weathered Leda clay crust.

4.4 Numerical Modelling

During the late phase of valley formation (Figure 2.10) in the Ottawa region, weathered crust tends to form on the surface of the slopes (i.e., including the crest, head, and toe of the slope). The slopes tend to be exposed to the atmosphere more and more as they transition towards the last stage of valley formation. This allows the weathering of the surface layer either by environmental or chemical factors. Therefore, by the time the valley formation reaches the last stage, the entire surficial layer undergoes weathering. In addition, such slopes typically undergo shallow failures, with the slip surface passing within the weathered layer.

This is due to the difference in permeability between the weathered and intact layer of Leda clay. The rainfall infiltration may not be able to infiltrate the intact layer because of saturated permeability that is two to three magnitudes lower (Lefebvre 1986) than the weathered layer. This makes the weathered surficial layer vulnerable to shallow landslides in Leda clay slopes. Hence, this study attempts to adapt the Leda clay slope model for numerical studies according to the late phase of the valley formation. This allows the numerical studies to represent the region's in-situ geometry of Leda clay slopes.

As discussed above, Leda clay slopes in the Ottawa region shows evidence of weathering in the surficial layer and this zone is desiccated and in an unsaturated condition. The matric suction changes associated with water and air phases have a significant influence on the unsaturated behavior of the soils. In other words, one of the key stress state variables, matric suction influences

mechanical (i.e., shear strength and volume change) and hydraulic (i.e., flow) behavior of the Leda clay that cannot be rationally explained using the principles of saturated soil mechanics. Therefore, this study extends unsaturated soil mechanics principles to determine the pore-water and FS variations in the weathered layer during rainfall infiltration.

Several landslides in the Ottawa region have occurred due to rainfall or snowmelt infiltration (Mitchell 1969; Eden and Mitchell 1970; Mitchell and Markell 1974; Williams et al. 1979; Hugenholtz and Lacelle 2004; Al-Umar 2018). This study attempts to investigate the influence of rainfall infiltration on Leda clay slopes with weathered curst (i.e., shallow slope failures).

4.4.1 Numerical Model Description

The height and width of the model slope investigated in the study are 23 m and 37 m, respectively (Figure 4.3). This provides a slope inclination angle of approximately 28°. These dimensions have been adapted by referencing the "Pineview Golf Club" landslide on the west bank of Green Creek adjacent to Pineview Golf Club to establish a numerical model that resembles an existing Leda clay slope (Mitchell 1970; Mitchell and Markell 1974; Williams et al. 1979). The 3 m of surficial layers are assumed to represent the average depth of weathered Leda clay crust around the Ottawa region (Eden and Crawford 1957). The weathered surface is defined using the surface layer drawing tool in SEEP/W. Ten different surface layers with a height of 0.3 m make up the model's 3 m weathered crust layer. This is done to increase the number of data points that can be collected after numerical analysis, which subsequently increases the accuracy of results.

The mesh size for the weathered layer is predominantly smaller than for the intact layer (i.e., assumed to be homogeneous). The global mesh size was set to 0.25 m and applied to the surface layers with 0.3 m height. The 0.3 m height of the surface layer is further reduced by adding

five nodes to the vertical line. Therefore, a quadrilateral mesh size of 0.06 by 0.25 m is used for the surficial layers (i.e., see "zoomed in" view in Figure 4.3).

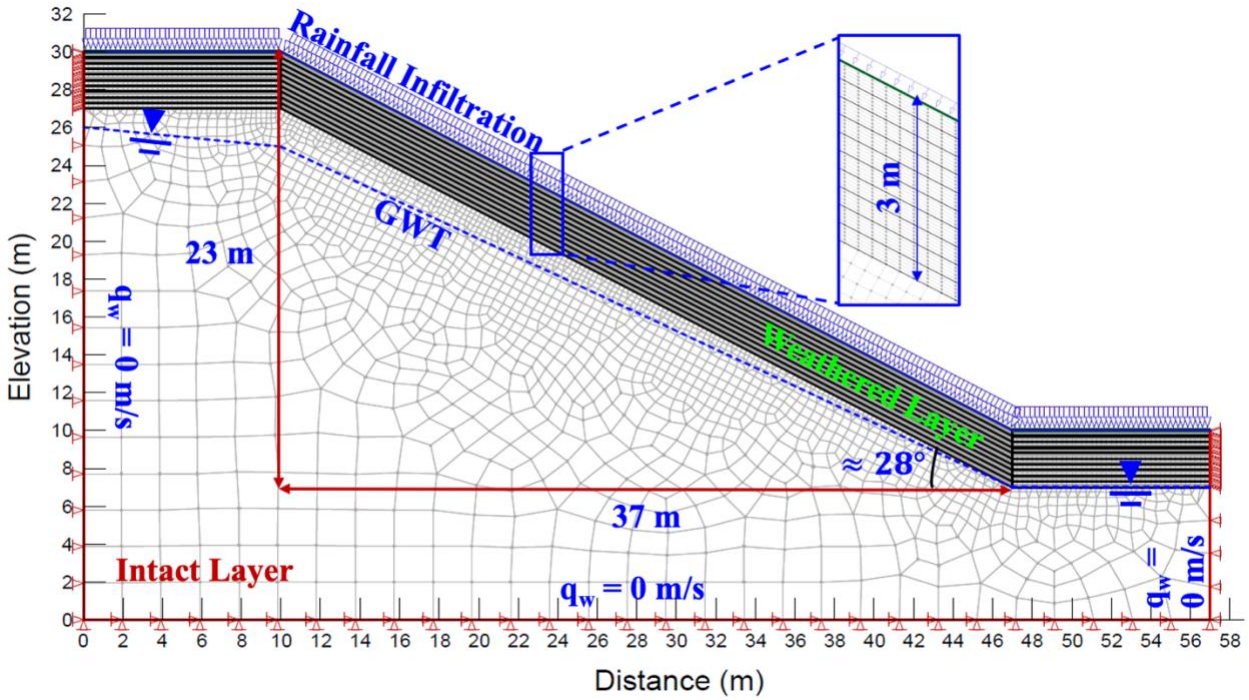

Figure 4.3 Established model slope depicting various characteristics, including boundary conditions

The advantage of adding vertical nodes to the quadrilateral elements is to collect the pore-water pressure (PWP) data to study its variation with depth in this study. The quadrilateral elements are highly recommended to model the intense response of the surface layer to infiltration than the triangular elements. Triangular elements bring about fluctuations in the results in thin surface layers, which, if required, can be mitigated by reducing the mesh size further (GeoSlope International Ltd. 2007a; Qi and Vanapalli 2015c). The mesh size in the intact layer is eight times bigger than the global mesh size of 0.25 m. The contrasting allocation of mesh size is related to the efficiency (i.e., computational time) and efficacy (i.e., significance of the results). In addition, the distinctive distribution of the mesh size shows that the study demands more accuracy in investigating the weathered Leda clay crust than the intact layer.

The Ottawa region generally has a shallow groundwater table (GWT) that fluctuates from 0.5 to 3.6 m depth from natural ground surface as per the research studies from the literature (see Appendix B). Since the weathered crust depth is approximately 3 m around the Ottawa region, the GWT is simulated to be at a depth of at least 3 m. If the GWT is less than 3 m deep, then the study of PWP profile variation for the entire weathered crust will be limited as part of it will be saturated prior to water infiltration. Therefore, the GWT is assumed to be 4 m at the crest, 5 m just below the head of the slope, and 3 m at the toe of the slope (see Figure 4.3). According to the GWT distribution, the maximum and minimum matric suction in the slope is at 50 kPa (i.e., 5 m below ground surface) and 30 kPa (i.e., 3 m below ground surface), respectively.

4.4.2 Boundary Conditions

The hydraulic and mechanical boundary conditions (i.e., defined in red along the boundaries) for the numerical study are defined in Figure 4.2. For SEEP/W analysis, the rainfall flux with no ponding is applied at the horizontal and slope sections at the model's top. GWT is defined as discussed above, and zero flux boundary conditions are applied around the two lateral and bottom boundaries. The conditions set are practical as the two lateral boundaries are almost 10 m further away from the sloping surface and therefore, would have minimum effect on the water flow in the sloping surface. In addition, the bottom boundary is also relatively at a greater depth than the sloping surface; hence, the effect of rainfall infiltration on it would be minimal. Several researchers (Zhang et al. 2004; Qi and Vanapalli 2015a; b; c; Tan and Vanapalli 2021) have used similar boundary conditions in their numerical studies on the influence of rainfall infiltration in slope stability or PWP profile variations.

On the other hand, for SIGMA/W, mechanical stress allowing displacement along the *y*-axis is defined on the left and right boundaries. In contrast, zero displacement in the *x*-*y* direction

is determined at the bottom of the model. It should be noted that initial conditions for SIGMA/W analysis require the definition of mechanical and hydraulic stresses for the coupled analysis. In some cases, as discussed earlier, the hydraulic stresses can be defined using SEEP/W and then incorporated into the SIGMA/W analyses, yielding a weak-coupled analysis.

4.4.3 Soil Properties

The soil properties of Leda clay to be used during the numerical studies have been summarized in Table 4.1. The table includes soil parameters for both weathered Leda clay crust and the intact layer. Three bimodal SWCCs are estimated in Chapter 3 to represent the weathered Layer, of which the SWCC with air entry value (AEV) of 15 kPa is used throughout the numerical studies. The choice of AEV = 15 kPa SWCC is based on the median value from the estimation studies. More discussions related to the influence of AEV variation on FS is discussed in section 4.5.1. Figure 4.4 illustrates the bimodal and unimodal SWCC representing the weathered and intact layer of Leda clay, respectively. The first AEV is 15 kPa followed by the second AEV of approximately 400 kPa.

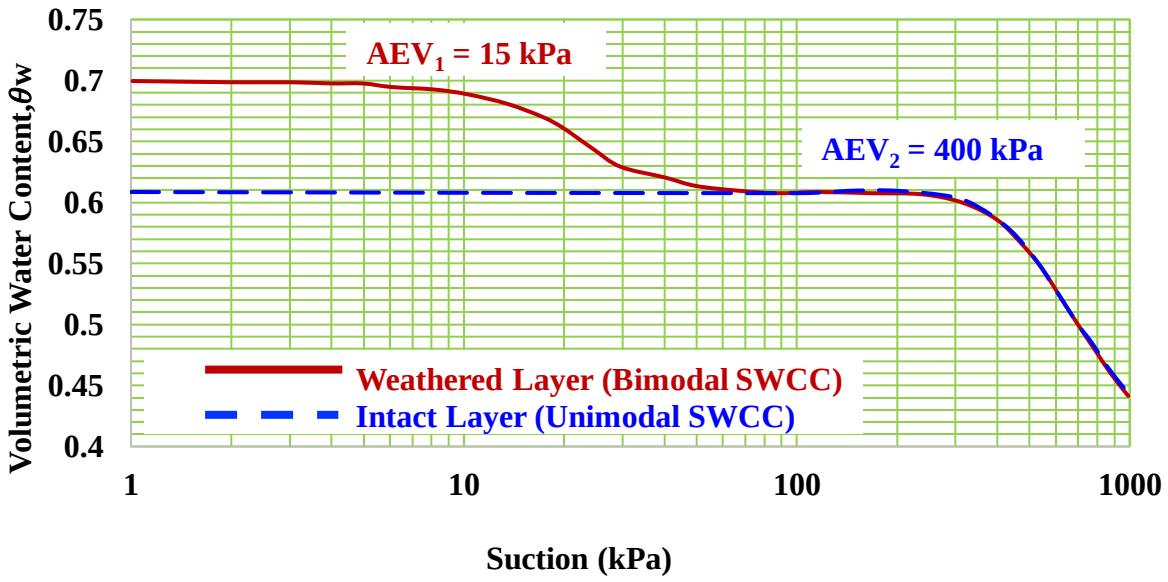

Figure 4.4 SWCCs of Leda Clay

Table 4.1 Summary of Leda clay soil properties used for numerical modelling

Properties	Weathered Layer	Intact Layer	Figure	Reference
First AEV (kPa)	15	400	Fig. 4.4	This Study & Taha (2010)
Second AEV (kPa)	400	----		
Saturated water content (m^3/ m^3)	0.7	0.6		
Residual water content (m^3/ m^3)	0.1	0.1		
k_{sat} (m/s)	$3.0x10^{-7}$	$3.0x10^{-9}$	Fig. 4.5	Nader (2014)
Modulus of elasticity, E (kPa)	15,000	15,000		Lo and Lee (1974)
Poisson's ratio, μ	0.3	0.3		
Unit weight, γ (kN/m^3)	16	16		Assumed based on this study
Effective internal friction angle, ϕ' (°)	30	28		Assumed based on Mitchell (1969)
Unsaturated shear strength angle, ϕ^b (°)	15	----		Assumed based on Batali and Andreea (2016)
Effective cohesion, c' (kPa)	----	----		

The hydraulic conductivity of unsaturated Leda clay (k_{unsat}) (Figure 4.5) has been estimated using the saturated hydraulic conductivity (k_{sat}). There is limited experimental data concerning the k_{sat} of weathered Leda clay in the Ottawa region. Nader (2014) conducted several tests on Leda clays around the Ottawa region, that also include hydraulic conductivity tests, to determine various soil properties. Rigorous discussions in the literature with respect to k_{sat} values for the weathered crust in Leda clay are not available; however, they are typically higher at the weathered surface layers and lower at greater depths (Nader 2014). In addition, the k_{sat} of weathered layers is generally two to three magnitudes higher (Lefebvre 1986; Qi and Vanapalli 2015c) than the intact layer due to the influence of cracks on the permeability. Therefore, the k_{sat} for the intact layer was estimated using the results obtained from Nader (2014), and the weathered layer k_{sat} is assumed to

be two magnitudes higher than the intact layer, as shown in Table 4.1 and Figure 4.5. Similar to the estimation of the bimodal SWCC, the bimodal hydraulic conductivity curve is derived using the in-built spline functions in GeoStudio software.

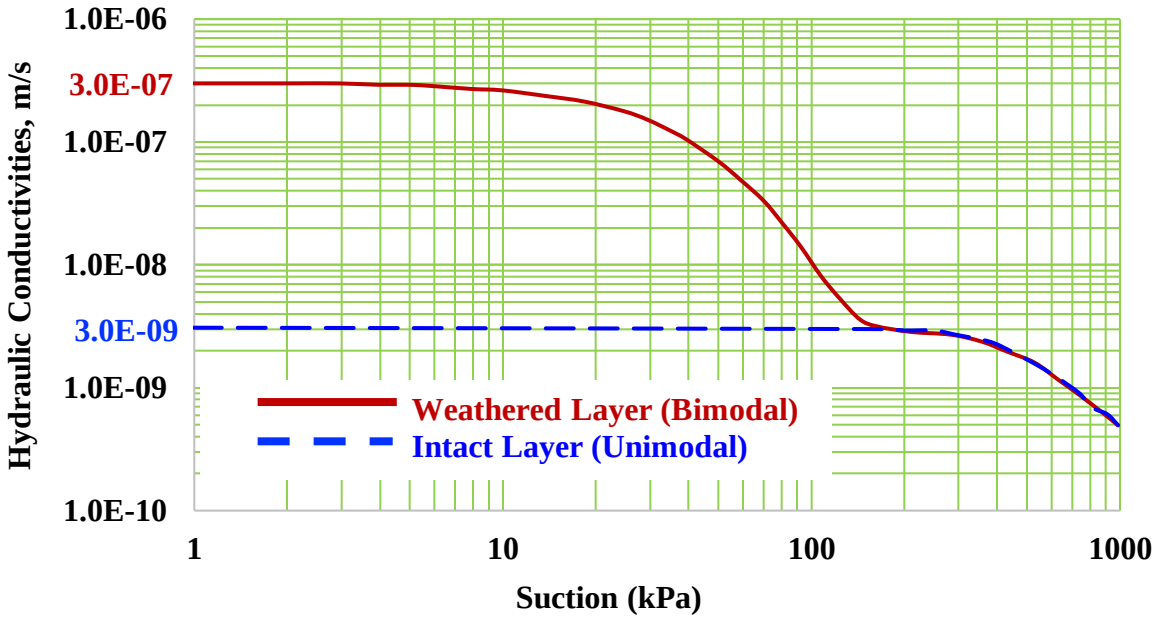

Figure 4.5 Variation of hydraulic conductivity in Leda clay with respect to suction

The modulus of elasticity and Poisson's ratio is required to conduct the coupled analysis using SIGMA/W. The values used for numerical modelling are assumed based on the information derived from the studies conducted by several researchers on Champlain Sea clay and Leda clay in the region (Bozozuk 1963; Hanna and Adams 1968; Lo and Lee 1974). The modulus of elasticity value varies according to the loading and unloading scenario or the depth of the soil layers (Qi and Vanapalli 2015c). The modulus of elasticity for unsaturated soils can be estimated by using Eq. 4.11 proposed by Oh et al. (2009).

$$E_{unsat} = E_{sat}\left[1 + \alpha \frac{(u_a - u_w)}{\frac{P_a}{101.3}} S^{\beta}\right] \qquad \text{Eq. (4.11)}$$

where E_{unsat} and E_{sat} are the modulus of elasticity of unsaturated and saturated soil, respectively. P_a is the atmospheric pressure. The SWCC and two fitting parameters, α and β are required to

predict the unsaturated modulus of elasticity. The GeoStudio software does not incorporate the semi-empirical method above to compute the variation of modulus of elasticity with matric suction.

In this study, the Leda clay soil does not undergo swelling or severe volume change upon wetting. Therefore, a linear-elastic material model is sufficient to evaluate the minimal volume change in the surficial weathered Leda clay crust. Since the volume change variation is assumed to be minimal, a constant modulus of elasticity value (i.e., 15,000 kPa) is used for both weathered and intact layer during the SIGMA/W analysis. The analysis is focused for the weathered Leda clay layer, hence, the soil parameters for the intact layer may not largely influence results collected.

Bozozuk (1963) suggests the Poisson's ratio for Leda clays to be 0.4 or slightly less. On the other hand, Lo and Lee (1974) used values of 0.35 for Poisson's ratio in their study of landslides in the Ottawa region. Moreover, Bäckström and Linder (2021) conducted a case study on a landslide that occurred in Rävekärr, Sweden where they use a weathered crust Poisson's ratio input parameter of 0.3 based on in situ soil parameters. Therefore, an assumption is made to represent the dilative and contractive behaviour of weathered Leda clay by using a Poisson's ratio of 0.3.

The unit weight of Leda clay was assumed based on data collected for SWCC estimation in Chapter 3. In addition, a general assumption is also made to keep the unit weight of the weathered and intact clay equal. This is done to simplify the computation and recognize that soil unit weight does not essentially influence the FS (GeoSlope International Ltd. 2007a).

The effective friction angle, ϕ' has been assumed based on Greens Creek slope stability studies conducted by numerous researchers (Mitchell 1969; Eden and Mitchell 1970; Sangrey and Paul 1971; Lo and Lee 1974). The friction angle, ϕ' is assumed based on the best-fit slip circle observed failure for the Greens Creek slide of November 1967. The ϕ' used to represent the

weathered Leda clay crust in this study is greater than that of the intact layer of the slope. Since the weathered Leda clay crust behaves like a densely packed granular soil (Eden 1975), its ϕ' is assumed to be greater than the intact soft clay in this study. The ϕ' is typically greater than 30 for dense granular soils (i.e., sand) compared to soft clays (Peck et al. 1974; AASHTO 1982).

The angle of internal friction, ϕ^b associated with matric suction is used to determine the linear shear strength at failure using Eq. 2.6. In this study, a comparison is made to understand the influence of linear and non-linear unsaturated shear strength equations (see section 4.5.3) on the FS of slopes. The ϕ^b value can vary between 0° and ϕ' over a large suction range. In this study, ϕ^b is assumed to be half of the effective friction angle, as suggested when other test results are unavailable (GeoSlope International Ltd. 2007a). The ϕ^b for the intact layer has not been defined as the current study focuses on slope stability within the weathered crust. The slip surface is defined within the weathered layer; thus, the value of ϕ^b in the intact layer does not influence the FS results.

4.5 Results and Discussions

The numerical results are presented in this section with reference to the slope FS within the weathered Leda clay layer at three different locations: upslope, mid-slope, and toe slope (see Figure 4.6 below). The results are collected from each of the three locations and presented in this section for analysis and discussion. The choice of locations for the slip surfaces in this research have mainly been influenced by the need to understand the behaviour of the surficial weathered layer at different elevations in the slope. For example, a shallow failure can occur at the head of the slope if the rainfall infiltration can reduce the suction strength faster compared to the scenario at midslope location. Adding to the discussions in section 4.4, the saturated permeability of the

intact layer is 2 to 3 magnitudes lower compared to the weathered crust of Leda clay. This shows that the rainfall infiltration can infiltrate within the weathered layer which can result in shallow slope failures.

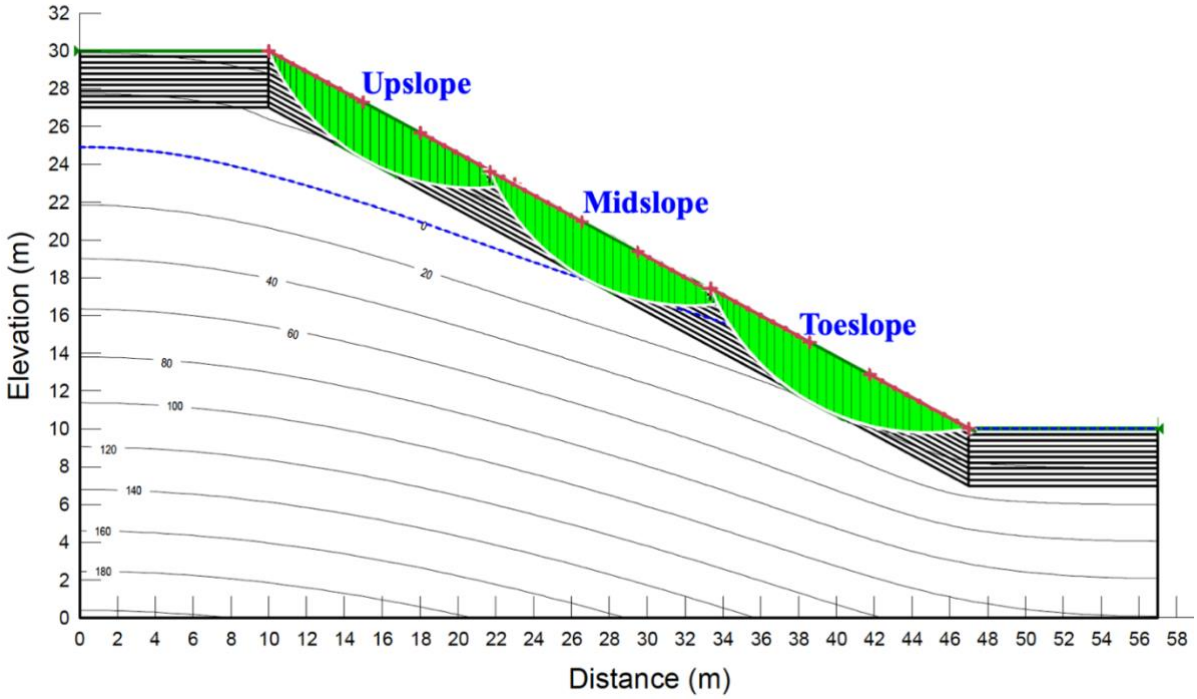

Figure 4.6 Model Slope illustrating the approximate slip surfaces used to determine FS at three different locations on the slope

A circular slip surface has been assumed in this study to compute the slope stability of weathered Leda clay crust. The slip surface is optimized in SLOPE/W such that it provides the critical FS at the different locations illustrated in Figure 4.6. The shape of the failure slip surface is assumed circular in this study based on shallow rotational landslide observed in the Ottawa region (Eden and Mitchell 1970). It is also possible to have non-circular slip surfaces due to the non-uniform soil structure in the weathered crust. There are several other optimization options incorporated in SLOPE/W that can be used to represent different shapes slip surface failure. However, it is beyond the scope of this research and may be explored in future studies.

Different rainfall intensities, which include 0.04, 1.08 and 10 mm/hr, were used in the analyses. Table 4.2 summarizes rainfall intensities used in the numerical studies of this study. The main reason for the variation in rainfall intensities is to observe the variation of the results for different studies. This enables comparisons to be made with existing similar research work (i.e., using low and high rainfall intensity) pursued in the literature.

Table 4.2 Summary of rainfall intensities used in different numerical studies

Section No.	Numerical Study	Rainfall Intensity	
		m/s	mm/hr
4.5.1	Influence of AEV	3.0×10^{-07}	1.08
4.5.2	Coupled-Uncoupled analysis		
4.5.3	Linear and Non-linear ϕ^b	1.0×10^{-08}	0.04
4.5.4	Unimodal and Bimodal	2.78×10^{-06}	10
4.5.5	Influence of varying rainfall intensities	2.78×10^{-06} 1.0×10^{-08}	10 0.04

The conventional slope stability analysis is not the primary focus of this study; for this reason, it is only discussed in the numerical studies results presented in section 4.5.1. The saturated conditions of the slope are established by assuming the GWT at the model's surface and defining saturated soil properties for weathered Leda clay as input parameters in SLOPE/W (see Table 4.1). The conventional slope stability analysis yielded FS values of 0.454, 0.451 and 0.426 at upslope, mid slope, and toe slope, respectively. These values are considerably less than 1, therefore, they are not meaningful based on the limit equilibrium method. However, they are used in section 4.5.1 below to highlight the difference between saturated FS and unsaturated FS for weathered Leda clay slopes.

4.5.1 Influence of AEV on the wetting front and FS

In Chapter 3, three SWCCs (i.e., with AEV = 5 kPa, AEV = 15 kPa and AEV = 80 kPa) are chosen based on the range of SWCCs predicted using the Fredlund et al. (2002) model. Although the bimodal SWCC with AEV = 15 kPa is used throughout the numerical studies, the influence of different AEV SWCCs on PWP and FS variation is investigated in this section. In addition, rainfall flux, q, and k_{sat} are of equal value with 3.0 x 10^{-07} m/s (1.08 mm/hr) for numerical studies in this section. The duration of numerical studies is adjusted to allow the wetting fronts to propagate to greater depths, as observed in Figure 4.7.

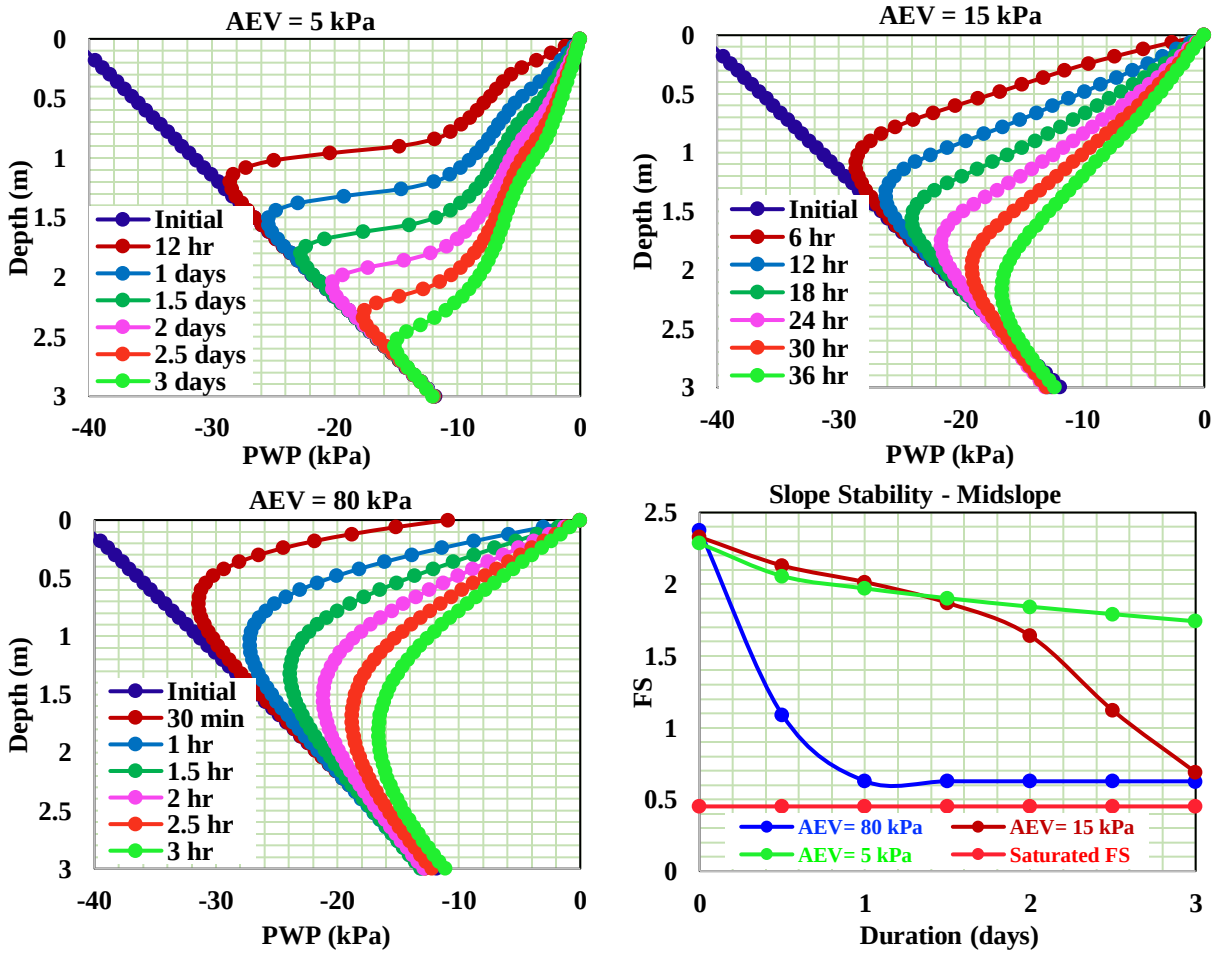

Figure 4.7 Influence of AEV on PWP and FS

Lumb (1962) defined the "wetting front" or "wetting band" as the sharp separation between the wetted zone and the initial condition. The difference in water storage functions can be used to understand the rate of wetting front movement for SWCCs with different AEVs (Zhang et al. 2004). The SWCC with a lower AEV tends to have a greater water storage capacity. Thus, the movement of the wetting front is much slower for AEV = 5 kPa and faster for AEV = 80 kPa. It takes three days for the wetting fronts to reach the depth of 3 m for AEV = 5 kPa, while it only takes 3 hours for AEV = 80 kPa. Zhang et al. (2004) achieved similar PWP profile variations for SWCCs with different AEV and the ratio of q/k_{sat} is equal to 1.

The wetting fronts propagated to greater depths faster for SWCC with AEV = 80 kPa (i.e., 3 hours), followed by AEV = 15 kPa (i.e., 36 hours) and finally AEV = 5 kPa (i.e., 3 days). Consequently, the FS values for AEV = 80 kPa are lowest and highest for AEV = 5 kPa (Figure 4.7). The mid slope slip surface determines the FS values for the current section. As the PWP increases (i.e., reducing the suction), the wetting fronts propagate to greater depths, reducing the shear strength and FS of the slip surface.

The FS of the mid slope assuming saturated soil conditions has been plotted in Figure 4.7 to compare with the results with the FS assuming unsaturated soil conditions. The unsaturated soil condition FS is higher (i.e., 0.6) than the saturated condition (i.e., 0.45). As discussed in the previous section, the FS values less than 1 have been used in this research for comparison purposes only. This result can be explained by the presence of unsaturated soil zones with higher suction in the slopes. In addition, the shear strength of the unsaturated soils tends to be greater than the saturated soil condition. Oh et al. (2014) reported similar results performing slope stability analysis for a shallow slope failure in Green's Creek. The contribution of unsaturated soil zones is visually

illustrated in their study. Therefore, the results and the model in this study tend to represent unsaturated soil conditions with relative accuracy.

4.5.2 Variation of PWP and FS for coupled and uncoupled analysis

The rainfall flux for this section is also equal to the saturated hydraulic conductivity, $3x10^{-07}$ m/s (1.08 mm/hr). Figure 4.8 presents PWP profile variations predicted using coupled and uncoupled analysis. The negative PWPs are equal to matric suction value with a sign difference, which means, for example PWP of -15 kPa is equal to a matric suction of 15 kPa. This is based on the definition the PWP is essentially equal to matric suction when they are measured with respect to atmospheric conditions. The data points for the PWP variations have been collected from the centre of the slip surface (i.e., approximate reference) locations specified in Figure 4.6. The data points for both coupled and uncoupled are collected from the same location to enable reasonable comparison.

The PWPs in the weathered layer (i.e., 3 m depth) are highlighted as this study focuses on the influence of rainfall infiltration in the top layer (i.e., weathered crust). The initial PWP distribution is at hydrostatic in nature for coupled and uncoupled analysis. However, the PWP values vary at the three locations (i.e., upslope > mid slope > toe slope) based on the proximity to the GWT. The PWPs tend to immediately increase towards zero once the rainfall infiltration commences at the slope surface. The PWP data presented in Figure 4.8 is collected from each element node spaced at 60 mm along the vertical. There are visible differences in the PWP profiles of coupled and uncoupled analysis at different locations. These differences may be a result of incorporating hydro-mechanical properties for the coupled analysis. The mechanical properties induce larger volume changes (i.e., soil softening upon wetting) resulting in even bigger changes

in the soil suction (Qi and Vanapalli 2015c). Therefore, the wetting fronts of coupled analysis tend to be sharper and reduce to greater depths faster than the uncoupled analysis.

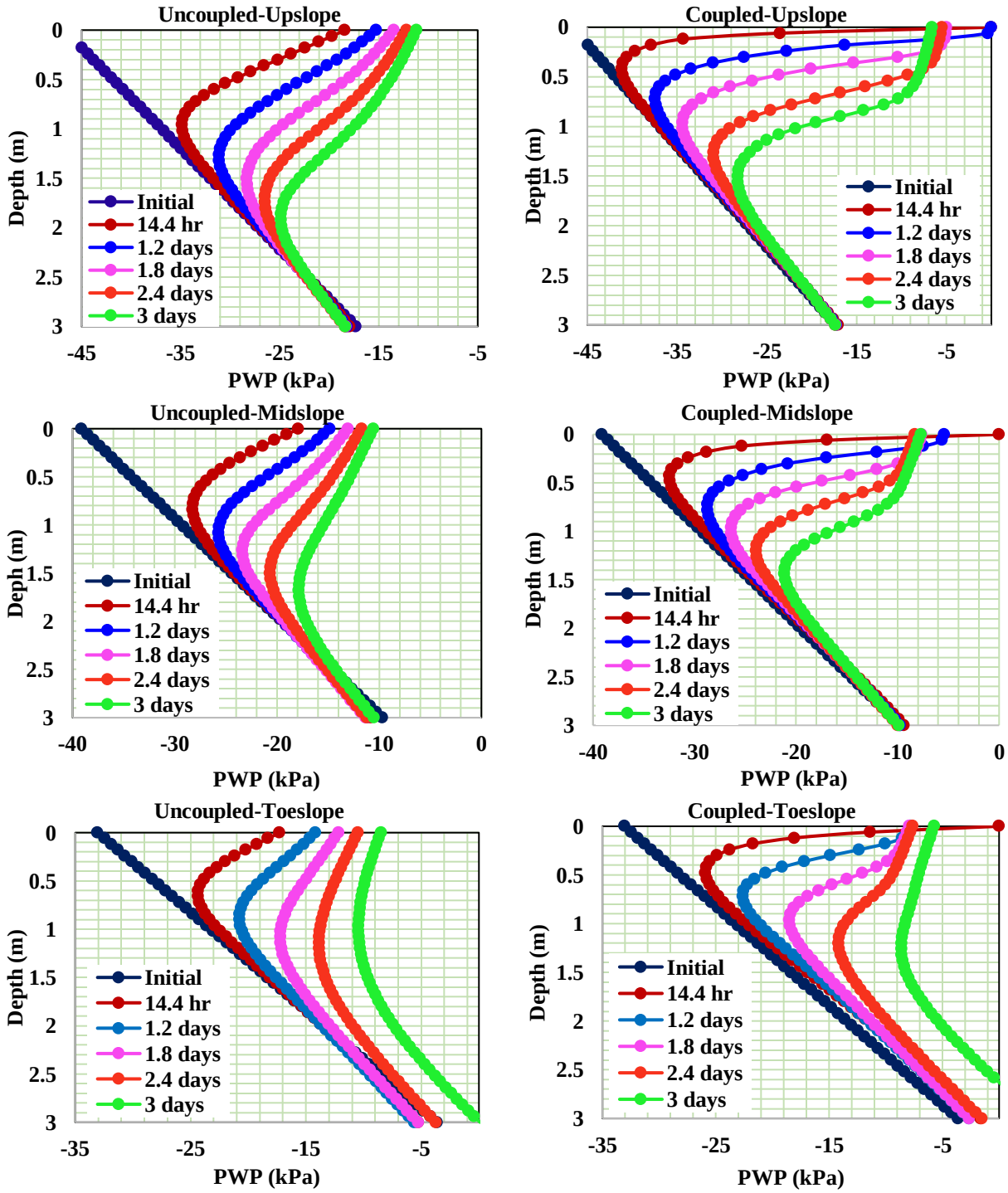

Figure 4.8 Comparison of PWP variations for coupled and uncoupled analysis

For example, the PWP variation at 14.4 hours is sharper for coupled analysis and gradual for uncoupled analysis at all locations. The mid slope and toe slope PWP variations are relatively similar for both coupled and uncoupled. However, the rate of downward movement of the coupled wetting fronts is marginally faster. Notably, several researchers (Qi and Vanapalli 2015b; c; Tran and Trinh 2019; Tan and Vanapalli 2021) present comparable PWP profile variations in coupled and uncoupled analysis. These researchers also consider the influence of coupled hydro-mechanical stresses on the distinctive PWP profile variation in coupled and uncoupled analysis.

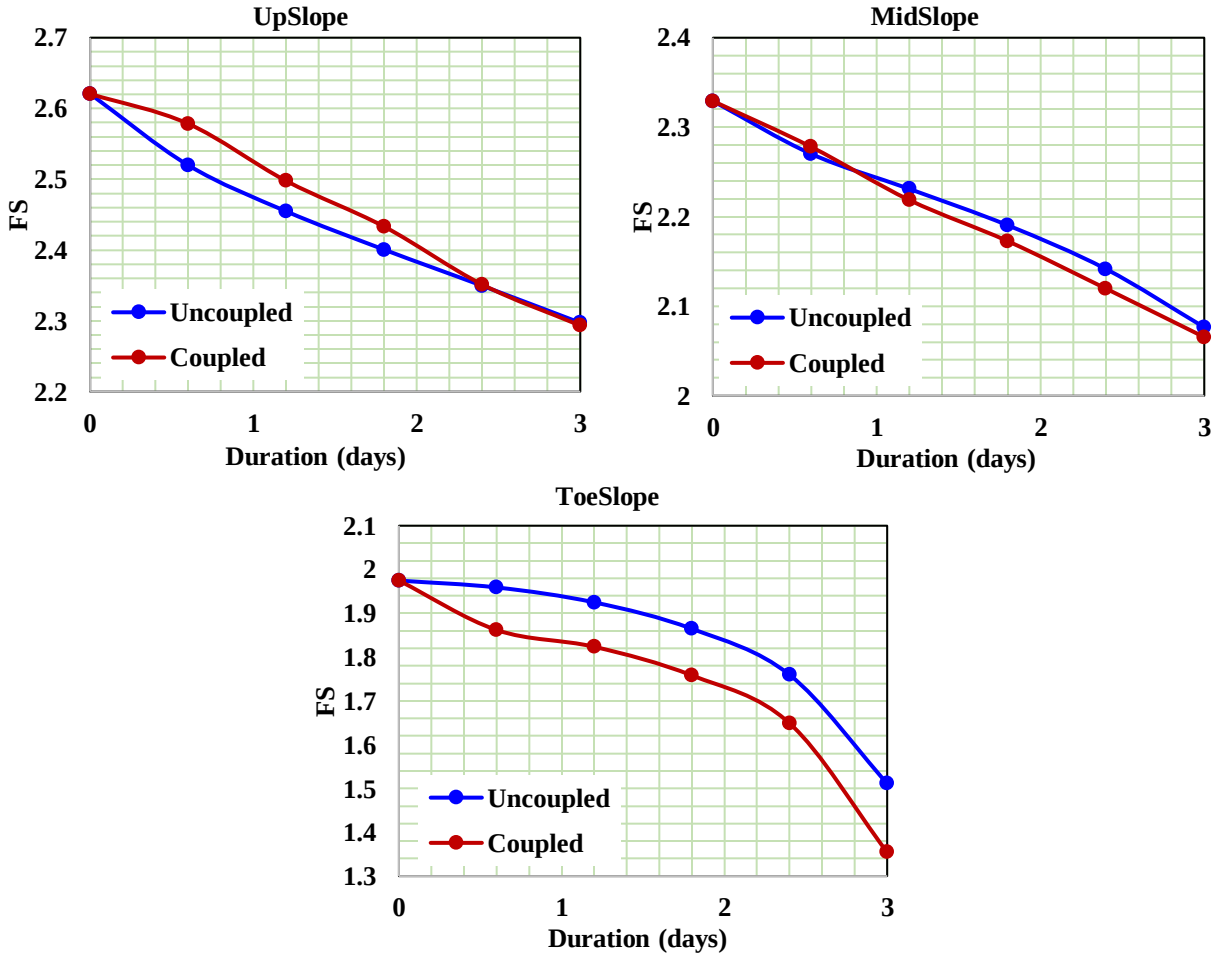

Figure 4.9 Variation of FS for coupled and uncoupled analysis

The factor of safety (FS) of the weathered layer is affected by the downward movement of the wetting fronts. Figure 4.9 shows the variation of FS with depth at different locations along the

slope, which is consistent with the PWP profile variations in Figure 4.8. The downward propagation of wetting fronts reduces the suction in the weathered layer, leading to a reduction in the shear strength and FS of the soil slope. Thus, the FS values generally decrease as the wetting fronts propagate to greater depths.

However, this study also investigates the influence of coupled hydro-mechanical stress on the FS of a weathered slope. The rate of downward propagation of wetting fronts influences the difference between the coupled and uncoupled FS results. In coupled hydro-mechanical analyses, the soil undergoes volume change due to soil softening upon wetting, while the uncoupled analyses do not consider the variations in volume change behavior. Therefore, the PWP infiltrates faster in the coupled analysis compared to the uncoupled analysis. This means that the matric suction, shear strength and FS also reduce at a faster rate (see Figure 4.9).

The variation of FS down the slope (i.e., from upslope to mid slope to toe slope) shows a steady decrease in the FS of safety values. The higher values for FS in the upslope location followed by midslope and toeslope can be explained by the higher suction values compared to other locations. This shows that it will take more time to fail compared to the toeslope location. It should be noted that the initial suction value near the head of the slope was 50 kPa compared to 30 kPa at the toeslope. In addition, the proximity of GWT to the toeslope also influences a faster failure condition compared to other locations. Furthermore, the duration of the FS study in this scenario is only 3 days and may not be sufficient to induce a slope failure. If the investigations are extended for longer duration, it is likely FS values will be lower and likelihood of slope failures increase. There are more comparisons of FS related to coupled and uncoupled analysis in the section in which comparisons are provided for understanding the influence of varying rainfall intensities (see section 4.5.5).

4.5.3 Influence of linear and non-linear unsaturated shear strength equations on FS

In the linear unsaturated shear strength equation (Eq. 2.6) the shear strength always increases linearly with respect to soil suction. This may not always be representative especially when the soil suction is very high, as a result, the shear strength may be overestimated (GeoSlope International Ltd. 2007a). SLOPE/W uses the non-linear shear strength equation proposed by Vanapalli et al. (1996) (Eq. 4.9) to alleviate this limitation. This equation uses the SWCC and the saturated shear strength parameters for predicting the shear strength of unsaturated soils. Both linear and non-linear method computation can be conducted using the SLOPE/W software. Therefore, a comparison is attempted using a rainfall influx of 1.0×10^{-08} m/s and other soil parameters, as provided in Table 4.1.

The FS for using a linear unsaturated shear strength equation tends to be lower than that of a non-linear equation at all three locations (Figure 4.10). The difference in FS at the upslope and mid slope is much more significant than at the toe slope. It should also be noted that the slope does not fail at the first two locations but fails at the toe slope. This may be due to the proximity of the toe slope slip surface to the GWT. The GWT may cut through or submerge the toe slope slip surface after 150 days of rainfall. The shear strength reduces due to the PWP profile, thus contributing to the reduction of FS. However, the disparity between the FS values for linear and non-linear shear strength equations can result from the assumption that constant ϕ^b is half of ϕ' in this study. The linear equation tends to provide a lower shear strength value than the non-linear equation. Therefore, the linear method yields a lower FS value than the non-linear one in this research.

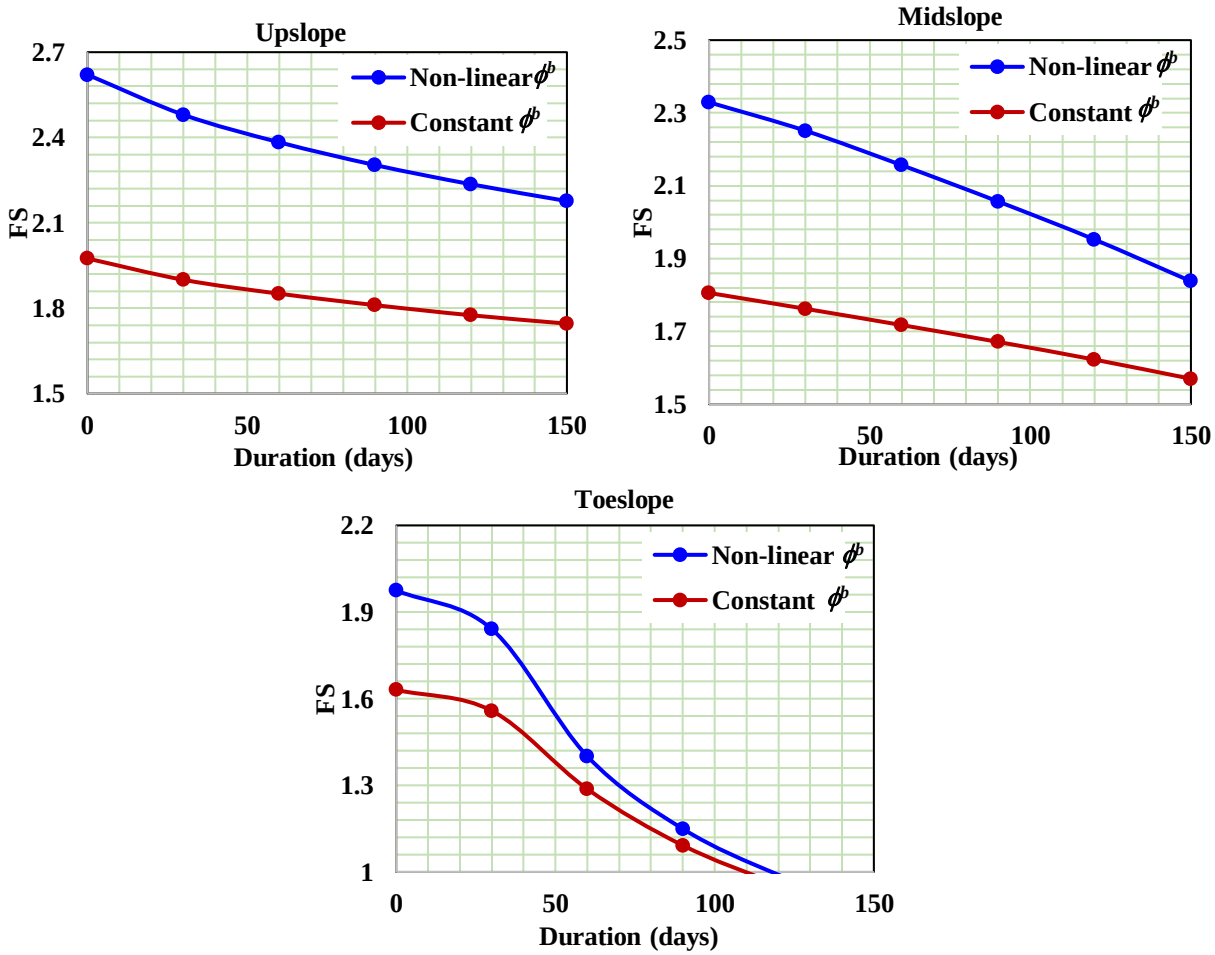

Figure 4.10 Variation of FS for non-linear and constant fb shear strength equations

Similar trends are observed by other researchers (Xinpo et al. 2006; Batali and Andreea 2016) who have attempted to study the contribution of different shear strength equations to slope stability analyses. Batali and Andreea (2016) examined numerous shear strength equations to evaluate the FS for a case study on a site vulnerable to landslides in Cluj-Napoca, Romania. The compared methods included the linear and non-linear shear strength equations preferred in this study. The results of their research had lower and higher FS values for linear and non-linear shear strength equations, respectively.

In addition, Xinpo et al. (2006) used a theoretical model to study the rainfall-induced instability of infinite loess slopes. Their study presents the relationship between ϕ' and FS of a

slope with an inclination angle of 27° (i.e., close to the model in this study with 28°). As expected, the lower frictional angle yielded a lower FS value. Therefore, the results obtained in this study are reasonable.

4.5.4 Influence of unimodal SWCC and bimodal SWCC on the FS

The weathered layer in this study is represented using a bimodal SWCC to consider the coupled influence of both macro and micro pores that contribute to differences in flow of infiltrating water due to the influence of cracks. A comparison is presented in Figure 4.11 that illustrates the influence of unimodal SWCC and bimodal SWCC on PWP profile variation and the FS value.

The numerical studies were conducted simulating a 10 mm/hr rainfall influx for 40 hours with other soil properties input from Table 4.1. It should also be noted that the results represent uncoupled analysis. The observation at the upslope location shows the wetting fronts for the bimodal SWCC moving down faster than the unimodal SWCC. Such a trend can be attributed to the simulation of cracks in bimodal SWCC that may allow the water to infiltrate more quickly than the unimodal SWCC. A close investigation of the wetting front after 16 hours at upslope shows that the bimodal wetting front is slightly deeper than the unimodal (Figure 4.12).

In contrast, the mid slope PWP profile variations (Figure 4.11) tend to resemble each other to a greater extent. In addition, results summarized in Figure 4.12 suggest that the wetting fronts seem to move down at a similar rate, but the bimodal is marginally deeper than the unimodal SWCC.

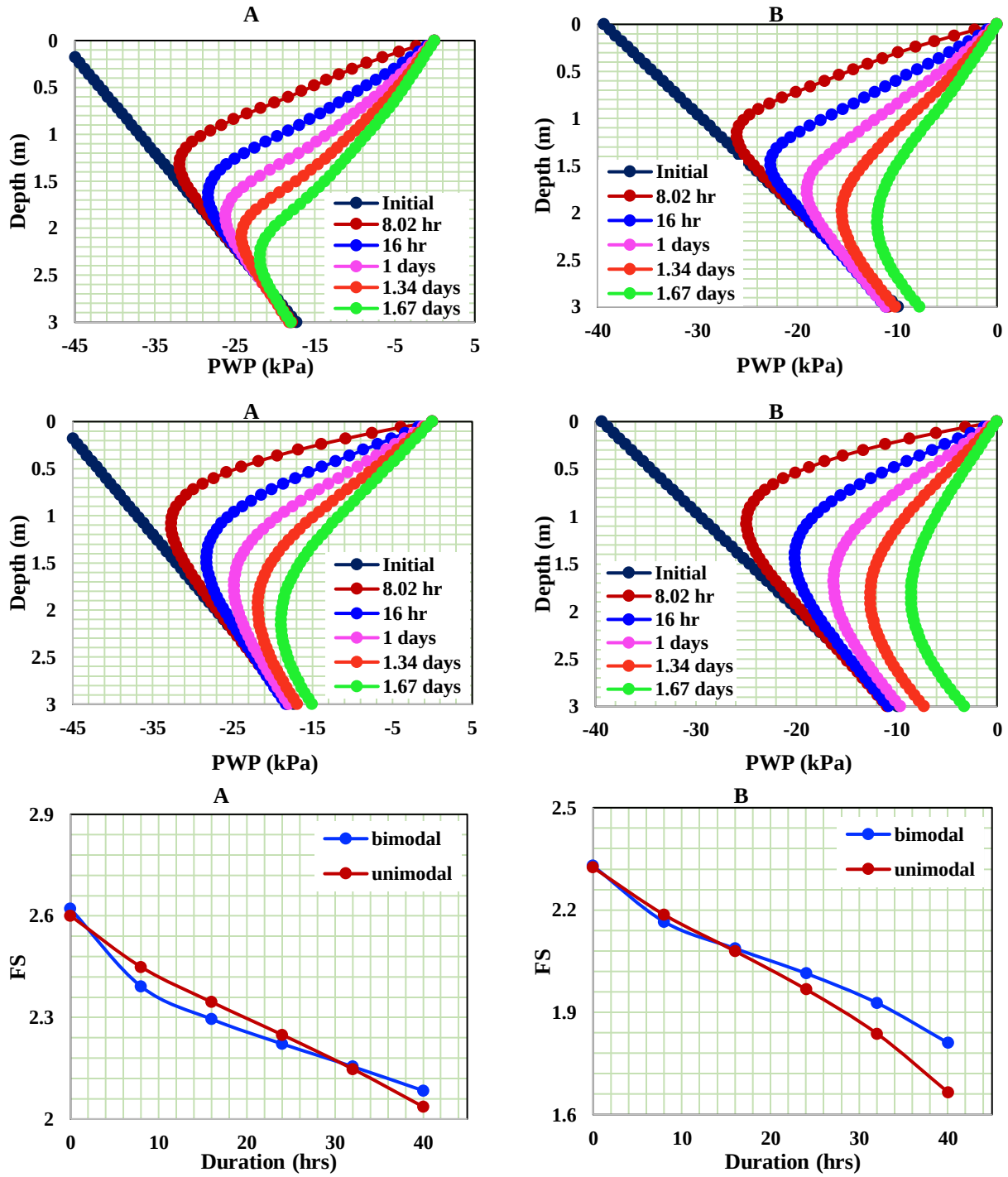

Figure 4.11 Slope stability analysis using BM-SWCC and UM-SWCC at different locations on the slope; (A) Upslope, (B) Midslope

The FS results in Figure 4.11 follow the same trend with the PWP profile variation, as the bimodal SWCC yields a lower FS when the wetting fronts move down faster. It can be observed

that the unimodal FS increases towards the 40-hour duration; this can be seen in the PWP profile variation, where the unimodal wetting fronts tend to move faster than the bimodal wetting fronts.

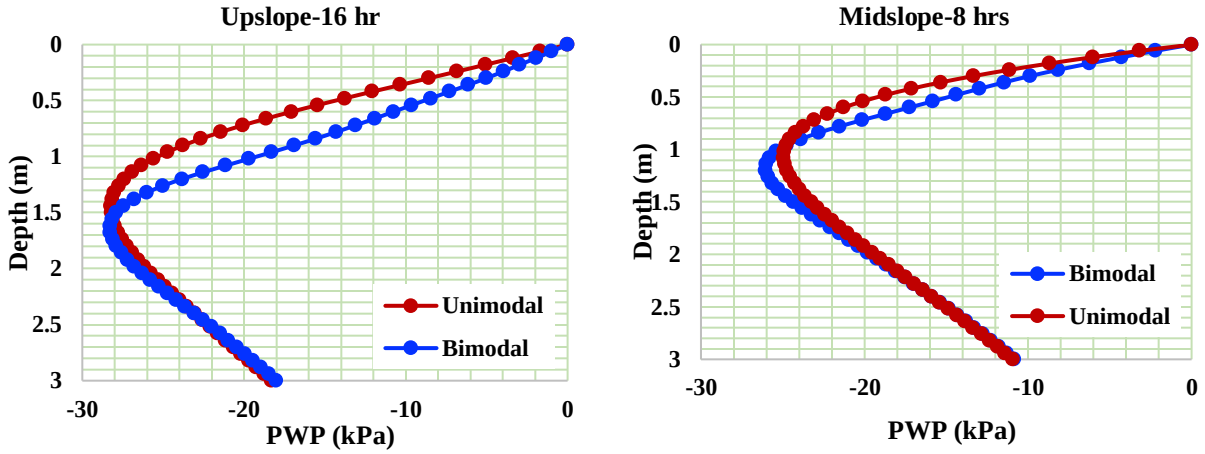

Figure 4.12 Comparison of bimodal and unimodal wetting fronts at upslope and midslope

Qi and Vanapalli (2015b) also observed a similar trend when comparing the FS values using unimodal and bimodal SWCCs. Therefore, bimodal SWCC provide reasonable FS values as it better incorporates the weathering phenomenon in the analysis.

4.5.5 Influence of varying rainfall intensity on coupled and uncoupled FS

This section compares the trends of coupled and uncoupled FS for different rainfall intensities. It's possible for the rainfall intensity to be greater or lower than the k_{sat} of the weathered layer. For this reason, analysis is undertaken for rainfall intensities higher (i.e., 2.78x10-6 m/s or 10 mm/hr) and lower (i.e., 1.0x10-8 m/s or 0.04 mm/hr) than the saturated hydraulic conductivity (i.e., 3.7x10-7 m/s). The results show that the coupled FS tends to be higher than the uncoupled FS for rainfall influx of 10 mm/hr over 2 days. However, for rainfall influx of 0.04 mm/hr over 150 days, the coupled FS is lower than the uncoupled FS.

Figure 4.13 (B) depicts the results of the low-intensity rainfall, which align with the discussion in section 4.5.2. This discussion highlights how the rate of downward movement of

wetting fronts affects the FS values of the slope. The coupled analysis moves to a greater depth faster due to the mechanical stress that softens the soil upon increased rainfall infiltration.

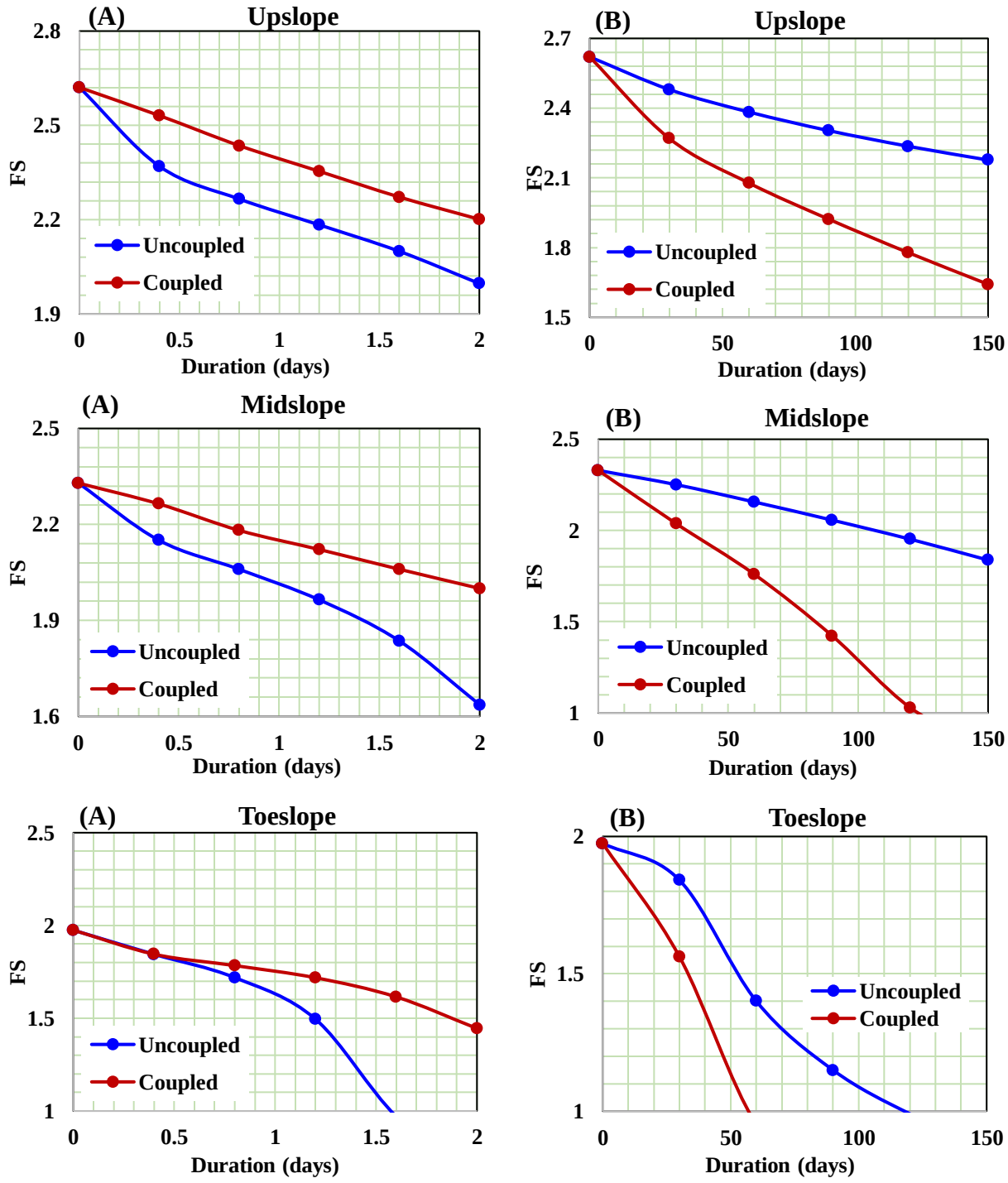

Figure 4.13 Influence of varying rainfall intensity on FS using coupled and uncoupled comparison; (A) 2.78x10-06 m/s (10 mm/hr), and (B) 1.0x10-08 m/s (0.04 mm/hr)

Qi and Vanapalli (2015a and 2015c) investigated the influences on rainfall intensities of slopes in expansive soils with values below and slightly above the saturated hydraulic conductivity, respectively. Their findings indicate that when rainfall intensities are below or slightly above the soil's saturated hydraulic conductivity, the resulting FS variations are similar to those observed in the low-intensity rainfall results of this study. The contrasting results for the high-intensity rainfall (i.e., Figure 4.12 (A)) with a higher coupled and lower uncoupled FS may be related to the saturated hydraulic conductivity being lower than the rainfall influx.

Insights into the impact of rainfall intensity on the analysis of weathered Leda clay slope, for both coupled or uncoupled conditions, are provided from the findings in sections 4.5.2 and 4.5.5. It was noted that low-intensity rainfall led to a lower FS for both coupled and uncoupled analyses over a longer duration. The intensity of rainfall influx being low, the occurrence of slope failure could be relatively longer than in the event of high-intensity rainfall. In the current scenario, the coupled analysis takes approximately 60 days, whereas the uncoupled analysis takes 120 days to induce slope failure at the toeslope. On the other hand, even after 150 days, the rainfall infiltration at the upslope is not adequate to penetrate the weathered crust entirely and reduce the shear strength contribution arising from suction.

These conclusions are consistent with the FS patterns results of Qi and Vanapalli's (2015) research for low-intensity rainfall (0.04 mm/hr and 1.08 mm/hr) on the weathered crust. However, Qi and Vanapalli (2015) research did not investigate high-intensity rainfall, so their findings cannot be compared to those of this study for high-intensity rainfall.

4.6 Conclusion

In this chapter, a series of numerical studies were conducted on a model slope representing a typical weathered Leda clay slope in the Ottawa region. To gain a comprehensive understanding

of the theoretical aspects of the modelling, a succinct overview of slope stability, with a particular focus on the hydro-mechanical coupling method, is presented. The numerical model is specifically designed to examine the third stage of valley formation in the Ottawa region, discussed in section 2.2.1. This stage involves a complete weathering of the slope's surficial layer from head to toe. To ensure a rational numerical analysis, the model considers the hydro-mechanical behavior changes that occur in the weathered zone. This zone is represented by a bimodal SWCC, which contrasts with the intact layer that features little variation in pore sizes and is represented by a unimodal curve. Moreover, the assumptions made in the analysis regarding boundary conditions and soil properties are justified in relation to the numerical model.

The section on results and discussion provides a detailed examination of the factors that impact the stability of weathered Leda clay slopes. The study explores how different AEV affects the downward movement of wetting fronts, which in turn influences shear strength and FS. Additionally, the analysis compares using unimodal and bimodal SWCC in numerical studies, with the latter presenting lower FS values due to its dual porosity nature that allows for faster water infiltration and shear strength loss. The study also investigates the impact of using linear and non-linear unsaturated shear strength equations on the FS of the slope. The results highlight that the non-linear equation provides higher FS values than the linear one. Finally, the study compares coupled and uncoupled analyses under varying rainfall influx and constant saturated hydraulic conductivity. The coupled analysis tends to have lower FS values for low-intensity rainfall, but higher FS values for high-intensity rainfall.

The variation of the PWP profile (i.e., a series of wetting fronts) has the potential to serve as a crucial indicator of the weathered surficial slope's shear strength. This information can be utilized

to determine the slope's FS and is particularly helpful in anticipating and preparing for potential landslide hazards triggered by rainfall.

CHAPTER 5: CONCLUSIONS AND RECOMMENDATIONS

5.1 Introduction

There is a notable change in climate trends in the Ottawa region associated with global warming. Due to this reason, the risk of instability of slopes and landslides increases with anticipated increases in rainfall infiltration that can have a significant impact on sensitive Leda clays in Ottawa region. Therefore, it is crucial to study and understand the behaviour of Leda clay slopes to ensure the safety of geotechnical structures considering the influence of different likely scenarios associated with climate changes.

Environmental fluctuations such as freezing-thawing and wetting-drying cycles affect the surficial layers of Leda clay slopes as they undergo weathering. The weathered crust typically is desiccated and contributes to cracks in the surficial layers of the Leda clay slope, which are typically in an unsaturated state. Conventional slope stability analysis using saturated soil mechanics may not reliably represent the in-situ conditions in the slope. Therefore, unsaturated soil mechanics can be used as a tool to conduct rigorous slope stability analyses on the weathered Leda clay slope. During the last two decades, significant advancements were made in the implementation of the state-of-the-art understanding the mechanics of unsaturated soils using numerical methods. In these methods, the soil-water characteristic curve (SWCC) and the saturated soil properties are used for the analysis.

Since the weathered Leda clay develops cracks that lead to the formation of macro and micro pores, a bimodal SWCC is used as a tool for reasonably predicting the hydro-mechanical behavioural properties. As direct measurements of the bi-modal SWCC are time consuming and need elaborate testing equipment, simple tools for approximating the SWCC for weathered Leda

clay will be valuable for use in engineering practice applications. There is limited data on the measured SWCC for Leda clay; however, they are not representative of the in-situ conditions. To address this data deficiency, a representative SWCC is estimated extending the model proposed by Fredlund et al. (2002) by utilizing soil properties obtained from borehole logs in the Ottawa region.

The key objective study is to suggest a numerical technique that the practicing engineers can use to conduct numerical analysis for the rational design of slopes considering the influence of various rainfall infiltration scenarios in weathered Leda clay slopes.

5.2 Conclusions

The work presented in this thesis encompasses two primary research objectives: (i) estimating the bimodal-SWCC that can be used for representing the weathered and intact layer and use it in the slope stability analysis (ii) coupled numerical analysis technique to rigorously investigate the influence of rainfall infiltration on weathered Leda clay slope stability in the Ottawa region.

The following conclusions can be derived from the research work performed:

1. The estimation of weathered crust SWCC considers the in-situ conditions of the Ottawa region. This is made possible by collecting borehole log data from geotechnical reports for regional projects containing weathered Leda clay. The Fredlund et al. (2002) model is used to estimate the unimodal SWCC using GSD curves and other relevant soil properties. The upper, median, and lower bound AEV SWCCs are selected to represent the weathered Leda clay from a range of estimated SWCCs. The estimated unimodal-SWCCs and Taha's (2010) -SWCC for the intact layer were used to derive three bimodal-SWCCs to represent the SWCCs with AEV = 5 kPa, AEV = 15 kPa, and 80 kPa, respectively.

2. The numerical model extended in this study closely simulates typical weathered Leda clay slopes around Greens Creek in the Ottawa region. An attempt was made to ensure that the boundary conditions and soil properties were representative of the in-situ conditions by using input data from various literature works related to slope stability in the Ottawa region.
3. The results from numerical analysis and comparisons are required for comprehending the impact of rainfall on weathered Leda clay. A typical SWCC with a lower AEV and a steeper slope in a weathered clay leads to a higher water storage capacity as compared to a higher AEV. This, in turn, influences the rate of downward movement of wetting fronts and affects the FS of slopes. The coupled analysis shows a lower FS than the uncoupled analysis owing to the impact of mechanical stress on soil particles, increases the infiltration rate and softens them. However, the study notes that the coupled analysis has a higher FS during high-intensity rainfall. The reason for this phenomenon can be attributed to the intensity of rainfall, which exceeds the soil's capacity to absorb water. As a result, the soil pores become saturated, hindering further infiltration. This reduction in infiltration rate minimizes the loss of shear strength, leading to an increase in the factor of safety.
4. In this study, it was found that the semi-empirical non-linear shear strength equation produced a higher FS value for the intact layer compared to the linear unsaturated shear strength equation, which resulted in a lower FS value for the weathered slope. The reason for this is that the bimodal SWCC, which represents the cracked or weathered crust, has a first AEV of only 15 kPa, significantly less than the intact layer AEV of 400 kPa. The shear strength behaves linearly up to the AEV of the soil, meaning that the contribution of the linear unsaturated shear strength equation is considerably less when dealing with a bimodal

SWCC. If the SWCC were unimodal, the shear strength from the linear equation would be greater and could potentially overestimate the FS value.

5.3 Recommendations for future works

More research studies are required on weathered Leda clay slopes to address the limitations of the current work. These limitations stem from factors such as complexity, cost, and time. The following recommendations provide valuable insights on how to improve our understanding:

- Conduct extensive experimental research studies on samples collected from in-situ weathered crust of Leda clay in the Ottawa region and measure the bimodal SWCC. The gathered data will be valuable for proposing reliable estimation techniques for the bimodal SWCC that is more representative of the weathered crust.
- The estimation of the bimodal SWCC is an area of research that may benefit from the use of advanced methods such as Artificial Intelligence (AI), provided that a sufficiently large dataset is available. However, to enhance the reliability of the results obtained from such studies, it is necessary to acquire a more extensive dataset. In this regard, it is worth noting that the dataset used in this study for estimating the bimodal SWCC for weathered crust was limited to approximately 100 data lines. Therefore, to yield more reasonable estimates, it is crucial to expand the dataset for AI-based studies or general estimation.
- The characteristics of soil in a cracked or weathered crust can vary frequently as the environment changes. Relying on a single bimodal SWCC to capture this phenomenon is not reasonable. The bimodal SWCC of weathered crust is sensitive to environmental factors. Therefore, additional research is necessary to establish a numerical modelling technique that reasonably reflects the worst-case scenario in-situ conditions of weathered Leda clay slopes.

References

AASHTO. 1982. “Standard specifications for transportation materials and methods of testing and sampling.” American Association of State Highway and Transportation Officials. Washington, DC, USA

Aldaeef, A. A., and M. T. Rayhani. 2015. “Hydraulic performance of compacted clay liners under simulated daily thermal cycles.” *J Environ Manage*, 162: 171–178. Academic Press. https://doi.org/10.1016/j.jenvman.2015.07.036.

Alexander, A. E., and P. Johnson. 1949. *Colloid Science*. Oxford: Clarendon Press.

Al-Khazaali, M. 2019. Soil-pile, pile group foundations and pipeline systems interaction behavior extending saturated and unsaturated soil mechanics. Ottawa.

Al-Umar, M. 2018. “GIS based assessment of climate-induced landslide susceptibility of sensitive marine clays in the Ottawa region, Canada.” Ph.D. Ottawa: University of Ottawa.

Al-Umar, M., M. Fall, and B. Daneshfar. 2022. “GIS based assessment of rainfall-induced landslide susceptibility of sensitive marine clays: a case study.” *Geomechanics and Geoengineering*, 17 (5): 1458–1484. Taylor and Francis Ltd. https://doi.org/10.1080/17486025.2021.1955152.

Alves, R. D., G. de F. N. Gitirana, and S. K. Vanapalli. 2020. “Advances in the modeling of the soil–water characteristic curve using pore-scale analysis.” *Computer Geotech*, 127. Elsevier Ltd. https://doi.org/10.1016/j.compgeo.2020.103766.

Andrews J. T. 1972. “Post-Glacial Rebound.” *The National Atlas of Canada*, 35–36.

Arya, L. M., F. J. Leij, M. Th. van Genuchten, and P. J. Shouse. 1999. “Scaling Parameter to Predict the Soil Water Characteristic from Particle-Size Distribution Data.” *Soil Science Society of America Journal*, 63 (3): 510–519. Wiley. https://doi.org/10.2136/sssaj1999.03615995006300030013x.

Arya, L. M., and J. F. Paris. 1981. “A Physicoempirical Model to Predict the Soil Moisture Characteristic from Particle-Size Distribution and Bulk Density Data.” *Soil Science Society of America Journal*, 45 (6): 1023–1030. Wiley. https://doi.org/10.2136/sssaj1981.03615995004500060004x.

Aubertin, M., M. Mbonimpa, B. Bussière, and R. P. Chapuis. 2003. "A model to predict the water retention curve from basic geotechnical properties." *Canadian Geotechnical Journal*, 40 (6): 1104–1122. https://doi.org/10.1139/t03-054.

Aylsworth, J. M., D. E. Lawrence, and J. Guertin. 2000. "Did two massive earthquakes in the Holocene induce widespread landsliding and near-surface deformation in part of the Ottawa Valley, Canada?" *Geology*, 28 (10): 903. https://doi.org/10.1130/0091-7613(2000)28<903:DTMEIT>2.0.CO;2.

Azam, S., and M. Ito. 2011. "Unsaturated soil properties of a fissured expansive clay." *14th Pan-American Conference on Soil Mechanics and Geotechnical Engineering*. Toronto, ON.

Bäckström, K. and Linder, A. 2021. Fault Tree Analysis of Quick Clay Slides (Dissertation). Retrieved from https://urn.kb.se/resolve?urn=urn:nbn:se:kth:diva-299065

Barbour, S. L. 1998. "Nineteenth Canadian Geotechnical Colloquium: The soil-water characteristic curve: a historical perspective." *Canadian Geotechnical Journal*, 35 (5): 873–894. https://doi.org/10.1139/t98-040.

Batali, L., and C. Andreea. 2016. "Slope Stability Analysis Using the Unsaturated Stress Analysis. Case Study." *Procedia Eng*, 284–291. Elsevier Ltd.

Bechai, M. 1974. "Determination of the Preconsolidation Pressure for a Sensitive Marine Clay." Master of Applied Science. Ottawa: University of Ottawa.

Bennet, R. H. 1976. "Clay Fabric and Geotechnical Properties of Selected Submarine Sediment Cores from the Mississippi Delta." PhD. Texas A&M University.

Bentley, S. P., and I. J. Smalley. 1978. "Mineralogy of sensitive clays from Quebec." *The Canadian Mineralogist*, 16: 103–112.

Bouma, J. 1989. "Using soil data for quantitative land evaluation." *Advances in Soil Science*, 9: 177–213.

Bozozuk, M. 1963. "The modulus of elasticity of Leda clay from field measurements." *Canadian Geotechnical Journal*, 1 (1): 43–51.

Brady, N. C., and R. R. Weil. 2008. *The Nature and Properties of Soil*. Upper Saddle River, NJ.

Brooks, R. H., and A. T. Corey. 1964. "Hydraulic properties of porous media." *Hydrology Paper No. 3. Southern Cooperative Series Bulletin*, Colorado State University. Hydrology papers, no. 3, (A. T. Corey, ed.), 1964.

Brydon, J. E., and L. M. Patry. 1961. “Mineralogy of Champlain Sea sediments and a Rideau clay soil profile.” *Canadian Journal of Social Science*, 41 (2): 169–181.

Burger, C. A., and C. D. Shackelford. 2001. “Evaluating dual porosity of pelletized diatomaceous earth using bimodal soil-water characteristic curve functions.” *Canadian Geotechnical Journal*, 38 (1): 53–66. Canadian Science Publishing. https://doi.org/10.1139/cgj-38-1-53.

Catana, M. C. 2006. “Compaction and Water Retention Characteristics of Champlain Sea Clay.” MASc. Ottawa: University of Ottawa.

Catana, M. C., S. K. Vanapalli, and V. K. Garga. 2006. “The Water Retention Characteristics of Compacted Clays.” *Unsaturated Soils 2006*, 1348–1359. Reston, VA: American Society of Civil Engineers.

CFEM. 2006a. “Identification and Classification of Soil and Rock.” *Canadian Foundation Engineering Manual*. Canadian Geotechnical Society.

CFEM. 2006b. “Identification and Classification of Soil and Rock.” *Errata - Canadian Foundation Engineering Manual*, 18. Canadian Geotechnical Society.

City of Ottawa. 2020. *Climate Change Master Plan*. Ottawa.

City of Ottawa. 2023. “Development Applications Search.” *City of Ottawa*. Accessed October 8, 2023. https://devapps.ottawa.ca/en/.

Climate Atlas of Canada. 2021. “Climate Atlas Report Region: OTTAWA RCP 8.5: High Carbon climate future GHG emissions continue to increase at current rates.”

Crawford, C. B. 1968. “Quick clays of eastern Canada.” *Eng Geol*, 2 (4): 239–265. https://doi.org/10.1016/0013-7952(68)90002-1.

Cruden, D. M. 1991. “A simple definition of a landslide.” *Bulletin of the International Association of Engineering Geology*, 43 (1): 27–29. https://doi.org/10.1007/BF02590167.

Cruden, D. M., and D. J. Varnes. 1996. “Chapter 3-Landslide types and processes.” *Landslides: investigation and mitigation, Transportation research board special report*, 247: 37–75.

Das, T., V. D. Rao, and D. Choudhury. 2022. “Numerical investigation of the stability of landslide-affected slopes in Kerala, India, under extreme rainfall event.” *Natural Hazards*, 114 (1): 751–785. Springer Science and Business Media B.V. https://doi.org/10.1007/s11069-022-05411-x.

Demers, D., D. Robitaille, P. Locat, and J. Potvin. 2014. “Inventory of Large Landslides in Sensitive Clay in the Province of Québec, Canada: Preliminary Analysis.” 77–89.

Dreimanis, A. 1976. “Tills: Their origin and properties.” *Royal Society of Canada Special Publication*, 12: 11–49.

Du, Y., M. Xie, and J. Jia. 2020. “Stepped settlement: A possible mechanism for translational landslides.” *Catena (Amst)*, 187: 104365. https://doi.org/10.1016/j.catena.2019.104365.

Ebrahimi-Birang, N., & Fredlund, D. G. 2016. “Assessment of the WP4-T device for measuring total suction.” *Geotechnical Testing Journal*, 39(3), 500-506. https://doi.org/10.1520/GTJ20150118

Eden, W. J. 1966. “An Evaluation of the Field Vane Test in Sensitive Clay.” *Van Shear and Cone Penetration Resistance Testing of In-Situ Soils*, 8-8–10. 100 Barr Harbor Drive, PO Box C700, West Conshohocken, PA 19428-2959: ASTM International.

Eden, W. J., and C. B. Crawford. 1957. “Geotechnical properties of Leda clay in the Ottawa area.” *International Conference of Soil Mechanics and Foundation Engineering*, 22–27. London.

Eden, W. J., and J. J. Hamilton. 1957. “The Use of a Field Vane Apparatus in Sensitive Clay.” *Symposium on Vane Shear Testing of Soils*, 41-41–13. 100 Barr Harbor Drive, PO Box C700, West Conshohocken, PA 19428-2959: ASTM International.

Eden, W. J., and R. J. Mitchell. 1970. “The mechanics of landslides in Leda clay.” *Canadian Geotechnical Journal*, 7 (3): 285–296.

Eden, W. J. 1975. “Mechanism of landslides in Leda clay with special reference to the Ottawa area.” Division of Building Research, National Research Council

Elson, J. A. 1969. “Late Quaternary marine submergence of Quebec.” *Revue de géographie de Montréal*, 23 (3): 247–258.

Farrell, D. A., and W. E. Larson. 1972. “Modeling the pore structure of porous media.” *Water Resour Res*, 8 (3): 699–706. https://doi.org/10.1029/WR008i003p00699.

Fransham, P. B., and N. R. Gadd. 1977. “Geological and geomorphological controls of landslides in Ottawa Valley, Ontario.” *Canadian Geotechnical Journal*, 14 (4): 531–539. https://doi.org/10.1139/t77-054.

Fredlund, D. 2015. “Use of unsaturated soil mechanics for environmental protection and sustainability.” *The International Conference on Multiphysical Interaction and Environment Mine*.

Fredlund, D. G. 2006. “Unsaturated Soil Mechanics in Engineering Practice.” *Journal of Geotechnical and Geoenvironmental Engineering*, 132 (3): 286–321. https://doi.org/10.1061/(ASCE)1090-0241(2006)132:3(286).

Fredlund, D. G., and N. R. Morgenstern. 1977. “Stress State Variables for Unsaturated Soils.” *Journal of the Geotechnical Engineering Division*, 103 (5): 447–466. https://doi.org/10.1061/AJGEB6.0000423.

Fredlund, D. G., N. R. Morgenstern, and R. A. Widger. 1978. “The shear strength of unsaturated soils.” *Canadian Geotechnical Journal*, 15 (3): 313–321. https://doi.org/10.1139/t78-029.

Fredlund, D. G., H. Rahardjo, and M. D. Fredlund. 2018. “Understanding the Family of Soil-Water Characteristic Curves.” *Geo Edmonton*. Edmonton: Canadian Geotechnical Society.

Fredlund, D. G., D. Sheng, and J. Zhao. 2011. “Estimation of soil suction from the soil-water characteristic curve.” *Canadian Geotechnical Journal*, 48 (2): 186–198. https://doi.org/10.1139/T10-060.

Fredlund, D. G., and A. Xing. 1994. “Equations for the soil-water characteristic curve.” *Canadian Geotechnical Journal*, 31 (4): 521–532. https://doi.org/10.1139/t94-061.

Fredlund, M. D. 1999. “The role of unsaturated soil property functions in the practice of unsaturated soil mechanics.” Ph.D. Saskatoon: University of Saskatchewan.

Fredlund, M. D., D. G. Fredlund, and G. W. Wilson. 1997. “Prediction of the Soil-Water Characteristic Curve from Grain-Size Distribution and Volume-Mass Properties.” *3rd Brazilian Symposium on Unsaturated Soils*, 13–23. Rio de Janeiro.

Fredlund, M. D., G. W. Wilson, and D. G. Fredlund. 2002. “Use of the grain-size distribution for estimation of the soil-water characteristic curve.” *Canadian Geotechnical Journal*, 39 (5): 1103–1117. https://doi.org/10.1139/t02-049.

Gadd, N. R. 1975. “Geology of Leda clay.” *In Fourth Guelph symposium on geomorphology*, 137–151.

Gadd, N. R. 1976. *Surficial geology and landslides of Thurso-Russell map-area, Ontario: 31 G/6E and 31 G/11E (Ontario portion)*. Paper (Geological Survey of Canada); 75-35. book. Ottawa: Geological Survey of Canada, Energy, Mines, and Resources Canada.

Gardner, W. R. 1958. “Some steady-state solutions of the unsaturated moisture flow equation with application to evaporation from a table.” *Soil Sci*, 85 (4): 228–232.

Garga, V. K., M. A. Khan, and S. K. Vanapalli. 2006. "Stress-path dependent behavior of a weathered clay crust." *Geotechnical and Geological Engineering*, 24 (6): 1481–1509. https://doi.org/10.1007/s10706-005-2635-3.

van Genuchten, M. Th. 1980. "A Closed-form Equation for Predicting the Hydraulic Conductivity of Unsaturated Soils." *Soil Science Society of America Journal*, 44 (5): 892–898. Wiley. https://doi.org/10.2136/sssaj1980.03615995004400050002x.

GeoSlope International Ltd. 2007a. "Slope/W User's Guide for Slope Stability Analysis." *GEO-SLOPE International Ltd*, 2007.

GeoSlope International Ltd. 2007. "Seep/W User's Guide for Finite Element Seepage Analysis." *GEO-SLOPE International Ltd*, 2007.

GeoSlope International Ltd. 2007b. "Sigma/W User's Guide for Stress-Deformation Analysis." *GEO-SLOPE International Ltd*, 2007.

Gillot, J. E. 1987. "Chapter 4 - Composition and Fabric of Clays." *Developments in Geotechnical Engineering*, J. E. GILLOTT, ed., 91–142. Elsevier.

Gupta, S. C., and R. P. Ewing. 1989. "Modeling water retention characteristics and surface roughness of tilled soils." *Proceedings of the International Workshop on Indirect Methods for Estimating the Hydraulic Properties of Unsaturated Soils*, 379–388. Riverside, California.

Han, Z., and S. K. Vanapalli. 2016. "Relationship between resilient modulus and suction for compacted subgrade soils." *Eng Geol*, 211: 85–97. Elsevier B.V. https://doi.org/10.1016/j.enggeo.2016.06.020.

Han, Z., G. tao Zhao, J. guo Lin, K. wei Fan, and W. lie Zou. 2022. "Influences of temperature and moisture histories on the hydrostructural characteristics of a clay during desiccation." *Eng Geol*, 297. Elsevier B.V. https://doi.org/10.1016/j.enggeo.2022.106533.

Hanna, T. H., and J. I. Adams. 1968. "Comparison of Field and Laboratory Measurements of Modulus of Deformation of a Clay." *Highway Research Record*, (243).

Haverkamp, R., and J. Parlange. 1986. "Predicting the Water-Retention Curve from Particle Size Distribution." *Soil Sci*, 142 (6): 325–339.

Holtz, R. D., W. D. Kovacs, and C. S. Thomas. 1981. *An introduction to Geotechnical Engineering*. Englewood Cliffs: Prentice-Hall.

Hugenholtz, C. H., and D. Lacelle. 2004. "Geomorphic controls on landslide activity in Champlain Sea clays along Green's Creek, Eastern Ontario, Canada." *Geographie Physique et*

Quaternaire, 58 (1): 9–23. Presses de l'Universite de Montreal. https://doi.org/10.7202/013108ar.

Issler, D., J. S. L'Heureux, J. M. Cepeda, and B. Quan Luna. 2014. "Towards a numerical run-out model for quick-clay slides." *Proceedings of INTERPRAEVENT*, 23–27. Nara.

Kenney, T. 1976. "Formation and geotechnical characteristics of glacial-lake varved soils." *Norwegian Geotechnical Institute Publication*, 15–39.

Kerr, P. F. 1963. "QUICK CLAY." *Sci Am*, 209 (5): 132–143. Scientific American, a division of Nature America, Inc.

Koekkoek, E. J. W., and H. Booltink. 1999. "Neural network models to predict soil water retention." *Eur J Soil Sci*, 50 (3): 489–495. https://doi.org/10.1046/j.1365-2389.1999.00247.x.

Kovacs, G. 1981. *Seepage Hydraulics*. Amsterdam: Elsevier Science Publishers.

Law, K.T., and M. Bozozuk. 1988 "Engineering problems in Leda clay." International Conference of Engineering Problems of Regional Soils, Beijing China 775–792

Lefebvre, G. 1986. *Slope instability and valley formation in Canadian soft clay deposits*. *Can. Geotech. J.*

Lefebvre, G. 1996. "Soft sensitive clays. Landslides -Investigation and Mitigation." *Transportation Research Board Special Report*, 247: 607–619.

Lefebvre, G., J.-J. Paré, and O. Dascal. 1987. "Undrained shear strength in the surficial weathered crust." *Canadian Geotechnical Journal*, 24 (1): 23–34. https://doi.org/10.1139/t87-003.

Lefebvre, G., and C. Poulin. 1979. "New Method of Sampling in Sensitive Clay." *Can Geotech J*, 16 (1): 226–233. https://doi.org/10.1139/t79-019.

Leroueil, S. 1997. "Geotechnical characteristics of eastern Canada clays." *International symposium on the characterization of soft marine clays*, 26–28. Yokosuka, Japan.

Leroueil, S., J. Locat, J. Vaunat, L. Picarelli, H. Lee, and R. M. Faure. 1996. "Geotechnical characterization of slope movements." *Landslides*, 53–74.

Li, Y., and S. K. Vanapalli. 2021. "A novel modeling method for the bimodal soil-water characteristic curve." *Computer Geotech*, 138. Elsevier Ltd. https://doi.org/10.1016/j.compgeo.2021.104318.

Li, Y., and S. K. Vanapalli. 2022a. “Prediction of soil-water characteristic curves using two artificial intelligence (AI) models and AI aid design method for sands.” *Canadian Geotechnical Journal*, 59 (1): 129–143. https://doi.org/10.1139/cgj-2020-0562.

Li, Y., and S. K. Vanapalli. 2022b. “Prediction of Soil–Water Characteristic Curves of Fine-grained Soils Aided by Artificial Intelligent Models.” *Indian Geotechnical Journal*, 52 (5): 1116–1128. Springer. https://doi.org/10.1007/s40098-022-00607-1.

Liu, S. Y., L. T. Shao, and H. J. Li. 2015. “Slope stability analysis using the limit equilibrium method and two finite element methods.” *Computer Geotech*, 63: 291–298. https://doi.org/10.1016/j.compgeo.2014.10.008.

Lo, K. Y., and C. F. Lee. 1974. “An Evaluation of the Stability of Natural Slopes in Plastic Champlain Clays.” *Canadian Geotechnical Journal*, 11 (1): 165–181. https://doi.org/10.1139/t74-010.

Locat, A. 2012. “Rupture progressive et étalements dans les argiles sensibles.” Ph.D. Université Laval.

Locat, A., D. Demers, P. Locat, and M. Geertsema. 2017. “Sensitive clay landslides in Canada.” *In Proceedings of the 70th Canadian Geotechnical Conference*. Ottawa.

Locat, J., G. Lefebvre, and G. Ballivy. 1984. “Mineralogy, chemistry, and physical properties interrelationships of some sensitive clays from Eastern Canada.” *Canadian Geotechnical Journal*, 21 (3): 530–540. https://doi.org/10.1139/t84-055.

Løken, T. 1970. “Recent research at the Norwegian geotechnical institute concerning the influence of chemical additions on quick clay.” *Geologiska Föreningen i Stockholm Förhandlingar*, 92 (2): 133–147. https://doi.org/10.1080/11035897009453673.

Lumb, P. 1962. “Effect of rain storms on slope stability.” *In Symposium on Hong Kong Soils*, P. Lumb, ed., 73–87. Hong Kong.

MAY, R. W. 1977. “Facies model for sedimentation in the glaciolacustrine environment.” *Boreas*, 6 (2): 175–180. https://doi.org/10.1111/j.1502-3885.1977.tb00346.x.

McRostie, G. C., L. Morissette, and M. W. St-Louis. 1996. “Bottom-heave control of a deep sensitive clay excavation in Ottawa, Canada.” *Canadian Geotechnical Journal*, 33 (6): 926–936. https://doi.org/10.1139/t96-122.

Minasny, B., and Alex. B. McBratney. 2002. “The Neuro-m Method for Fitting Neural Network Parametric Pedotransfer Functions.” *Soil Science Society of America Journal*, 66 (2): 352–361. https://doi.org/10.2136/sssaj2002.3520.

Ministry of Mines. 2023. “Ontario Geological Survey.” *Ministry of Mines*. Accessed October 8, 2023. https://www.geologyontario.mndm.gov.on.ca/ogsearth.html#sont.

Mitchell, J. K., and W. N. Houston. 1969. “Causes of Clay Sensitivity.” *Journal of the Soil Mechanics and Foundations Division*, 95 (3): 845–871. https://doi.org/10.1061/JSFEAQ.0001288.

Mitchell, R. J. 1969. *Landslides at Breckenridge, Pineview Golf Club, and Rockcliffe*. Ottawa.

Mitchell, R. J. 1970. *Landslides at Breckenridge, Pineview Golf Club, and Rockcliffe*. Ottawa, Canada.

Mitchell, R. J., and A. R. Markell. 1974. “Flowsliding in Sensitive Soils.” *Canadian Geotechnical Journal*, 11 (1): 11–31. https://doi.org/10.1139/t74-002.

Morgenstern, N. R. 1967. “Submarine slumping and the initiation of turbidity currents.” *Marine geotechnique*, 3: 189–220.

Moum, J., T. Løken, and J. K. Torrance. 1971. “A Geochemical Investigation of The Sensitivity of a Normally Consolidated Clay from Drammen, Norway.” *Géotechnique*, 21 (4): 329–340. https://doi.org/10.1680/geot.1971.21.4.329.

Moum, J., O. I. Sopp, and T. Loken. 1968. “Stabilization of undisturbed quick clay by salt wells.” *Norwegian Geotechnical Institute*, 81: 1–7.

MTO. 2022. “Foundation Library.” *Ministry of Transportation Ontario*. Accessed October 8, 2023. https://foundation.mto.gov.on.ca/Map.

Mualem, Y. 1976. “A new model for predicting the hydraulic conductivity of unsaturated porous media.” *Water Resources Res*, 12 (3): 513–522. https://doi.org/10.1029/WR012i003p00513.

Mualem, Y. 1986. “Hydraulic Conductivity of Unsaturated Soils: Prediction and Formulas.” *Methods of Soil Analysis, Part 1: Physical and Mineralogical Methods*, 799–823. wiley.

Nader, A. 2014. *Engineering Characteristics of Sensitive Marine Clays-Examples of Clays in Eastern Canada*. Ottawa.

Oh, W. T., S. K. Vanapalli, and M. Sheikhtaheri. 2014. “Slope stability analysis for Champlain Sea clay deposits using the mechanics of unsaturated soils.” *Unsaturated Soils: Research and*

Applications - Proceedings of the 6th International Conference on Unsaturated Soils, UNSAT 2014, 1521–1527. Taylor and Francis - Balkema.

Panikom, N. 2020. "Climate change impact on rainfall-induced landslides in Ottawa sensitive marine clays." Master of Applied Science. Ottawa: University of Ottawa.

Peck, R. B., Hanson, W. E. and Thornburn, T. H. 1974. *Foundation Engineering*. John Wiley, London, 514 pp.

Penner, E. 1965. "A study of sensitivity in Leda Clay." *Can J Earth Sci*, 2 (5): 425–441. https://doi.org/10.1139/e65-037.

Perret, D., J. Therrien, P. Locat, and D. Demers. 2019. "Influence of surficial crusts on the development of spreads and flows in Eastern Canadian sensitive clays." *72nd Canadian Geotechnical Conference*. St. John's, Newfoundland and Labrador.

Petley, D. N., M. H. Bulmer, and W. Murphy. 2002. "Patterns of movement in rotational and translational landslides." *Geology*, 30 (8): 719. https://doi.org/10.1130/0091-7613(2002)030<0719:POMIRA>2.0.CO;2.

Pineda, J. A., E. Romero, M. De Gracia, and D. Sheng. 2014. "Shear strength degradation in claystones due to environmental effects." *Géotechnique*, 64 (6): 493–501. https://doi.org/10.1680/geot.13.T.025.

Qi, S., and S. Vanapalli. 2015a. "Stability Analysis of an Expansive Clay Slope: A Case Study of Infiltration-Induced Shallow Failure of an Embankment in Regina, Canada." *International journal of geohazards and environment*, 7–19. Dalhousie Libraries. https://doi.org/10.15273/ijge.2015.01.003.

Qi, S., and S. K. Vanapalli. 2015b. "Numerical analysis of slope stability in expansive soil: a case study of field test in Henan province, China." *The 68th Canadian Geotechnical Conference & 7th Canadian Permafrost*.

Qi, S., and S. K. Vanapalli. 2015c. "Hydro-mechanical coupling effect on surficial layer stability of unsaturated expansive soil slopes." *Computer Geotech*, 70: 68–82. Elsevier Ltd. https://doi.org/10.1016/j.compgeo.2015.07.006.

Quigley, R. M. 1980. *Geology, mineralogy, and geochemistry of Canadian soft soils: a geotechnical perspective1*.

Rankka, K., Y. Andersson-Sköld, C. Hultén, R. Larsson, V. Leroux, and T. Dahlin. 2004. "Quick-Clay in Sweden." *Swedish Geotechnical Institute*, 65: 137.

Rasmussen, K. K. 2012. “An Investigation of Monotonic and Cyclic Behaviour of Leda Clay.” MASc. London: University of Western Ontario.

Retningslinjer for presentasjon av geotekniske undersökelser. 1974. Oslo, Norway.

Richards, L. A. 1931. “Capillary conduction of liquids through porous mediums.” *Physics (College Park Md)*, 1 (5): 318–333. https://doi.org/10.1063/1.1745010.

Rosenqvist, I. TH. 1953. “Considerations on the Sensitivity of Norwegian Quick-Clays.” *Géotechnique*, 3 (5): 195–200. https://doi.org/10.1680/geot.1953.3.5.195.

Sangrey, D. A., and M. J. Paul. 1971. “A Regional Study of Landsliding Near Ottawa.” *Canadian Geotechnical Journal*, 8 (2): 315–335. https://doi.org/10.1139/t71-026.

Satyanaga, A., and H. Rahardjo. 2019. “Unsaturated shear strength of soil with bimodal soil-water characteristic curve.” *Geotechnique*, 69 (9): 828–832. ICE Publishing. https://doi.org/10.1680/jgeot.17.P.108.

Satyanaga, A., H. Rahardjo, E. C. Leong, and J. Y. Wang. 2013. “Water characteristic curve of soil with bimodal grain-size distribution.” *Comput Geotech*, 48: 51–61. https://doi.org/10.1016/j.compgeo.2012.09.008.

Schaap, M. 1998. “Using neural networks to predict soil water retention and soil hydraulic conductivity.” *Soil Tillage Res*, 47 (1–2): 37–42. https://doi.org/10.1016/S0167-1987(98)00070-1.

Skempton, A. W., and R. D. Northey. 1952. “The Sensitivity of Clays.” *Géotechnique*, 3 (1): 30–53. https://doi.org/10.1680/geot.1952.3.1.30.

Smith, N. D. 1978. “Sedimentation processes and patterns in a glacier-fed lake with low sediment input.” *Canadian Journal of Earth Sciences*, *15*(5), 741-756. https://doi.org/10.1139/e78-081

Soderblom, R. 1974. “*Organic matter in Swedish clays and its importance for quick clay formation*.” In 26th proceedings of the Swedish Geotechnical Institute. Stockholm, Sweden.

Syvitski, J. P. M. 1978. “Sedimentological advances concerning the flocculation and zooplankton pelletization of suspended sediment in Howe Sound, British Columbia: a fjord receiving glacial meltwater.” PhD. University of British Columbia.

Syvitski, J. P. M. 1980. “Flocculation, agglomeration, and zooplankton pelletization of suspended sediment in a fjord receiving glacial meltwater.” *Fjord Oceanography*, 615–623.

Syvitski, J. P. M., and J. W. Murray. 1981. “Particle interaction in fjord suspended sediment.” *Marine Geology*, *39*(3-4), 215-242. https://doi.org/10.1016/0025-3227(81)90073-6

Taha, A., and M. Fall. 2014. “Shear behavior of sensitive marine clay–steel interfaces.” *Acta Geotech*, 9 (6): 969–980. Springer Verlag. https://doi.org/10.1007/s11440-014-0321-4.

Taha, A. M. 2010. “Interface shear behavior of sensitive Marine Clays-Leda Clay.” MASc. Ottawa: University of Ottawa.

Tan, M., and S. K. Vanapalli. 2021. “Performance estimation of a shallow foundation on an unsaturated expansive soil slope subjected to rainfall infiltration.” *MATEC Web of Conferences*, 337: 03009. EDP Sciences. https://doi.org/10.1051/matecconf/202133703009.

Tavenas F. 1984. “Landslides in Canadian sensitive clays - a state-of-the-art.” *4th International Symposium on Landslides*, 16–21. Toronto, ON.

Ter-Stepanian, G. 2000. “Quick clay landslides: their enigmatic features and mechanism.” *Bulletin of Engineering Geology and the Environment*, 59 (1): 47–57. https://doi.org/10.1007/s100640000052.

Thakur, V., and S. A. Dedago. 2014. “Identification of sensitive clays susceptible to flow slides using remolding energy concept.” *Proceedings of the Computer Methods and Recent Advances in Geomechanics*, F. Oka, S. Kimoto, R. Uzuoka, and Murakami A., eds., 1–6. Kyoto, Japan.

Torrance, J. K. 1975. “On the Role of Chemistry in the Development and Behavior of the Sensitive Marine Clays of Canada and Scandinavia.” *Canadian Geotechnical Journal*, 12 (3): 326–335. https://doi.org/10.1139/t75-037.

Torrance, J. K. 1979. “Post-depositional changes in the pore-water chemistry of the sensitive marine clays of the Ottawa area, eastern Canada.” *Eng Geol*, 14 (2–3): 135–147. https://doi.org/10.1016/0013-7952(79)90081-4.

Torrance, J. K. 1983. “Towards a general model of quick clay development.” *Sedimentology*, 30 (4): 547–555. https://doi.org/10.1111/j.1365-3091.1983.tb00692.x.

Torrance, J. K. 1988. “Mineralogy, pore-water chemistry and geotechnical behaviour of Champlain Sea and related sediments.” *The Late Quaternary Development of the Champlain Sea Basin, Geological Association of Canada*, 35: 259–275.

Torrance, J. K. 2013. “Landslides in quick clay.” *Landslides*, 83–94. Cambridge University Press.

Torrance, J. K., S. W. Hedges, and L. H. Bowen. 1986. “Mössbauer spectroscopic study of the iron mineralogy of post-glacial marine clays.” *Clays and Clays Minerals*, 34 (3): 314–322.

Tran, T. V., and M. T. Trinh. 2019. “Coupled and uncoupled approaches for the estimation of 1-D heave in expansive soils due to transient rainfall infiltration: A case study in central Vietnam.” *International Journal of GEOMATE*, 17 (64): 152–157. GEOMATE International Society. https://doi.org/10.21660/2019.64.11778.

Tyler, S. W., and S. W. Wheatcraft. 1989. “Application of Fractal Mathematics to Soil Water Retention Estimation.” *Soil Science Society of America Journal*, 53 (4): 987–996. Wiley. https://doi.org/10.2136/sssaj1989.03615995005300040001x.

van Genuchten, M.T. 1980. A Closed-form Equation for Predicting the Hydraulic Conductivity of Unsaturated Soils. Soil Science Society of America Journal, 44: 892-898. https://doi.org/10.2136/sssaj1980.03615995004400050002x

Vanapalli, S. K. 1994. “Simple test procedures and their interpretation in evaluating the shear strength of an unsaturated soil.” Ph.D. Saskatoon: University of Saskatchewan.

Vanapalli, S. K. 2010. “Shear strength of unsaturated soils and its applications in geotechnical engineering practice.” *4th Asia-Pacific Conf. on Unsaturated Soils*, Buzzi, Fityus, and Sheng, eds., 579–598. London: Taylor & Francis Group.

Vanapalli, S. K., and M. C. Catana. 2005. “Estimation of the soil-water characteristic curve of coarse-grained soils using one point measurement and simple properties.” *In Proceedings of an International Symposium on Advanced Experimental Unsaturated Soil Mechanics*, 401–410.

Vanapalli, S. K., D. G. Fredlund, D. E. Pufahl, and A. W. Clifton. 1996. “Model for the prediction of shear strength with respect to soil suction.” *Canadian Geotechnical Journal*, 33 (3): 379–392. National Research Council of Canada. https://doi.org/10.1139/t96-060.

Vanapalli, S. K., Sillers, W. S., & Fredlund, M. D. 1998. “The meaning and relevance of residual state to unsaturated soils”. In *51st Canadian geotechnical conference*, Vol. 8. Alberta, Canada: Edmonton.

Vanapalli, S. K., Fredlund, D. G., & Pufahl, D. E. 1999. “The influence of soil structure and stress history on the soil–water characteristics of a compacted till”. *Géotechnique*, *49*(2), 143-159. https://doi.org/10.1680/geot.1999.49.2.143

Varnes, D. J. 1958. “Landslide types and processes.” *Landslides and engineering practice*, 20–47.

Wang, D. Y., C. S. Tang, Y. J. Cui, B. Shi, and J. Li. 2016. “Effects of wetting-drying cycles on soil strength profile of a silty clay in micro-penetrometer tests.” *Eng Geol*, 206: 60–70. Elsevier B.V. https://doi.org/10.1016/j.enggeo.2016.04.005.

Wijaya, M., and E. C. Leong. 2016. “Equation for unimodal and bimodal soil-water characteristic curves.” *Soils and Foundations*, 56 (2): 291–300. Japanese Geotechnical Society. https://doi.org/10.1016/j.sandf.2016.02.011.

Williams, D. R., P. M. Romeril, and R. J. Mitchell. 1979. “Riverbank erosion and recession in the Ottawa area.” *Canadian Geotechnical Journal*, 16 (4): 641–650. https://doi.org/10.1139/t79-074.

Williams, J., R. Prebble, W. Williams, and C. Hignett. 1983. “The influence of texture, structure and clay mineralogy on the soil moisture characteristic.” *Soil Research*, 21 (1): 15. https://doi.org/10.1071/SR9830015.

Zapata, C. E. 1999. “Uncertainty in Soil-Water-Characteristics Curve and impacts on unsaturated Shear Strength Prediction.” Ph.D. Arizona State University.

Zhai, Q., H. Rahardjo, A. Satyanaga, G. Dai, and Y. Zhuang. 2020. “Framework to estimate the soil-water characteristic curve for soils with different void ratios.” *Bulletin of Engineering Geology and the Environment*, 79 (8): 4399–4409. https://doi.org/10.1007/s10064-020-01825-8.

Zhang, L. L., D. G. Fredlund, L. M. Zhang, and W. H. Tang. 2004. “Numerical study of soil conditions under which matric suction can be maintained.” *Canadian Geotechnical Journal*, 41 (4): 569–582. National Research Council of Canada. https://doi.org/10.1139/T04-006.

Appendix A: Fitted GSD curves from 15 different Leda clay samples

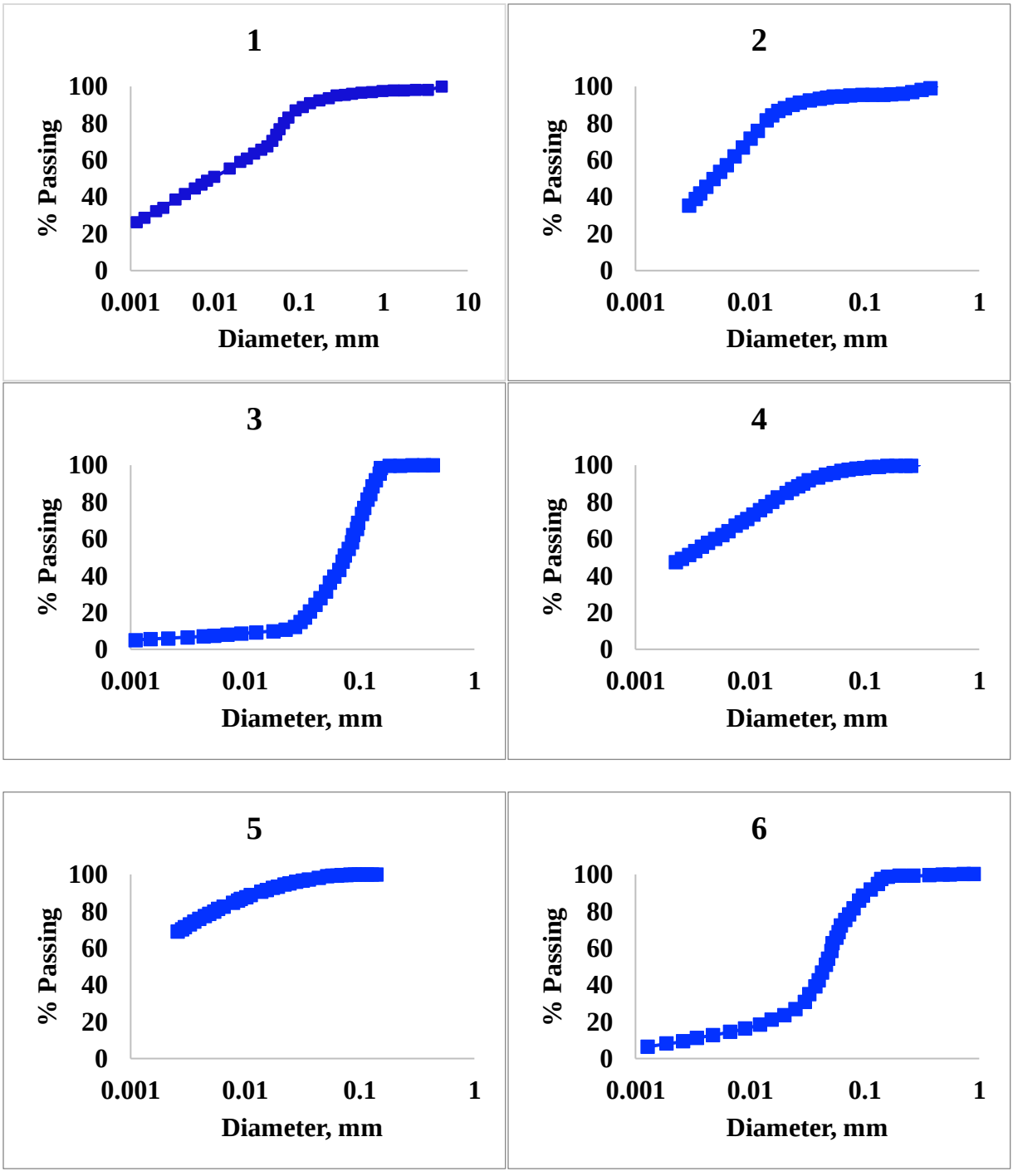

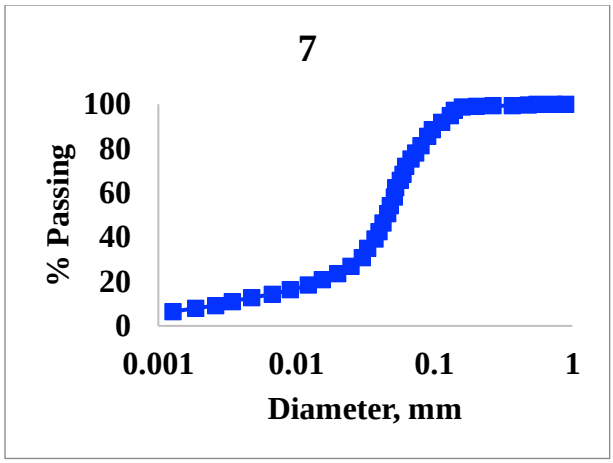
7
100
80
60
40
20
0
% Passing
0.001
0.01
0.1
1
Diameter, mm

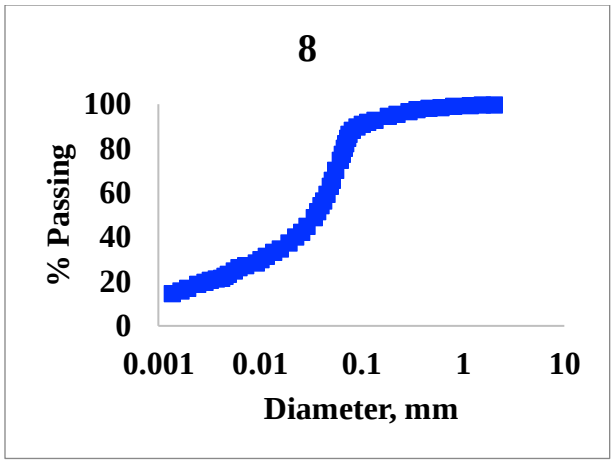
8
100
80
60
40
20
0
% Passing
0.001
0.01
0.1
1
10
Diameter, mm

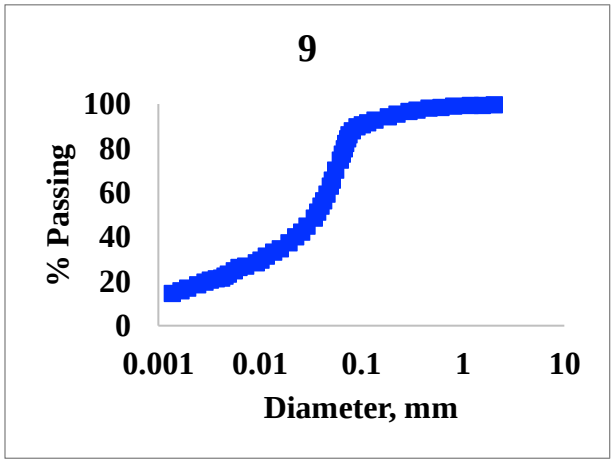
9
100
80
60
40
20
0
% Passing
0.001
0.01
0.1
1
10
Diameter, mm

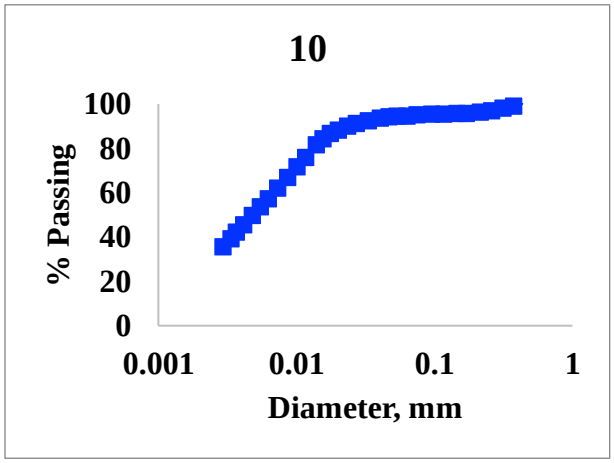
10
100
80
60
40
20
0
% Passing
0.001
0.01
0.1
1
Diameter, mm

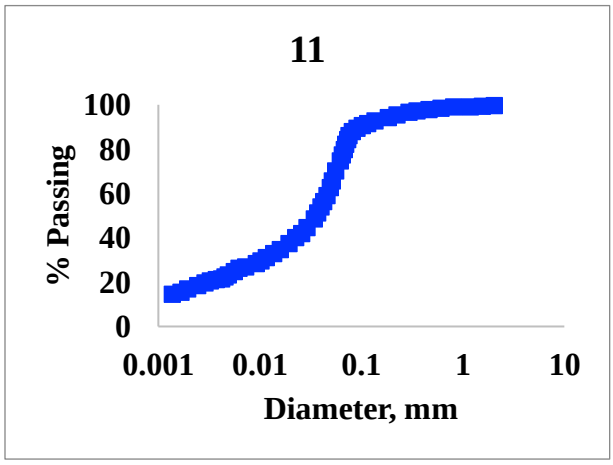
11
100
80
60
40
20
0
% Passing
0.001
0.01
0.1
1
10
Diameter, mm

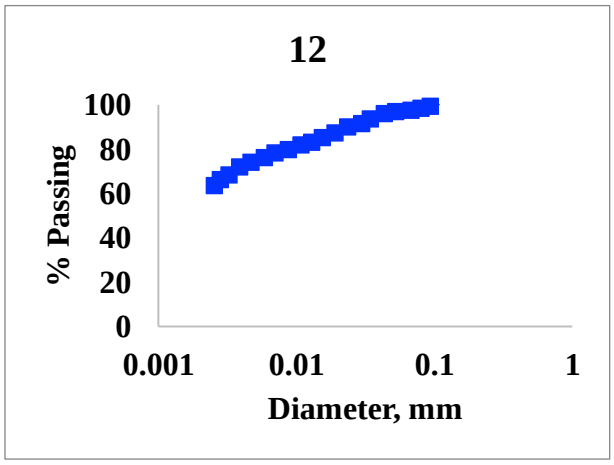
12
100
80
60
40
20
0
% Passing
0.001
0.01
0.1
1
Diameter, mm

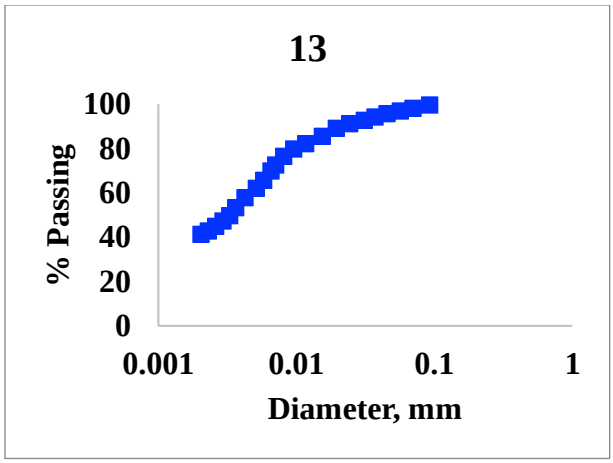
13
100
80
60
40
20
0
% Passing
0.001
0.01
0.1
1
Diameter, mm

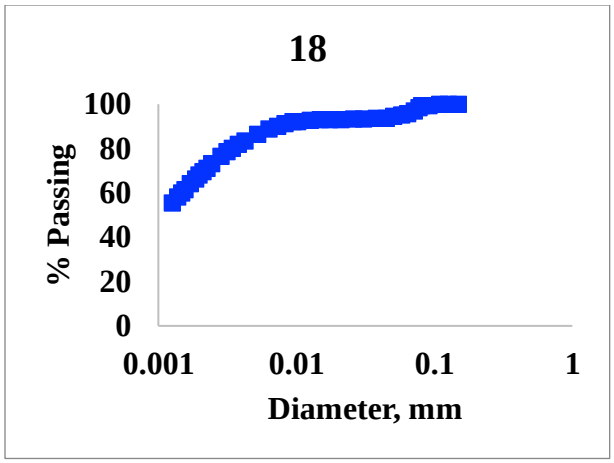
18
100
80
60
40
20
0
% Passing
0.001
0.01
0.1
1
Diameter, mm

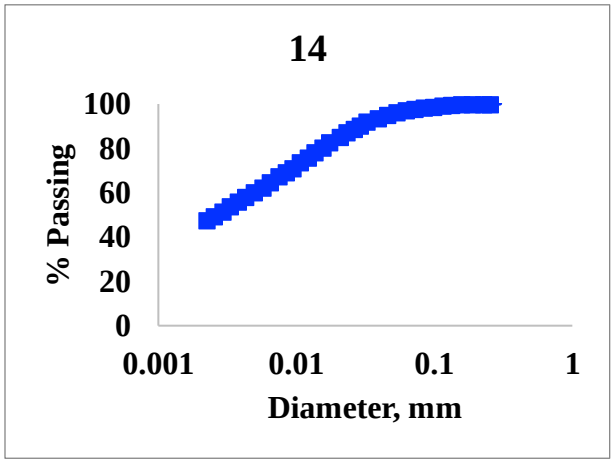
14
100
80
60
40
20
0
% Passing
0.001
0.01
0.1
1
Diameter, mm

Appendix B: Detailed information for weathered Leda clay soil properties used in this study

No.	GEOCRES	Latitude	Longitude	Year	GWT (m)	w (%)	e0	Depth (m)	LL (%)	PL (%)	PI (%)
1	31G00-059	45.340665	-74.9063	1970	3.6	50	1.521	1.6	41.3	19.4	21.9
2	31G05-090	45.384658	-75.58501	1972	1.5	58	1.702	1.8	63	23	40
3	31G00-240	45.338512	-75.47316	1974	0.9	74	1.89	2.0	80	21	59
4	31G05-089	45.39285	-75.5924	1972	1.8	56	1.472	2.1	64	25	39
5	31G05-088	45.384813	-75.58477	1972	1.7	58	1.75	2.2	66	26	40
6	31G00-240	45.338512	-75.47316	1974	0.9	74	1.955	2.3	70	23	47
7	31G00-240	45.338512	-75.47316	1974	0.9	86	2.34	2.4	70	21	49
8	31G00-227	45.30381	-75.07576	2005	2.2	49.9	1.465	2.6	54	20	34
9	31G00-227	45.30381	-75.07576	2005	2.2	80	2.265	2.6	66	23	43
10	31G05-090	45.384658	-75.58501	1972	1.5	60	1.058	2.7	52	24	28
11	31G00-227	45.30381	-75.07576	2005	2.2	60.3	1.62	2.7	49	27	22
12	31G05-092	45.398661	-75.58326	1973	1.8	52	1.604	2.9	67	25	42
13	31G05-079	45.389771	-75.59016	1971	1.2	52	1.68	2.9	62	25	37
14	31G05-089	45.39285	-75.5924	1972	1.8	50.5	1.398	2.9	53	24	29
15	31G05-087	45.396746	-75.59666	1972	1.8	52	1.388	2.9	41	24	17
16	31G00-034	45.362308	-75.48539	1968	2.6	87.5	2.34	3.1	77	26	51
17	31G05-143	45.494315	-75.48407	1986	0.5	66	1.804	3.1	64	24	40
18	31G00-240	45.338512	-75.47316	1974	0.9	80	2.14	3.1	73	31	42